ENGINEERING ANALYSIS OF LOW ENRICHED URANIUM FUEL USING IMPROVED ZIRCONIUM HYDRIDE CROSS SECTIONS

A Thesis

by

ROBERT WILCOX CANDALINO

Submitted to the Office of Graduate Studies of
Texas A&M University
in partial fulfillment of the requirements for the degree of

MASTER OF SCIENCE

August 2006

Major Subject: Nuclear Engineering

ENGINEERING ANALYSIS OF LOW ENRICHED URANIUM FUEL USING IMPROVED ZIRCONIUM HYDRIDE CROSS SECTIONS

A Thesis

by

ROBERT WILCOX CANDALINO

Submitted to the Office of Graduate Studies of
Texas A&M University
in partial fulfillment of the requirements for the degree of

MASTER OF SCIENCE

Approved by:

Chair of Committee,	William S. Charlton
Committee Members,	Marvin L. Adams
	Thomas R. Kiffe
Head of Department,	William E. Burchill

August 2006

Major Subject: Nuclear Engineering

ABSTRACT

Engineering Analysis of Low Enriched Uranium Fuel Using Improved Zirconium Hydride Cross Sections. (August 2006)

Robert Wilcox Candalino, B.S., Texas A&M University

Chair of Advisory Committee: Dr. William S. Charlton

A neutronic and thermal hydraulic analysis of the 1-MW TRIGA research reactor at the Texas A&M University Nuclear Science Center using a new low enriched uranium fuel (named 30/20 fuel) was completed. This analysis provides safety assessment for the change out of the existing high enriched uranium fuel to this high-burnup, low enriched uranium fuel design. The codes MCNP and Monteburns were utilized for the neutronic analysis while the code PARET was used to determine fuel and cladding temperatures. All of these simulations used improved zirconium hydride cross sections that were provided by Dr. Ayman Hawari at North Carolina State University. The neutronic and thermal analysis showed that the reactor will operate with approximately the same fuel lifetime as the current high enriched uranium fuel and stay within the thermal and safety limits for the facility. It was also determined that the control rod worths and the temperature coefficient of reactivity would provide sufficient negative reactivity to control the reactor during the fuel's complete lifetime.

An assessment of the fuel's viability for use with the Advanced Fuel Cycle Initiative's Reactor Accelerator Coupling Experiments program was also performed. The objective of this study was to confirm the continued viability of these experiments

with the reactor operating using this new fuel. For these experiments, the accelerator driven system must produce fission heating in excess of 1 kW when driven by a 20 kW accelerator system. This criterion was met using the new fuel. Therefore the change out of the fuel will not affect the viability of these experiments.

ACKNOWLEDGEMENTS

I would like to thank my advisor Dr. Charlton for his guidance, support and patience during this project. I would also like to thank Dr. Adams from the Nuclear Engineering Department and Dr. Kiffe from the Mathematics Department for serving on my committee. A special thanks to Dr. Hawari from North Carolina State University for providing valuable cross section sets that were used in this project.

In addition, I am very grateful to have received an Advanced Fuel Cycle Initiative fellowship from the Department of Energy. Their fellowship provided the inspiration for aspects of this thesis and helped support me financially. I would also like to thank the helpful people at the University Research Alliance for keeping me on track during this project.

Thanks to my parents and family for their love and support through my years at Texas A&M University and to all my friends.

TABLE OF CONTENTS

Page

Page

LIST OF TABLES

Page

LIST OF FIGURES

Page

Page

Page

Page

Page

Page

I INTRODUCTION

I.A. History of the NSCR

The Nuclear Science Center Reactor (NSCR) at Texas A&M University (TAMU) has been an integral part of nuclear education since it first achieved criticality on December 18, 1961. Since then it has served several TAMU campus departments, other universities, and other industrial and research organizations. Several changes have taken place at the reactor in regards to the type of fuel, operating power, and additional structures since 1961. The reactor operated until 1967 with MTR-type curved aluminum plate elements at an operating power level of 100 kW. General Atomic (GA) TRIGA (Training, Research, Isotopes, General Atomics) type fuel began use at the facility in 1968 and the power level was increased to 1 MW. While the initial core loading produced satisfactory operation, the experimental capability of the core was affected by the burnup of the fuel. Standard TRIGA fuel uses 20% enriched uranium in a uranium-zirconium hydride matrix with an 8.5% loading of uranium. Standard TRIGA fuel is generally limited to a peak fuel burnup of 0.5 MW-years per fuel element. To remedy this low burnup, additional fuel was periodically added to the core and graphite reflectors were added to four sides of the reactor to restore excess reactivity.[1]

Fuel followed control rods were included in the core in August 1970 to also help with the burnup problem. Modifications to the grid plate were made so that these new control rods could be utilized. Standard TRIGA fuel was used in the fuel followed

---

This thesis follows the style of *Nuclear Science and Engineering*.

control rods and thus the reactor still required frequent fuel addition due to the facility's high burnup rates of 100 MW-days per year per element.[1]

GA FLIP (Fuel Life Improvement Program) fuel was designed to alleviate the short fuel lifetime associated with standard TRIGA fuel. FLIP fuel has the same dimensions as standard TRIGA fuel, but with a different material composition. FLIP fuel has an enrichment of 70% and a H/Zr ratio of 1.6 while the Standard TRIGA fuel has an enrichment of 20% and a H/Zr ratio of 1.7. Thus, FLIP fuel uses high enriched uranium (HEU) whereas Standard TRIGA fuel uses low enriched uranium (LEU). FLIP fuel also has an expected lifetime of 9 MW-years which is considerably higher than the 1/2 MW-year life for Standard TRIGA fuel.[1]

Calculations revealed that the NSCR could safely operate with the FLIP fuel.[1] In June 1973, the NSCR was licensed to operate with this new fuel. The reactor operated from 1973 to 1979 with a mixture of FLIP and standard TRIGA fuel. More FLIP fuel was purchased during this time as the funds became available and by 1979 the core was entirely FLIP fuel.[1, 2] The reactor has been operating at a power of 1 MW with this fuel to the present day.

I.B. Objectives

I.B.1. Performance and Safety Parameters

Current U.S. policy states that research reactors must have a fuel enrichment of less than 20% due to the possible weapons use associated with HEU.[1] For this reason,

the NSCR must be converted back to a LEU fuel in order to help mitigate proliferation risks. This new fuel is termed 30/20 fuel since it consists of 30% by weight uranium in the uranium-zirconium hydride matrix while the uranium has an enrichment of 20% U-235. One of the main goals of this thesis is to verify that the NSCR performance and safety will not be degraded using 30/20 fuel with respect to neutronics and thermal characteristics. The NSCR performance and safety parameters that were evaluated included:

1. Maintain 30/20 fuel lifetime to be approximately the same as FLIP fuel lifetime.
2. Peak fuel and peak clad temperatures during steady-state operation are maintained below design setpoints throughout fuel lifetime.
3. Control rod shutdown reactivity maintained above technical specifications throughout fuel lifetime.
4. Prompt temperature coefficient of reactivity remains strongly negative throughout fuel lifetime.

To complete the first objective, an MCNP[3] input deck was written to model the entire NSCR. This input deck includes the isotopics and geometry of the main components that make up the core such as the fuel, control rods, cladding, coolant and reflectors. The program Monteburns[4] uses this MCNP input to simulate the reactor operating at a constant power level of 1 MW for an extended period of time. Monteburns keeps track of the criticality and isotopics in the fuel as a function of time. By simulating both 30/20 and FLIP fuel, a comparison can be made between the two

fuels in regards to the maximum fuel lifetime. A more detailed explanation of the codes MCNP and Monteburns can be found in sections I.C.1. and I.C.2. respectively.

The code PARET[5] was used to find the fuel centerline and cladding temperatures. The main input required for this code is the mass flow rate that is generated from natural convection and the axial power distribution. A mass flow rate of 8.026 kg/s was assumed since this is the same flow rate observed by the University of Texas at Austin's TRIGA reactor.[6] MCNP was used to tally the axial fission energy deposition in several regions in the NSCR. These tallies were used at different levels of burnup generated by Monteburns. Once the power distribution information is gathered, this becomes the input for the code PARET and the temperatures as a function of fuel lifetime can be generated. A more detailed description of PARET is found in section I.C.3.

Objectives three and four can be accomplished with MCNP. The criticality was calculated with the control rods fully inserted and fully withdrawn to determine the worths of the control rods. Also, the temperature coefficient of reactivity was calculated at several stages during the operational time period of the reactor. It is critical that the temperature coefficient of reactivity remains negative during the entire lifetime of the reactor. This ensures that as the power and temperature of the reactor increases more neutrons will be absorbed in non fissile materials thus returning the reactor back to a stable condition.

This coefficient is dominated by two main effects; the zirconium hydride effect as well as the Doppler broadening of the U-238 isotope. The first of these, zirconium hydride, has unique moderating characteristics for slow neutrons. The rise in temperature of the hydride increases the probability that the thermal neutron will gain energy. The use of Er-167 in the fuel ensures that some of these neutrons will be absorbed since this isotope of erbium has a particularly high absorption cross section at around 0.5 eV.[2,7]

The second contributor is the fact that as the temperature increases, the resonances in Uranium-238 broadens which increases the probability that neutrons in this energy region will be absorbed.[8] Both of these effects contribute to the safety of research reactors and these effects were evaluated for the new 30/20 fuel with respect to time.

I.B.2. The RACE Program

Another objective that must be met is a requirement set by the Department of Energy's (DOE) Advance Fuel Cycle Initiative (AFCI). In 2001, Congress authorized the AFCI program as an outgrowth of the Advanced Accelerator Applications (AAA). AFCI was officially launched in fiscal year 2003. The main objective that AFCI faces is to address important nuclear issues that face the U.S. These include waste management concerns, a decline in the infrastructure of nuclear energy, and leadership in nuclear

energy. The first of these objectives, improving nuclear waste management, will be addressed in this thesis.[9]

One barrier that inhibits the development of more nuclear reactors in the U.S. is the concern over waste management. The waste generated from nuclear power plants requires disposal and therefore a repository. One goal of the AFCI program is to develop the technology for waste transmutation. Waste transmutation involves transforming some of the long lived radioactive materials into short lived or even stable isotopes. The minor actinides that are of most concern include Np-237, Am-241, and Am-243. By transmuting these actinides, the long term radiotoxicity and heat load of the spent fuel can be reduced and will in turn lessen the burden for a repository.[9]

One way to transmutate these minor actinides is through an Accelerator Driven System (ADS). The Reactor Accelerator Coupling Experiments (RACE) is an AFCI project to study ADS technologies. The RACE project is a series of accelerator-driven subcritical systems (ADSS) experiments.[10] These experiments involve using an electron accelerator to bombard a heavy-metal target near the subcritical reactor with electrons which will produce Bremsstrahlung photons. The photons produce fast neutrons via photonuclear reactions. This provides the neutron source for the reactor. The neutrons produced in the heavy-metal target have energies that range from average fission energies of 1 MeV up to the energy of the incident electron from the accelerator (20 MeV for this thesis). These fast neutrons are required to transmutate the waste. Since the neutrons are multiplied through a subcritical system, there is a linear relationship

between the total power in the reactor and the power from the accelerator.[11] Therefore, if the accelerator is removed, the reactor will shutdown. This makes for an inherently safe way to transmutate spent nuclear fuel.

The RACE project consists of three experiments to be conducted at Idaho State University (ISU), the University of Texas at Austin (UT-Austin), and Texas A&M University (TAMU). The goal of these experiments is to demonstrate the capability to conduct ADSS experiments. They would also answer questions concerning the coupling efficiency, reactivity, and neutron multiplication.[10] The purpose of the first tests at ISU was to determine some basic understanding of RACE to provide valuable information for future experiments. This information includes operating procedures, performance of the systems, fission product production, and activation of the target. For the tests at UT-Austin, the objective was to produce enough power in the reactor so that temperature feedback effects could be observed.[11] This was not observed however since the target was not in a location close to the reactor. It is therefore necessary to conduct further experiments so these feedback mechanisms can be observed. These experiments will be performed at TAMU.

The objective of this thesis is to determine the feasibility of the RACE program with the new 30/20 fuel at the NSCR. It was originally assumed that FLIP fuel would be used for the RACE program at the NSCR. Since this is not the case anymore, an analysis must be made with this new fuel to ensure an adequate power level is achieved. To do this MCNP was used to model the NSCR with a tungsten target in the vicinity of

the reactor. An electron source was created on the top portion of the tungsten target to simulate the accelerator. MCNP can simulate the electron interactions within the target that produce Bremsstrahlung photons which in turn produce neutrons via photonuclear reactions. The amount of energy generated in the fuel due to neutron and photon interactions were tallied to determine whether or not a significant power level was achieved so that temperature feedback mechanisms could be observed.

I.C. Computer Codes

I.C.1. MCNP

MCNP is a coupled neutron, photon, and electron Monte Carlo transport code. The user creates an input file that specifies the geometry, materials, location and type of source, the type of answers desired, and any variance reduction techniques to be used to improve efficiency. The Monte Carlo method is useful to solve complex problems. Monte Carlo relies on random numbers to determine the outcome of the life of one particle. For example, a particle is created with characteristics specified by the user. A random number is generated to determine the distance this particle will travel given the materials that make up the problem. Another random number is generated to determine what type of interaction the particle will have. This continues until the particle is absorbed or escapes the boundaries set by the input. This process constitutes one history. As more histories are run, the neutron and photon distribution are better known.

The quantities of interest specified by the user are tallied along with an estimation of the error.[3]

The primary source of the continuous energy nuclear libraries comes from the Evaluated Nuclear Data File (ENDF) system. Data exists for neutron interactions, neutron induced photons, photon interactions and thermal particle scattering S(α, β). The S(α, β) treatment is particularly important for this thesis since it describes the moderating properties for ZrH. This scattering treatment includes molecular binding and crystalline effects that become particularly important for neutrons with low energy. All of these cross section data are important for accurately describing the problem at hand so that the correct solution can be found.[3]

Answers that are specified by the user can be tallied by MCNP. These tallies include: particle current, flux, and energy deposition. These tallies are normalized to be per source particle with the exception of criticality calculations. For MCNP, the criticality is defined as the number of fission neutrons in the current generation divided by the previous generation.[3]

MCNP will also print out the estimated relative error which is defined as one standard deviation of the mean divided by the mean. This informs the user the degree of confidence there is in the answer calculated by MCNP. For most purposes, it is desired to obtain a relative error less than 0.1 so that the results will be generally reliable.[3]

I.C.2. Monteburns

Monteburns is a Pearl script that acts as a link between the codes MCNP and ORIGEN2 (Ref. 12) to simulate the burnup in the reactor. The user specifies the geometry and materials in the MCNP input. The Monteburns input consists of the number of materials to be burned, isotopes in each material to keep track of, power level, total burn time, and the number of inner and outer burn steps. To start the burnup calculation, MCNP is used to determine one-group microscopic cross sections and fluxes. This information provides the input for ORIGEN2 (Ref. 12). ORIGEN2 will then perform decay and burnup calculations. ORIGEN2 keeps track of the isotopes and their concentrations in each material burned. This information is then used to produce a new MCNP input deck which will now have new isotopics for the materials that are being burned. Again, MCNP is run to obtain cross sections and fluxes for ORIGEN2. This process is repeated for each burn step until the total time to be burned is reached. This process is shown below (Fig.1). After each burn step, the criticality of the system and the mass of the isotopes are written to an output file. To improve accuracy, it is advised to use several burn steps for long irradiation times since the isotopics can change considerably over time.[4]

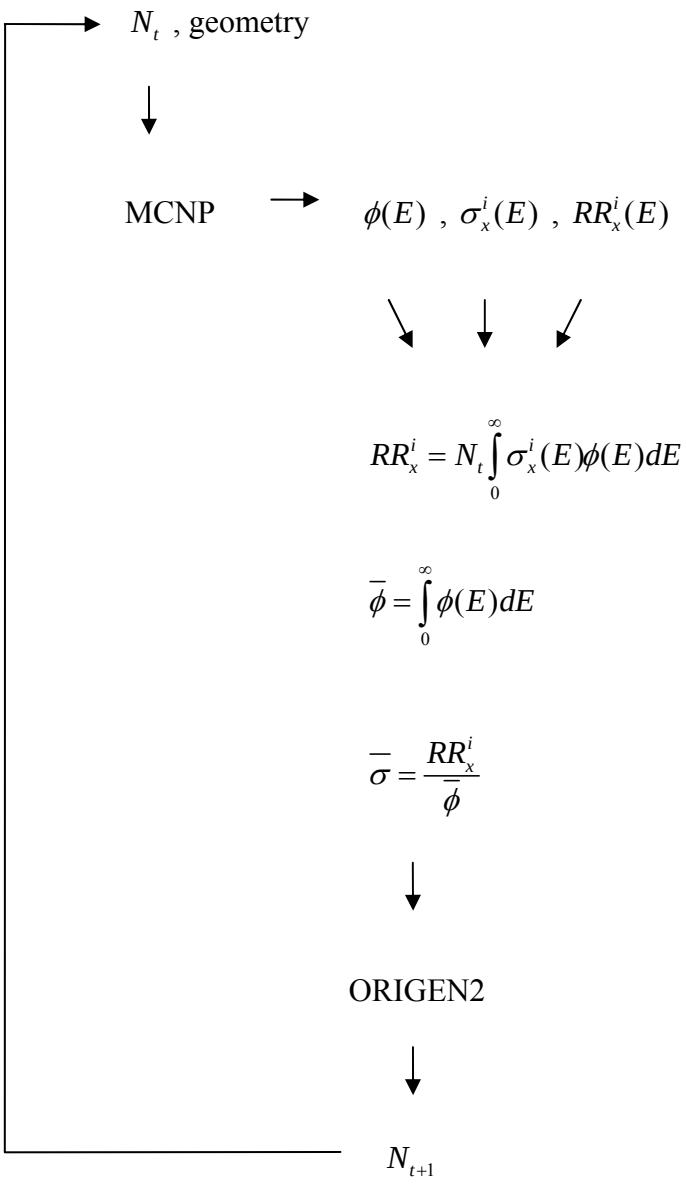

Fig. 1. Flow chart for burnup calculations.

I.C.3. PARET

PARET is a code developed by Argonne National Laboratory to provide a coupled thermal, hydrodynamic and point kinetics capability specifically for research reactors. The core can be represented by one to four regions, each with its own hydraulic parameters, coolant flow rates, and power distribution. Each coolant region can be divided up into as many as 21 axial sections. Each section describes the axial power distribution as a ratio between the power in that axial location and an average power for all axial sections of the core. The heat transfer in the fuel pin is treated as a one-dimensional problem in each axial section. Similarly, the hydrodynamics solution is treated as a one-dimensional problem. The output for PARET of interest is the fuel centerline, clad surface, and coolant temperatures. Feedback mechanisms such as the temperature coefficient of reactivity and control rod movements can also be simulated. This is particularly useful for pulsing simulations. These simulations were not performed however. PARET is still useful for calculating steady state temperatures which was done for this project.[5]

I.D. ZrH Scattering Cross Sections

Throughout these evaluations new zirconium hydride scattering cross sections will be used. These cross sections were obtained from Dr. Ayman Hawari from North Carolina State University. Dr. Ayman Hawari used atomistic simulations which treat the interactions between atoms quantum mechanically. These simulations produce the

forces between the atoms. A classical lattice dynamics code uses this force information to model the atomic structure using a dynamical matrix and generates the vibrational frequencies for the atoms. Although the cross sections provided had a hydrogen to zirconium ratio of 2.0 instead of the expected ratio of 1.6, they should still be acceptable for this thesis.[13]

II REACTOR DESIGN

The 30/20 fuel and the existing FLIP fuel in the NSCR have identical dimensions. The only difference between the fuels is isotopic composition. Since there are no geometry changes, a detailed description of the existing reactor systems is given below. Also, differences between the two fuels are provided in this section. The NSCR contains 86 fuel elements, four fuel followed shim safety control rods, one regulating control rod, and one transient control rod. These components are attached to a grid plate along with the graphite reflectors, experimental notches and instrumentation. The entire core is covered with 26 feet of water. Further descriptions of these components are provided below.

II.A. Mechanical Design

A bridge spans the reactor pool which provides support for the reactor core and its components such as the control rod drives and instrumentation systems. This bridge is mounted on four wheels so that it can be moved to different operating positions.[1] The two positions that were considered in this project were positions away from and near the thermal column. Figs. 2-4 give a general layout of the pool, stall, and reactor locations.

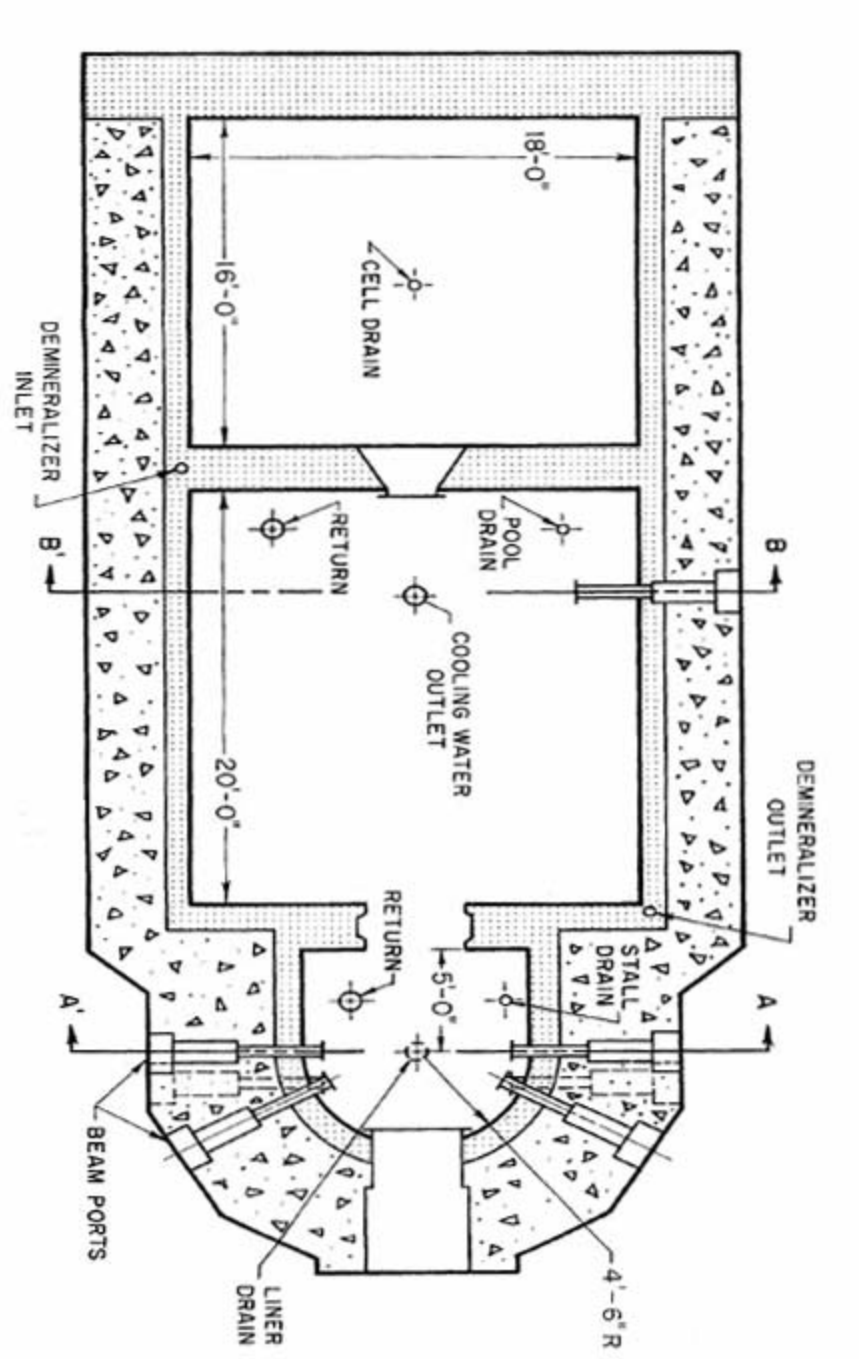

Fig. 2. Plan view of the NSC with dimensions.

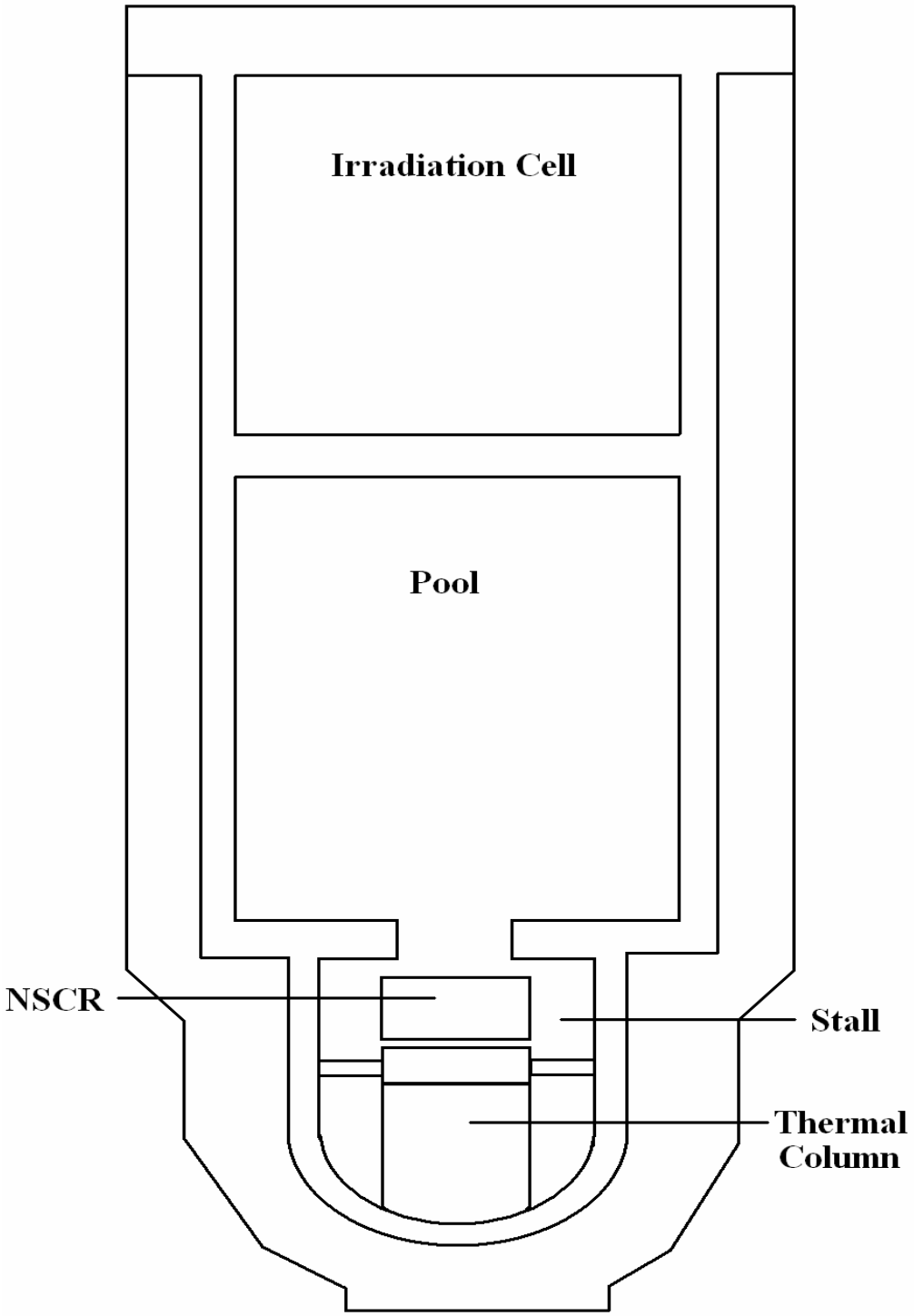

Fig. 3. Plan view of the NSC.

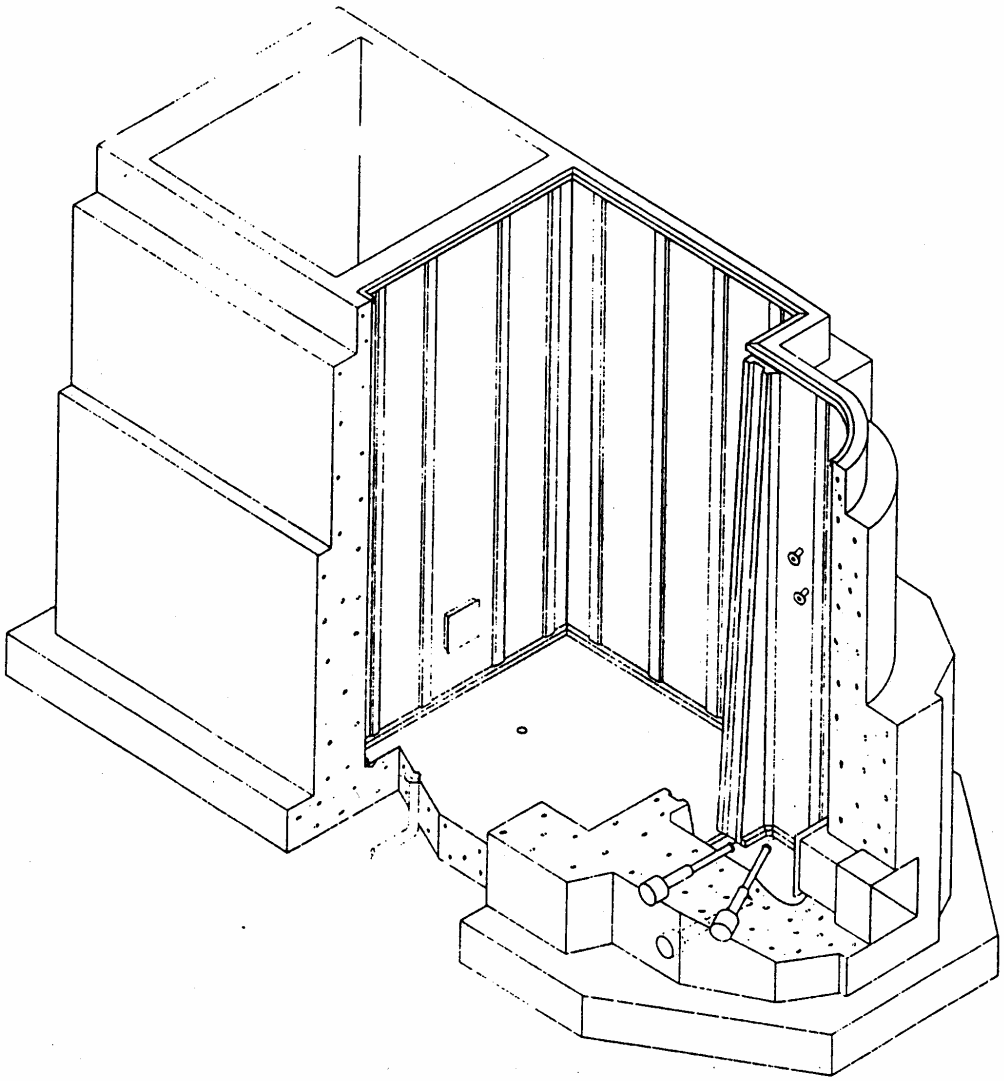

Fig. 4. NSC pool liner.

The reactor is supported by a grid plate which is welded to an aluminum suspension frame. The west side of the frame is left open to the pool to ensure an unrestricted flow of the cooling water. Stainless steel guides are mounted on the pool

floor. This is done so that accurate repositioning of the core can be achieved for experiments. It also allows for the core to be lowered to the bottom of the pool to prevent sway.

The grid plate (Fig. 5) contains a 9x6 array of 54 holes. Each hole can support one bundle assembly. Each bundle assembly can contain up to four fuel elements (or three fuel elements and a control rod). The typical core configuration is shown in Fig. 6. Note that each bundle assembly position is labeled with a letter and number designation (for example, "safety 1" is located in position C-9). A clearance hole is provided in the gird plate to allow for the movement of the control rods (Fig. 7).[1]

Both the FLIP and LEU fuel utilize zirconium hydride (ZrH) as a solid moderator. ZrH is homogeneously combined with the enriched uranium fuel. To facilitate hydriding of the uranium and zirconium, a 0.18" hole is drilled through the long end of the fuel slug. After the hydriding is complete, a zirconium rod is inserted. Graphite slugs measuring 3.5 inches in length are positioned at the top and bottom of the fuel to act as reflectors.[1] This is seen in Fig. 8. The fuel and graphite slugs each have a diameter of 1.371 inches and are contained in a 0.020-inch thick 304 stainless steel cladding. Additional fuel specifications for both the FLIP and 30/20 fuels are found in Table I.

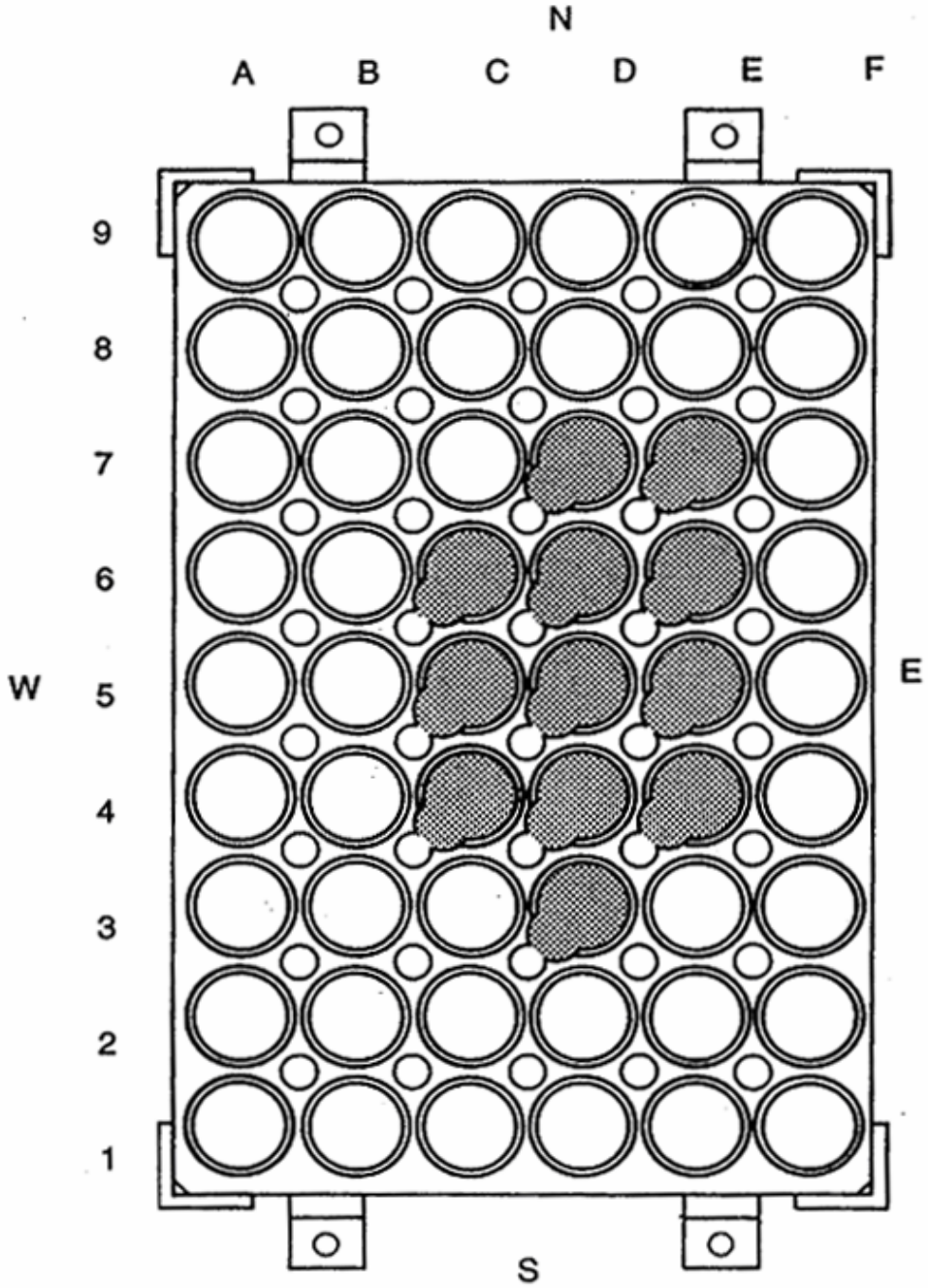

Fig. 5. NSC grid plate.

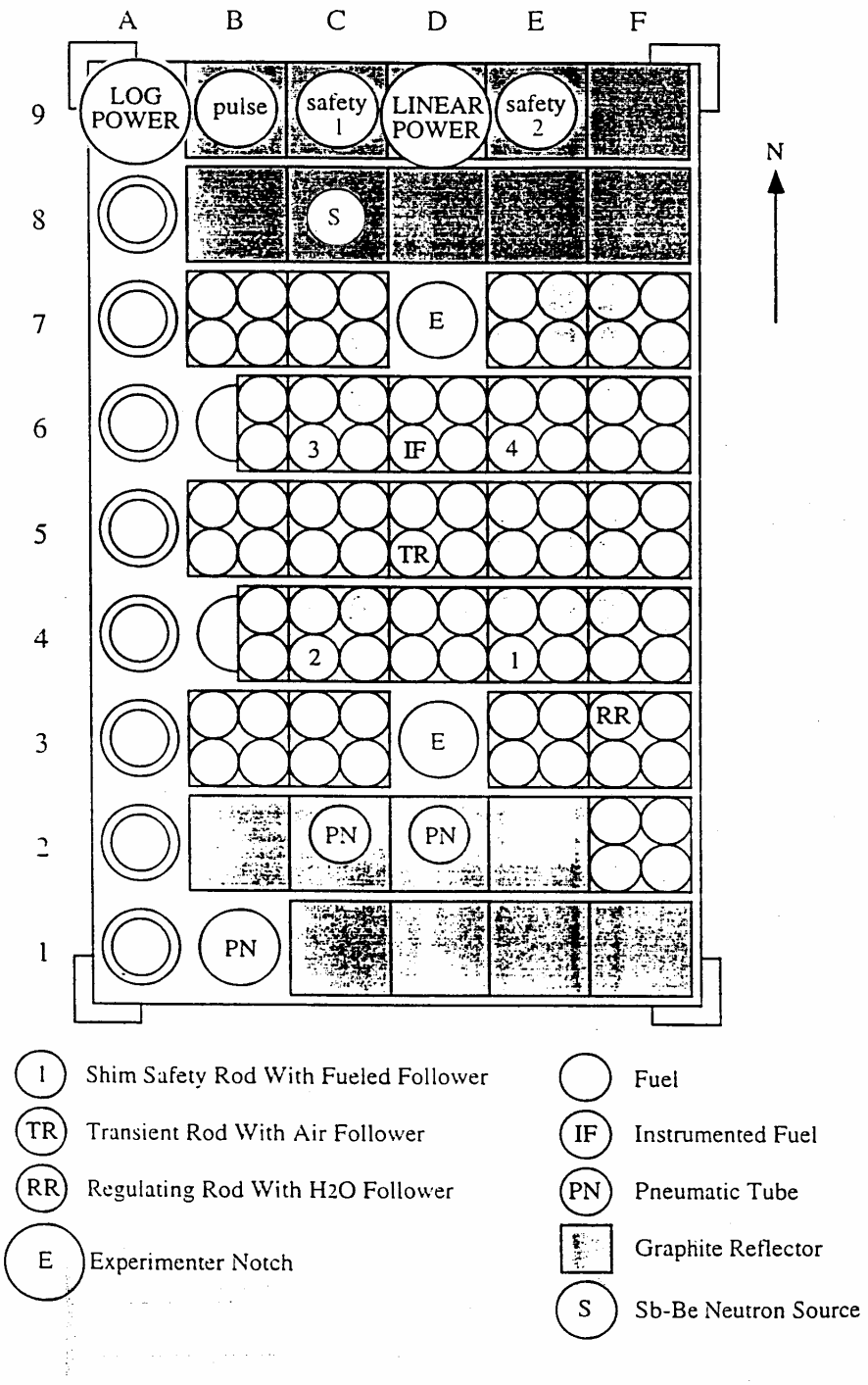

Fig. 6. Typical core configuration.

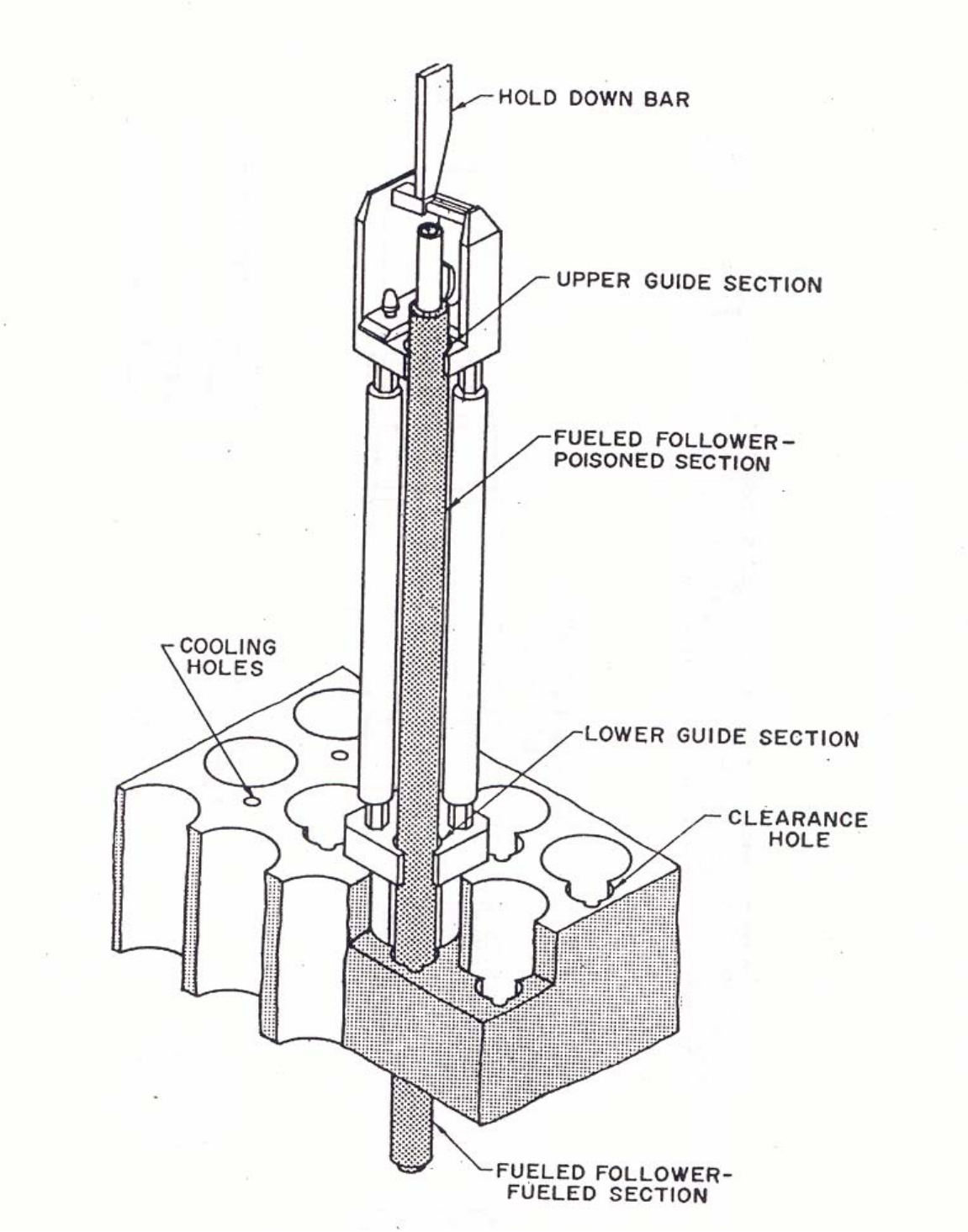

Fig. 7. Fuel followed shim safety rod installation.

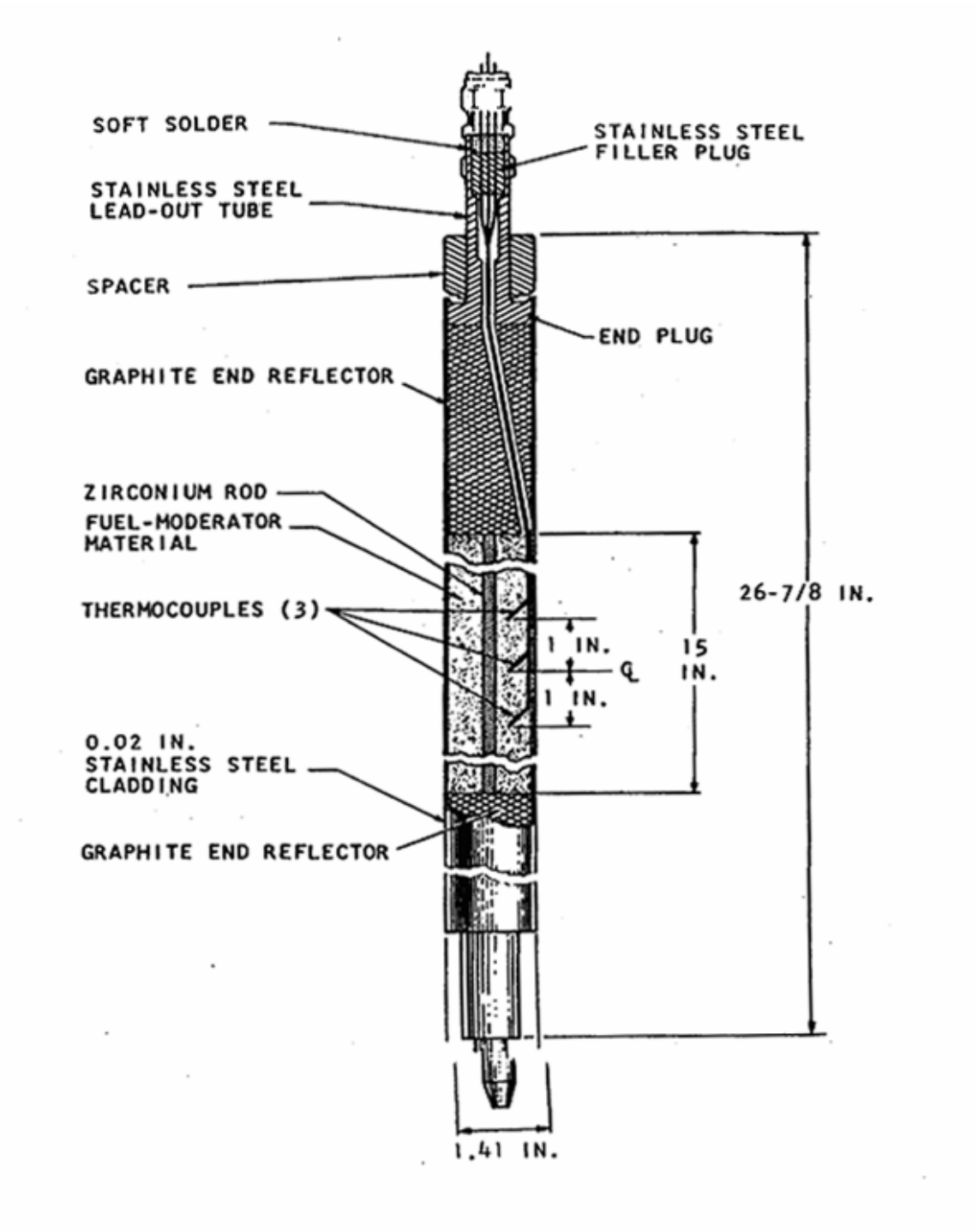

Fig. 8. NSCR fuel rod.

TABLE I

FLIP and LEU Specifications

	FLIP	**30/20**
Fuel-moderator material	U-ZrH	U-ZrH
Uranium content	8.5 wt%	30 wt%
U-235 enrichment	70%	20%
U-235 content per element	123 g	151 g
Burnable poison	natural erbium	natural erbium
Erbium content	1.5 wt%	0.9 wt%
Shape	cylindrical	cylindrical
Length of fuel	15 in	15 in
Diameter of fuel	1.371 in	1.371 in
Cladding type	304 SS	304 SS
Cladding thickness	0.020 in	0.020 in

One of the fuel rods contains three thermocouples to measure the fuel temperature during operation. The thermocouples are located halfway between the radial centerline and the outside edge of the fuel; one at the axial center and the other two are located one inch above and below the axial center. A stainless steel tube contains the lead out wires for the thermocouples and passes through the graphite slug (Fig. 8).[1]

The reactor has six control rods: four shim safety rods, one regulating rod, and one transient rod. The shim safety rods are fuel followed. This means that the bottom

portion of the rod contains fuel while the top portion contains borated graphite powder to be used as a poison. The poison section is 14 inches long while the fuel section is 15 inches long. Both are contained in the same stainless steel cladding that is used for the fuel rods. Both the transient rod and regulating rod are 15 inches in length. The shim safety and transient rods consists of borated graphite powder while the regulating rod is B_4C powder.[1]

Both the shim safety and regulating rods are moved via electromechanical drive mechanisms. The shim safety rods can be moved individually or in gang with a maximum withdrawal rate of 11.4 cm/min. The regulating rod can be operated manually or automatically. Its maximum withdrawal rate is 24.4 cm/min. The transient rod is mostly used during pulsing experiments where it can be pneumatically fired out of the core.[1]

Fig. 9 is the MCNP model for the NSCR. The isotopics and dimensions of the major components of the NSCR are provided in Figs. 10-19 and Tables II-VI. The dimensions are in centimeters. The difference in isotopics between the FLIP and 30/20 fuel is shown in Table II. The isotopics for the FLIP fuel are the same as that used by Brad Rearden[2] while the 30/20 composition was provided by Dr. William Whittemore.[14] The 30/20 fuel accounts for both carbon and hafnium that is present in the fuel. Carbon is present because carbon crucibles are used in the electric melt of fuel constituents. Therefore, some carbon enters the molten fuel. Carbon has undesired effects on other manufacturing aspects of the fuel so the amount of carbon is assayed. Hafnium is

present because it exists in the ore that bears zirconium. Even after some extensive processes to eliminate the impurities from zirconium, there are still trace amounts of hafnium. Since hafnium has a large thermal neutron cross section, it was accounted for.[14]

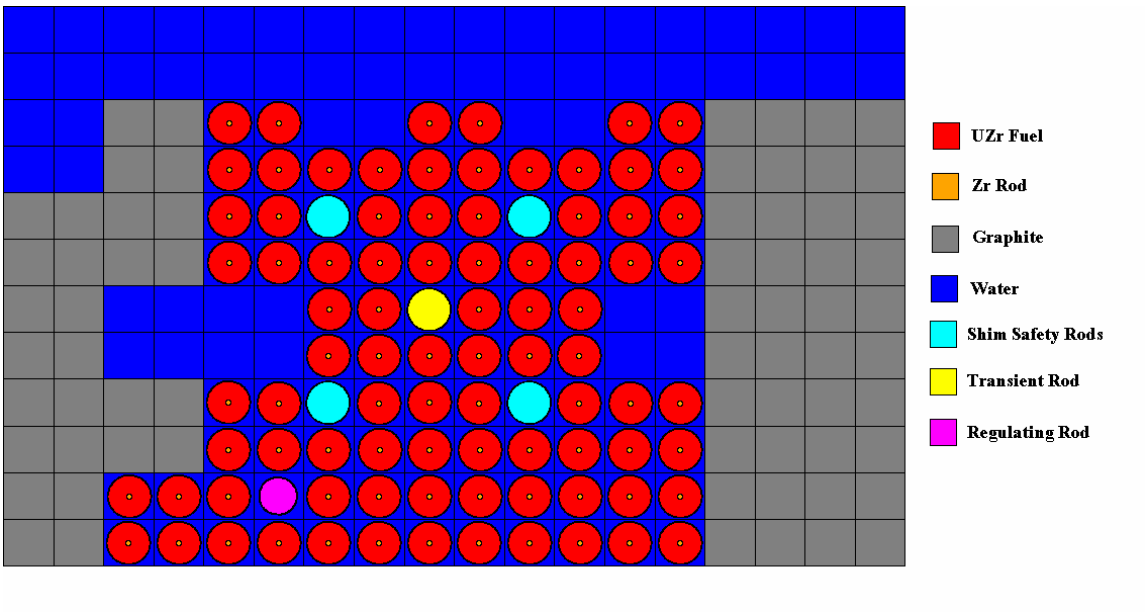

Fig. 9. Cross sectional view of MCNP model of the NSCR.

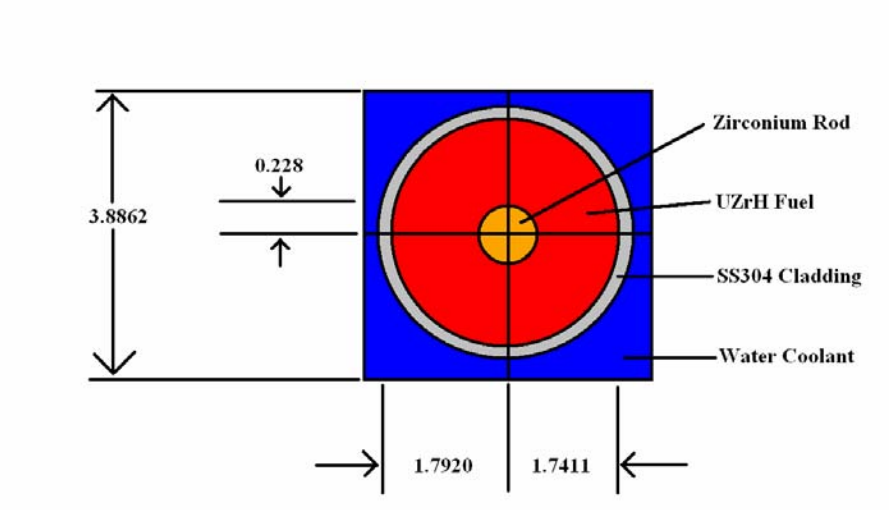

Fig. 10. NSCR fuel rod radial dimensions and materials.

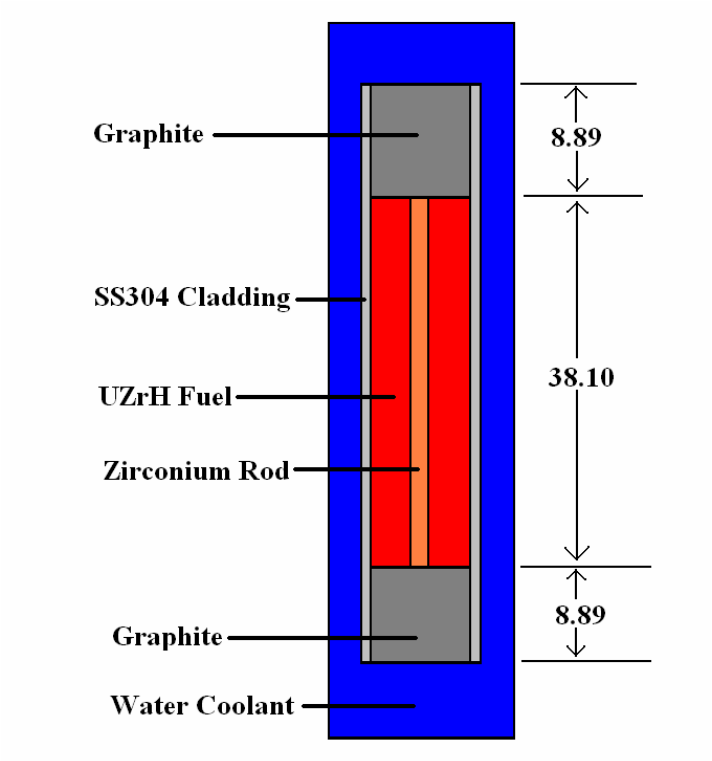

Fig. 11. NSCR fuel rod axial dimensions and materials.

TABLE II

NSCR Compositions for 30/20 and FLIP Fuel

Material	**Isotope**	**30/20 Fuel Atomic Density (atoms/b-cm)**	**FLIP Fuel Atomic Density (atoms/b-cm)**
Zirconium Rod	Zr	4.29757E-02	4.29090E-02
U-ZrH	U-234	8.32000E-06	
	U-235	1.08197E-03	8.83840E-04
	U-236	1.21000E-05	
	U-238	4.32127E-03	3.78780E-04
	Zr	3.22796E-02	3.39770E-02
	H-1	4.91576E-02	5.43640E-02
	Er-166	7.71700E-05	1.05600E-04
	Er-167	5.29900E-05	7.21320E-05
	C	1.78701E-03	
	Hf	1.93677E-06	
SS304 Cladding	Cr	1.73850E-02	1.73850E-02
	Fe	5.92060E-02	5.92060E-02
	Ni	7.69950E-03	7.69950E-03
	Mn	1.73200E-03	1.73200E-03
Water Coolant	H-1	6.6691E-02	6.6691E-02
	O-16	3.3346E-02	3.3346E-02

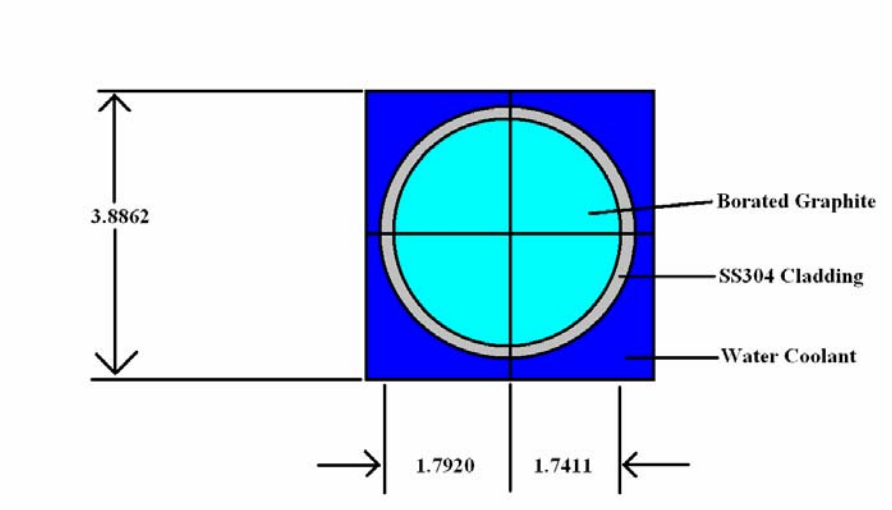

Fig. 12. NSCR shim safety control rod radial dimensions and materials.

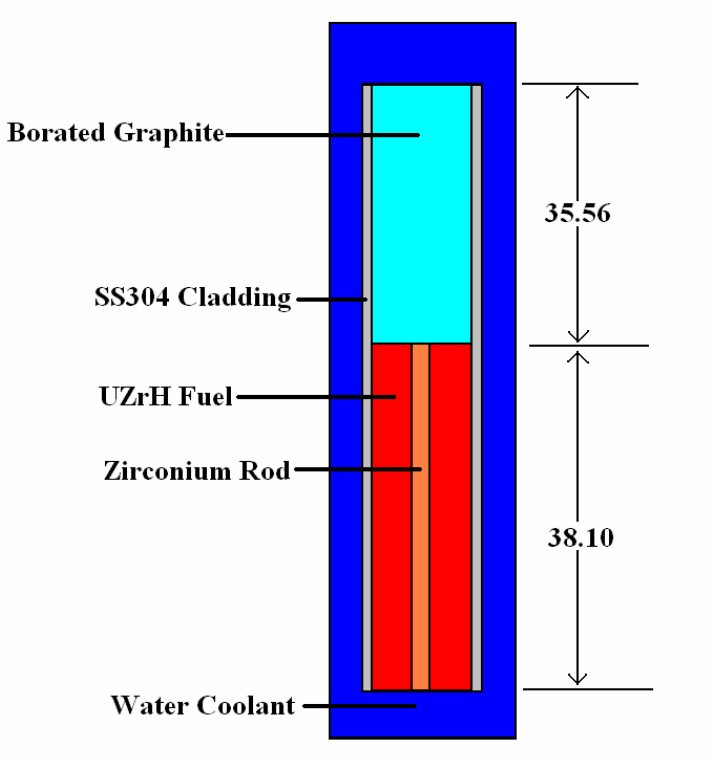

Fig. 13. NSCR shim safety control rod axial dimensions and materials.

TABLE III

NSCR Shim Safety Control Rod Material Compositions

Material	**Isotope**	**30/20 Fuel Atomic Density (atoms/b-cm)**
Borated Graphite	C	1.00824E-01
	B-10	2.18250E-02
	B-11	5.42218E-03
SS304 Cladding	Cr	1.73850E-02
	Fe	5.92060E-02
	Ni	7.69950E-03
	Mn	1.73200E-03
Water Coolant	H-1	6.6691E-02
	O-16	3.3346E-02

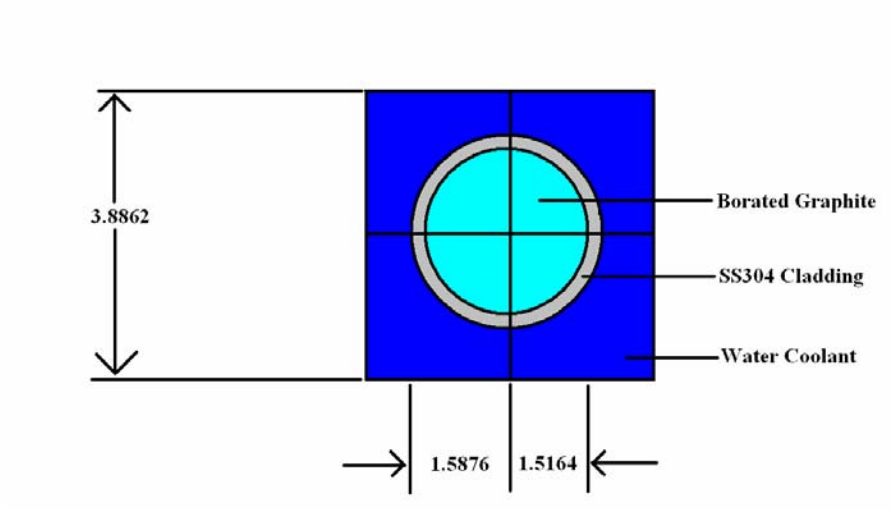

Fig. 14. NSCR transient control rod radial dimensions and materials.

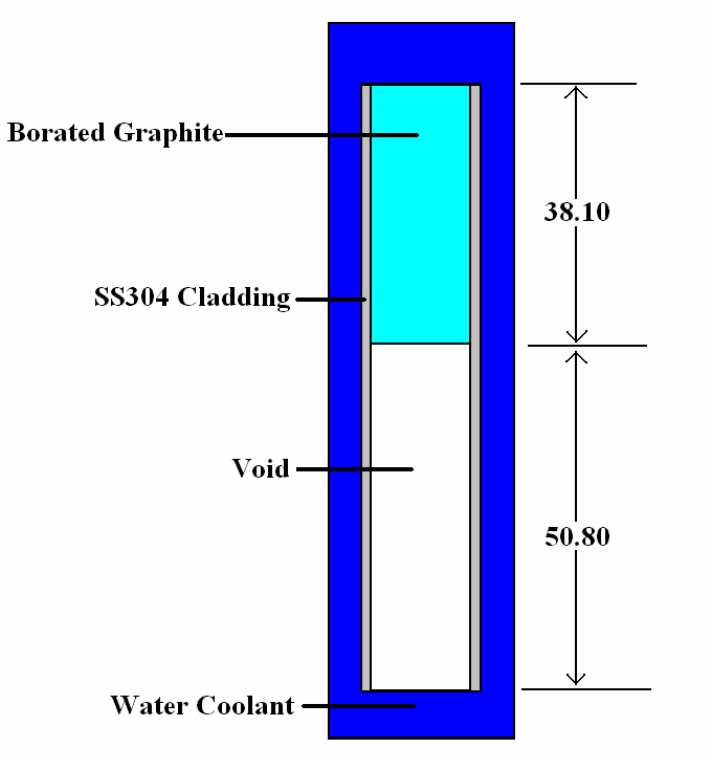

Fig. 15. NSCR transient control rod axial dimensions and materials.

TABLE IV

NSCR Transient Control Rod Material Compositions

Material	**Isotope**	**30/20 Fuel Atomic Density (atoms/b-cm)**
Borated Graphite	C	1.00824E-01
	B-10	2.18250E-02
	B-11	5.42218E-03
SS304 Cladding	Cr	1.73850E-02
	Fe	5.92060E-02
	Ni	7.69950E-03
	Mn	1.73200E-03
Water Coolant	H-1	6.6691E-02
	O-16	3.3346E-02

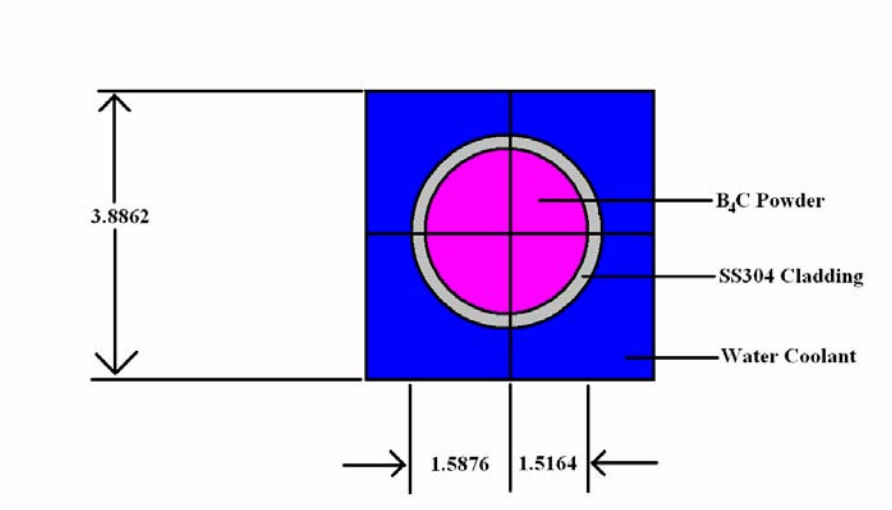

Fig. 16. NSCR regulating control rod radial dimensions and materials.

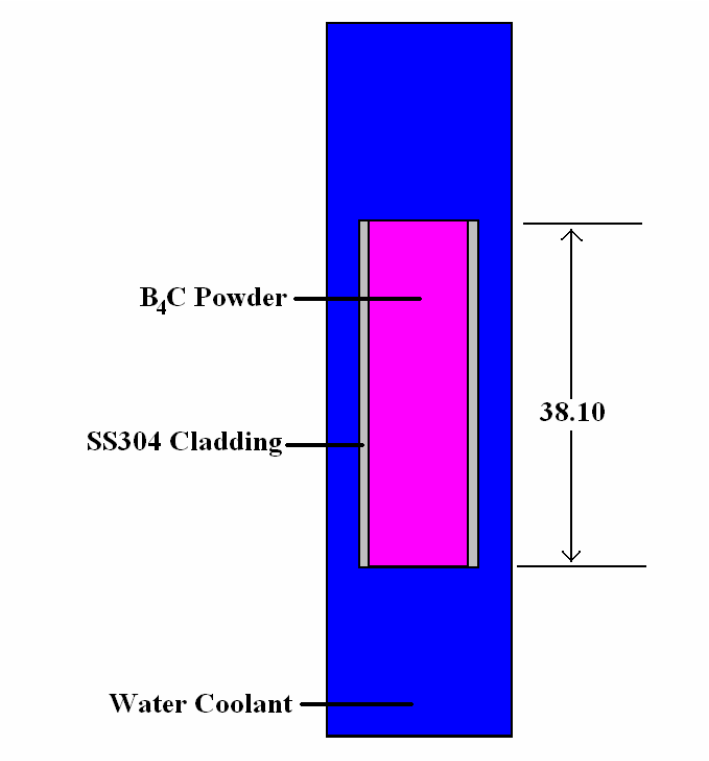

Fig. 17. NSCR regulating control rod axial dimensions and materials.

TABLE V

NSCR Regulating Control Rod Material Compositions

Material	**Isotope**	**30/20 Fuel Atomic Density (atoms/b-cm)**
B_4C Powder	C	2.72471E-02
	B-10	2.16887E-02
	B-11	8.72998E-03
SS304 Cladding	Cr	1.73850E-02
	Fe	5.92060E-02
	Ni	7.69950E-03
	Mn	1.73200E-03
Water Coolant	H-1	6.6691E-02
	O-16	3.3346E-02

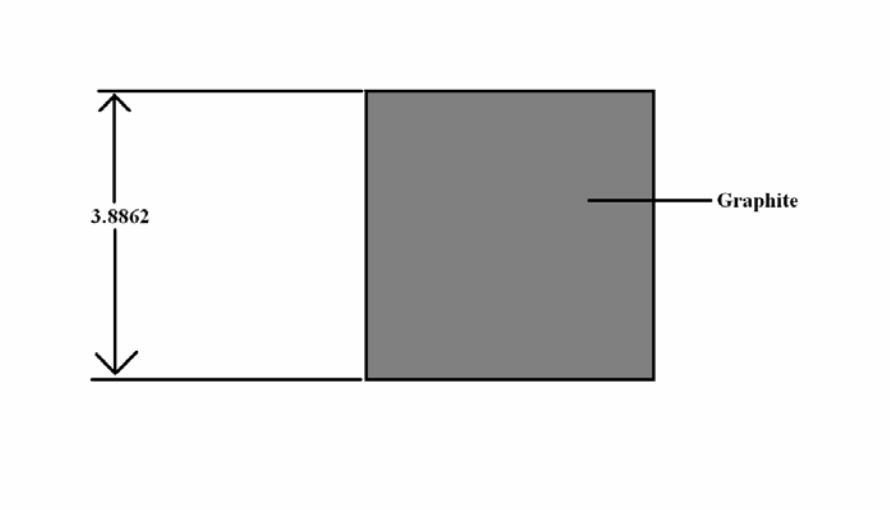

Fig. 18. NSCR graphite reflector element radial dimensions and materials.

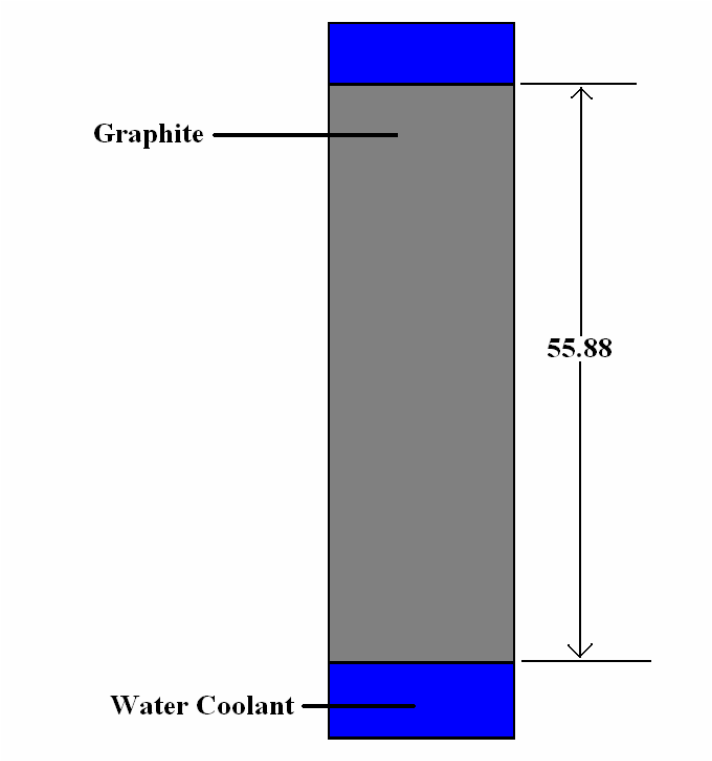

Fig. 19. NSCR graphite reflector element axial dimensions and materials.

TABLE VI

NSCR Graphite Reflector Element Material Composition

Material	Isotope	30/20 Fuel Atomic Density (atoms/b-cm)
Graphite	C	8.1299E-02

II.B. Thermal Design

The NSC reactor is located in a pool 26 feet below the surface of the water. It is cooled by natural convection through the 2 inch diameter holes in the grid plate. Water passes through this hole and through a cruciform opening (Fig. 20). The rod spacing is shown in Fig. 21. The spacing allows for good coolant flow. Coolant flow is enhanced by additional ½ inch diameter holes located at the corner of each four rod assembly (see Fig. 7).[1]

The main thermal concern is the dissociation of hydrogen from the uranium-zirconium hydride fuel. When hydrogen dissociates from the matrix, pressure increases which can lead to a failure in the cladding. Hydrogen tends to migrate from the hot radial center of the fuel rod to the periphery over time. There can be a 10% increase in the hydrogen to zirconium ratio along the edge of the fuel at a high burnup. Pulsing experiments also facilitate the dissociation of hydrogen since there is a momentary peak in fuel temperature at the edge. This increases the pressure inside and can lead to fuel deformations. The magnitudes of pulsing experiments are therefore more limited at high

burnups.[1] Studies show that in order to prevent these deformations the peak fuel temperature under any operating conditions may not exceed 950°C and the cladding temperature must remain below 500°C to avoid stress in the cladding.[15]

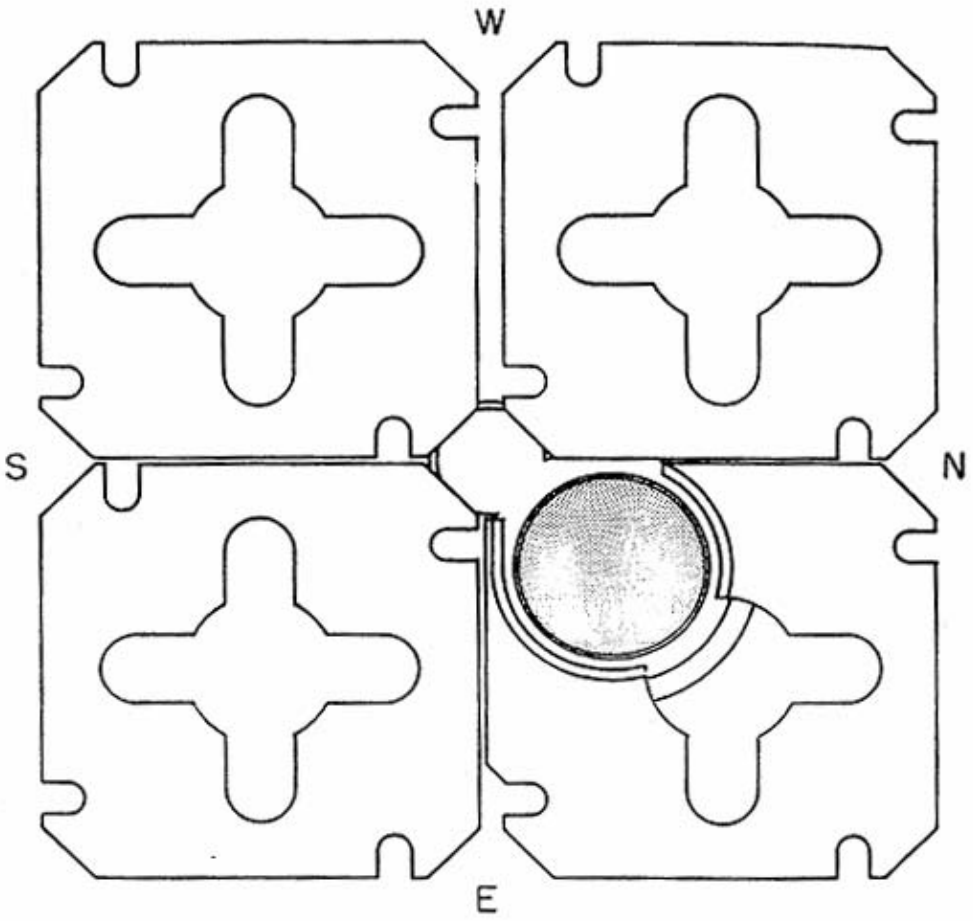

Fig. 20. Cruciform opening for coolant flow.

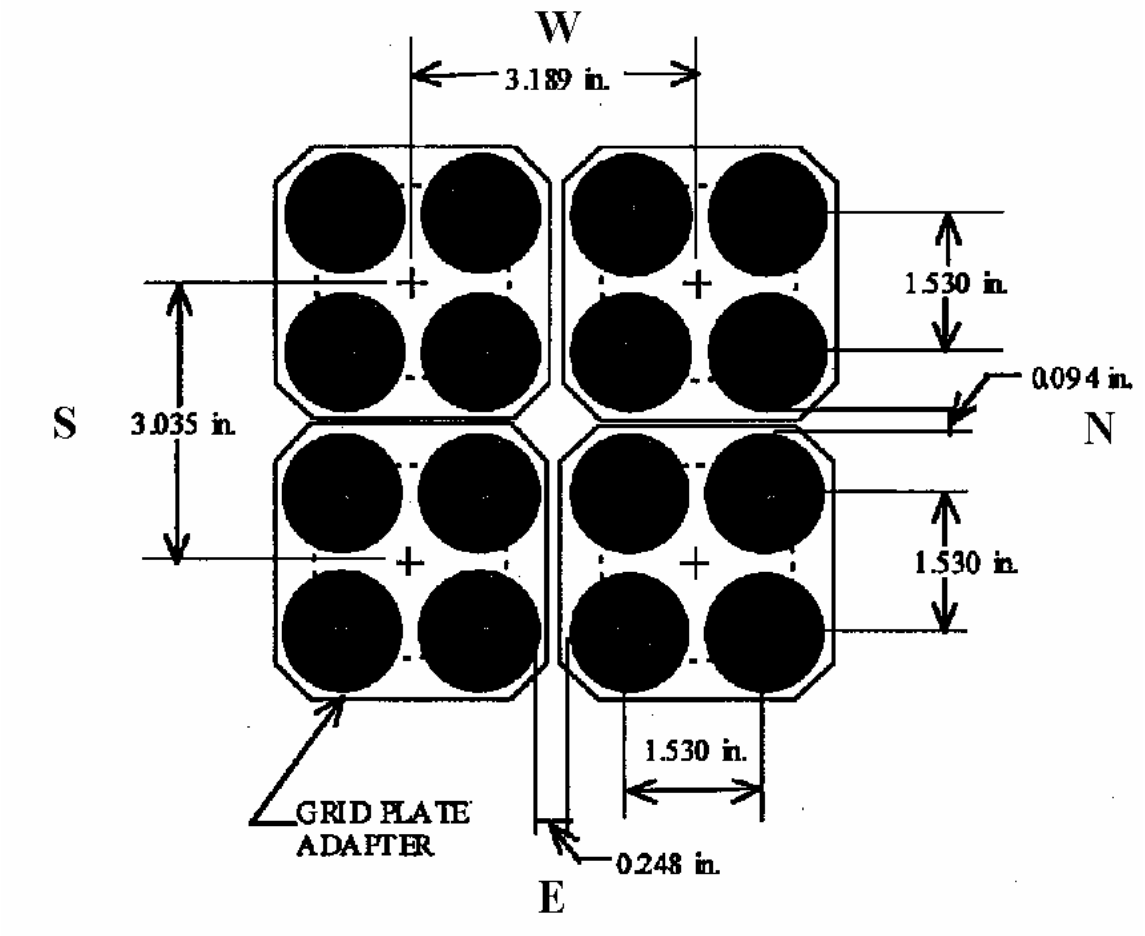

Fig. 21. Fuel rod spacing.

III NEUTRONIC ANALYSIS

An analysis of the neutronic aspects of the 30/20 fuel in the NSCR core is provided in this section. The programs MCNP and Monteburns were utilized for this process. Before the analysis of the 30/20 fuel started, a separate study to determine the validity of the new ZrH cross sections was performed. After satisfactory results were found from this test additional simulations were conducted. One of these was to determine the necessity of using more than one radial region in the fuel for burnup calculations. The conclusion was made that one radial region in the NSCR fuel can accurately predict the criticality of the reactor as well as the mass of various isotopes. The criticality and isotopics were tabulated as a function of time for both the FLIP and 30/20 fuels with and without a thermal column present. Also, the worths of the control rods were determined. These values were compared to previous analysis of LEU fuel.

III.A. Improved Zirconium Hydride Cross Sections

It is important to obtain accurate cross sections for the S(α, β) scattering since this plays a large role in the temperature feedback mechanism. ZrH is ineffective as a moderator for slowing down neutrons with energies less than 0.14 eV. For energies above 0.14 eV however, ZrH performs as well as a free hydrogen atom for slowing down neutrons. Thermal neutrons (0.025 eV) can actually gain energy as they pass through the ZrH lattice. As the temperature increases the probability that a thermal neutron will gain energy as it interacts with the oscillating hydrogen atom in the ZrH

lattice increases.[6] Er-167 has a large microscopic absorption cross section (several kilobarns) at 0.5 eV. The combination of the scattering properties of ZrH and the use of Er-167 provides a large temperature coefficient of reactivity.

MCNP has two sets of cross sections for the S(α, β) treatment for ZrH. One is from 1985, the other from 1999. Both are from the ENDF. This study is to see if the cross section sets from Dr. Hawari can more accurately predict the behavior of the reactor. A criticality calculation was performed for the NSCR using the standard ZrH cross sections in MCNP and was compared to the criticality calculated using the cross section sets provided by Dr. Hawari.

These results are shown in Table VII for the existing MCNP cross sections and Dr. Hawari's cross sections. Previous comparisons between MCNP models for critical rod height and the actual critical rod height data have shown that the MCNP model tends to underestimate the criticality. Since Dr. Hawari's cross sections show an increase in k_{eff}, these cross-sections produce a better prediction of the reactor behavior. It should be noted that the differences between the cross sections only applies to the S(α, β) treatment. It was therefore determined that these cross sections can be used for the remaining portions of this thesis.

TABLE VII

ZrH Cross Section Comparison

	K effective	Standard Deviation
1985 data	1.06048	0.000732
1999 data	1.06045	0.000700
Dr. Hawari data	1.06166	0.000690

The flux was also calculated with MCNP with these different cross sections and Figs. 22 and 23 show these results. Again, the interest here lies in how much difference there is among the ZrH cross sections. To obtain Fig. 22, an F4 tally with many energy bins was run with MCNP. MCNP essentially solves Eq. (1). Here, $N(\vec{r},E,t)$ can be thought of as a track length density. Therefore, by summing the track lengths an estimate for the average flux can be found and tallied in the appropriate energy bin.

$$\bar{\phi} = \frac{1}{V}\int dE \int dV \int ds N(\vec{r},E,t) \tag{1}$$

MCNP tallies are normalized to the source particle. Therefore, the units for the F4 tally are n/cm^2-source particle. This will give the correct shape for the neutron scalar flux, but not the correct magnitude. To obtain the desired magnitude and units of n/cm^2-sec, the quantity of neutrons per second needs to be known. To do this, a power level of 1 MW was assumed and the following constant was obtained in Eq. (2).

$$\frac{1E6J}{s}\times\frac{1MeV}{1.6022E-13J}\times\frac{fission}{200MeV}\times\frac{2.4neutrons}{fission}=7.4898E16\frac{n}{s} \qquad (2)$$

From Fig. 22 one can see that the three cross section sets seem to agree quite well with each other for predicting the scalar flux. Since the differences are hard to observe, Fig. 23 was created. Here, ratios were made between the 1999 data and the 1985 data and between Dr. Hawari's data and the 1985 data. This shows that there is a difference among the cross sections, but generally they agree with each other within a ratio of 0.875 and 1.075. Fewer neutrons were tallied in the energy bins below 1E-8 MeV. These energy bins have larger errors associated with them and may be the source of the discrepancies in Fig. 23.

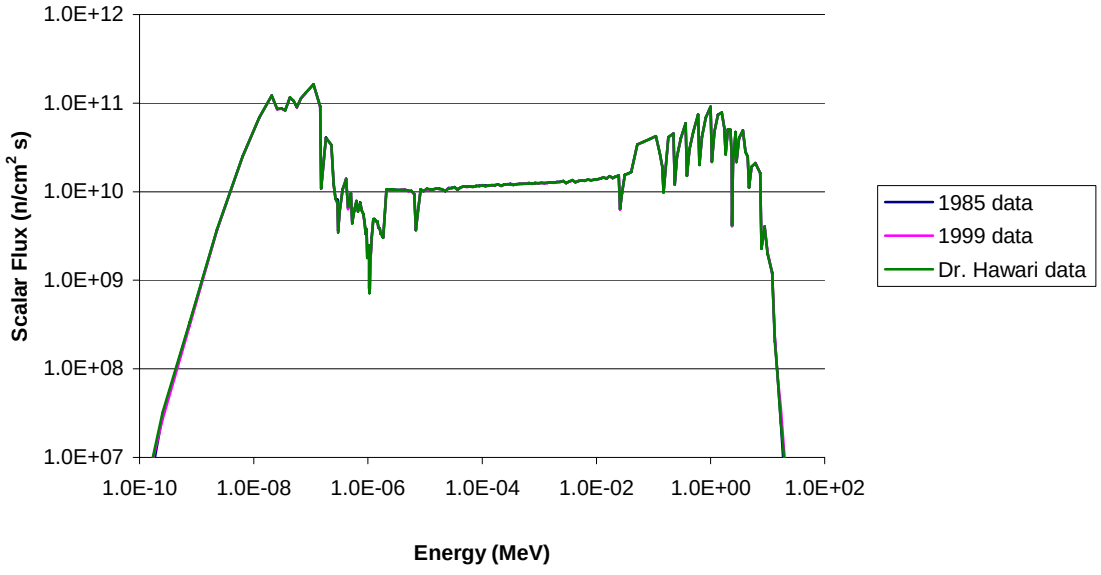

Fig. 22. Fluxes for various ZrH MCNP scattering cross sections.

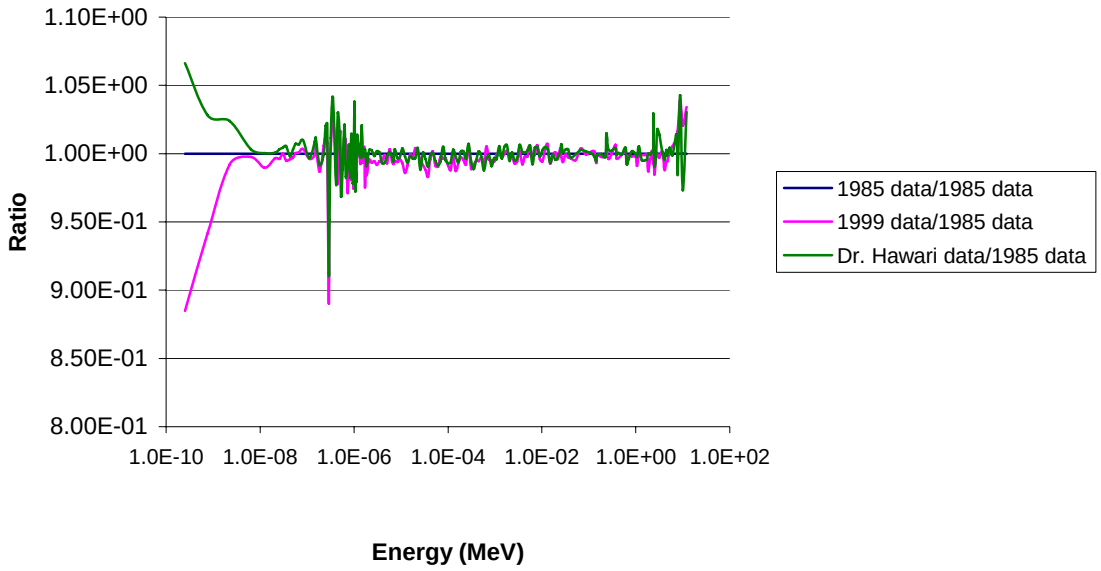

Fig. 23. Flux ratios.

III.B. Radial Region Comparison

In typical fuel pin simulations, multiple radial regions are used in the fuel to account for the buildup and depletions difference for self-shielding. The increased number of fuel regions accounts for the fact that the flux will vary with the radius. Since the TRIGA fuel has a moderator which is integrated with the fuel, it may not be necessary to use multiple fuel regions to acquire an accurate simulation. This is important in this work because of the use of a Monte Carlo transport simulation. In this simulation computation time increases significantly with an increase in the number of cells.

A simple test case was studied where one pin cell was modeled in MCNP (with reflecting boundary conditions applied to all six sides; thus simulating an infinite lattice of these fuel pins). Two models were made: one with only one radial fuel region, the other with eight radial fuel regions. Both models were input into Monteburns to simulate fuel burnup. The purpose of this test was to determine if a single fuel region was sufficient. MCNP and Monteburns input decks for this study are found in Appendix A.

The two pins were burned using Monteburns. k_{inf} as well as the mass of several isotopes of interest were tabulated as a function of time. These results are found in Figs. 24-33. While it can be seen that there is some difference between the two simulations, it does not appear that there is enough difference to have a major impact on pertinent results. The error between the two simulations was calculated by taking the difference between the two results and dividing by the results gathered from the 8 region simulation. The maximum error found in Figs. 24-33 is seen in Table VIII. The maximum error found was 13% for the differences in Am-243. All other isotopes had errors below 10%. It was decided that this error is acceptable. Thus for the remainder of this work single fuel regions were used to decrease the required computational time.

TABLE VIII

Error Between 1 Pin Cell with 1 Region and Pin Cell with 8 Regions

Isotope	% Error
U-235	0.000134
U-238	3.86
Np-237	0.63
Pu-239	4.44
Pu-240	6.63
Am-241	6.70
Am-242	6.33
Am-243	13.87
Er-167	0.11

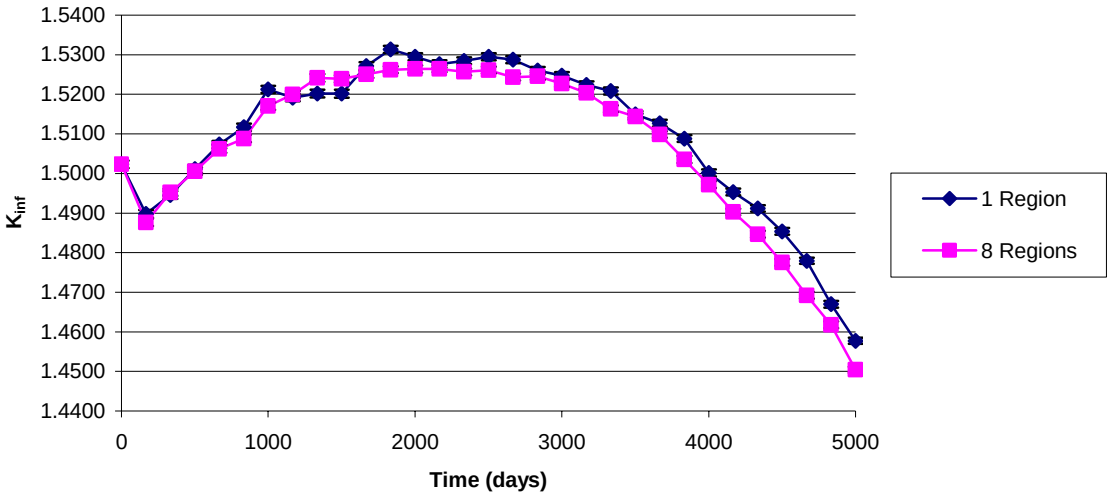

Fig. 24. k_{inf} versus time for pin cell with 1 fuel region and 8 fuel regions.

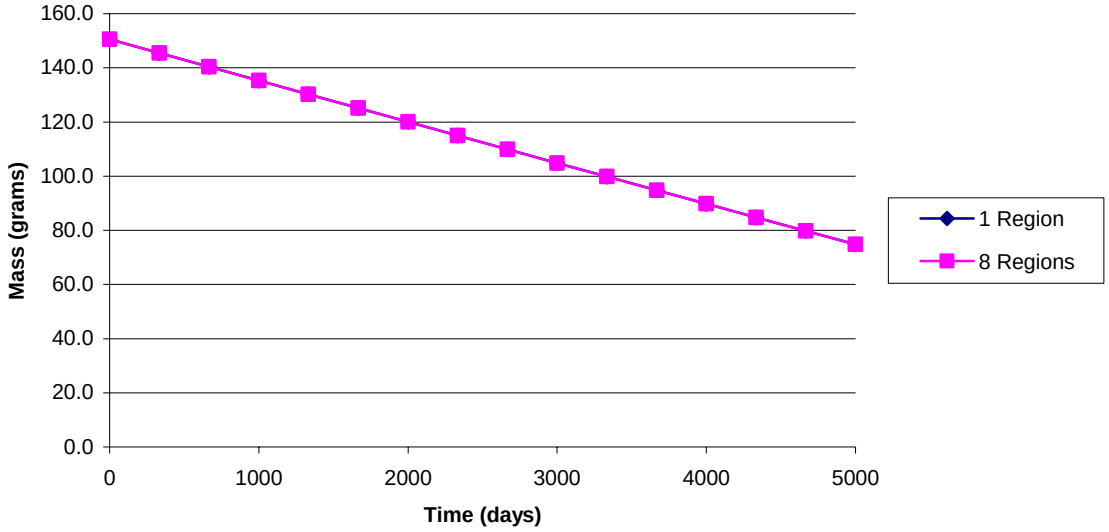

Fig. 25. U-235 mass versus time for pin cell with 1 fuel region and 8 fuel regions.

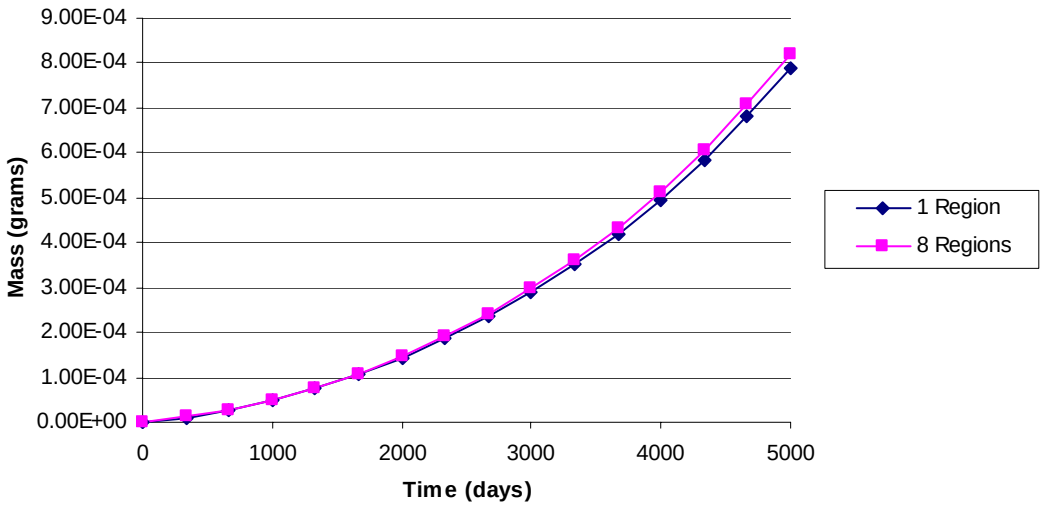

Fig. 26. U-238 mass versus time for pin cell with 1 fuel region and 8 fuel regions.

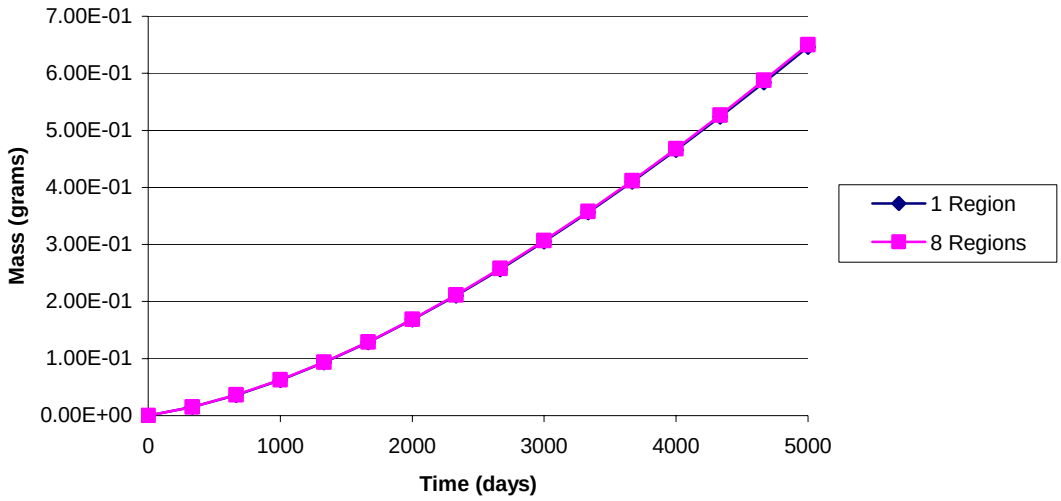

Fig. 27. Np-237 mass versus time for pin cell with 1 fuel region and 8 fuel regions.

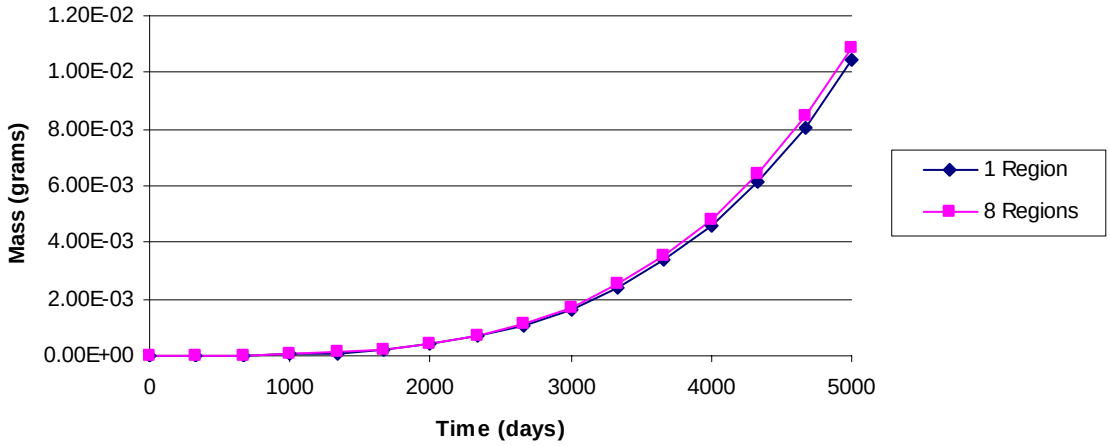

Fig. 28. Pu-239 mass versus time for pin cell with 1 fuel region and 8 fuel regions.

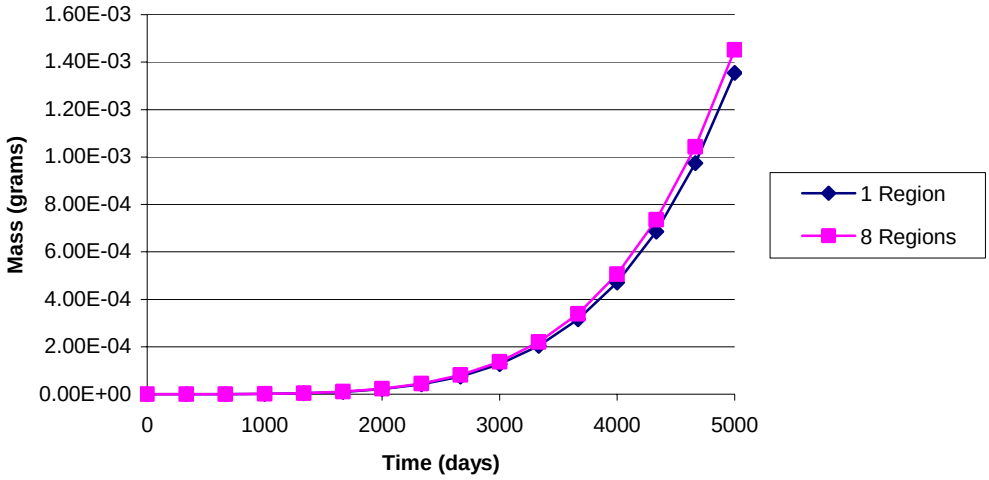

Fig. 29. Pu-240 mass versus time for pin cell with 1 fuel region and 8 fuel regions.

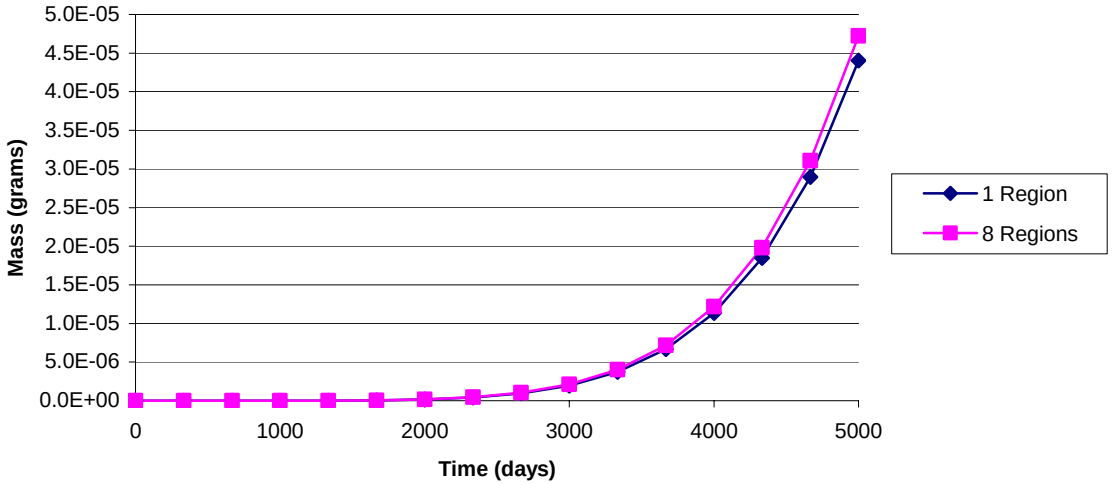

Fig. 30. Am-241 mass versus time for pin cell with 1 fuel region and 8 fuel regions.

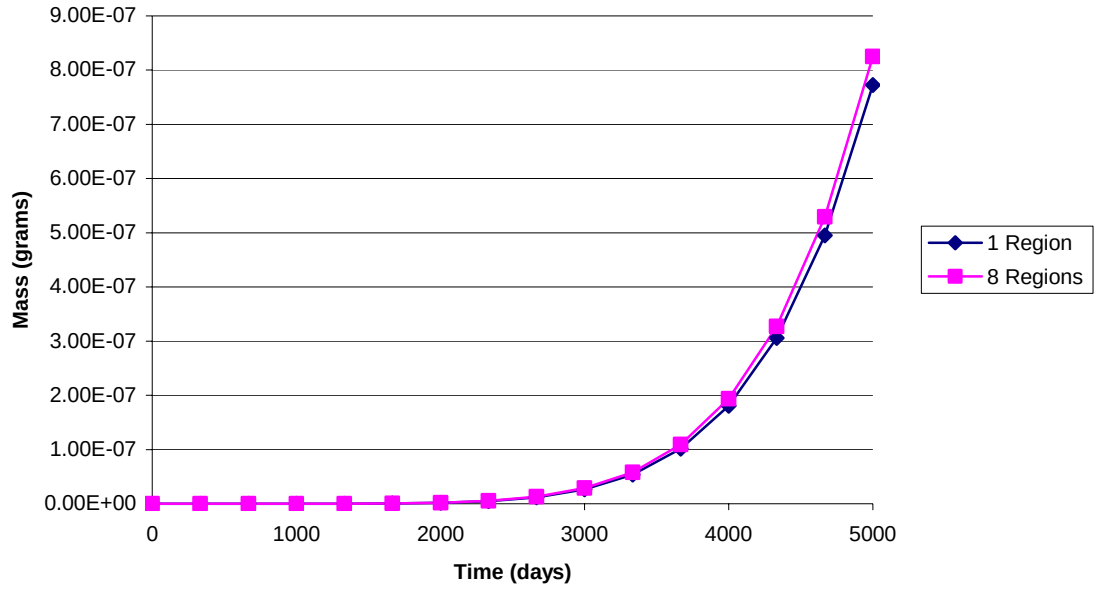

Fig. 31. Am-242 mass versus time for pin cell with 1 fuel region and 8 fuel regions.

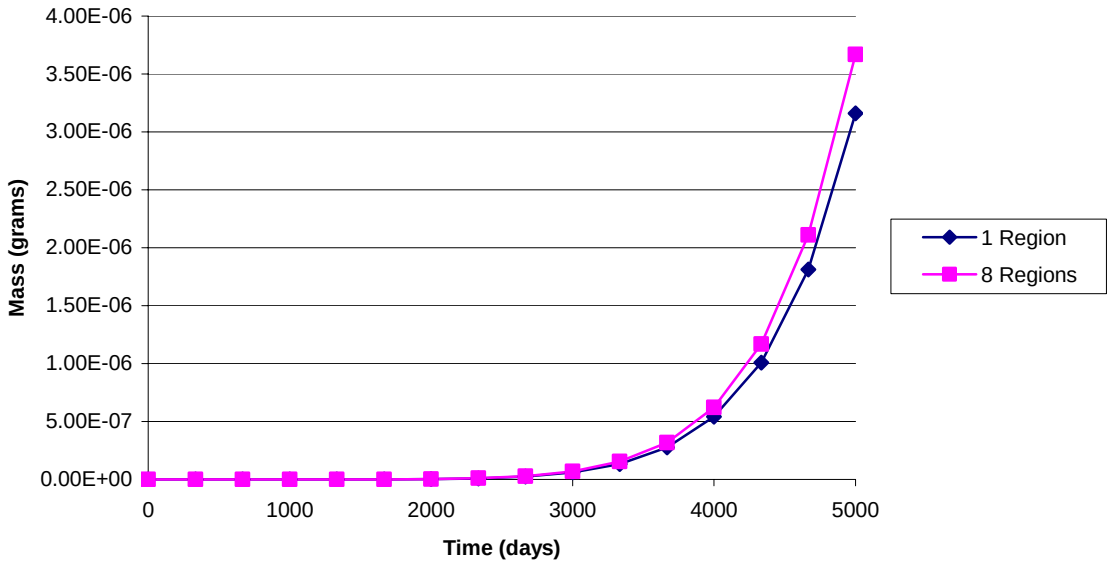

Fig. 32. Am-243 mass versus time for pin cell with 1 fuel region and 8 fuel regions.

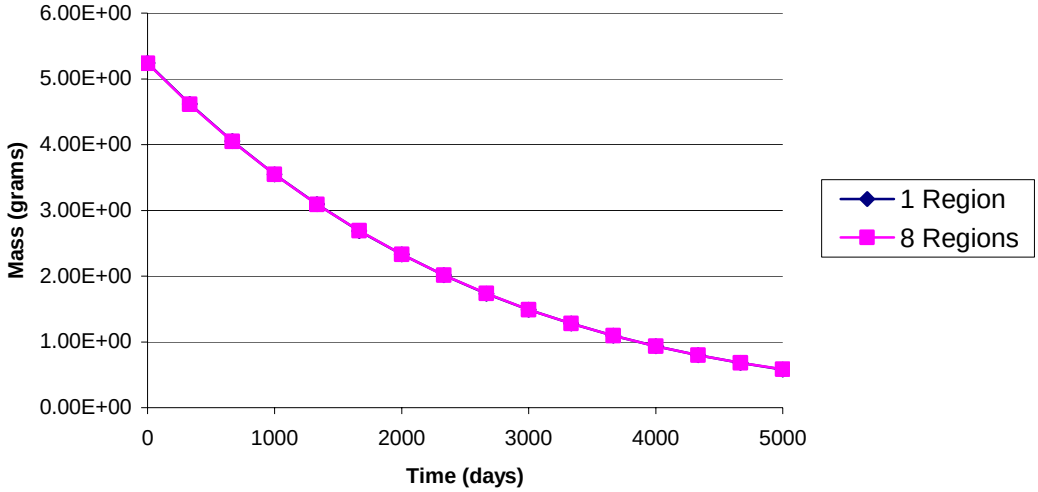

Fig. 33. Er-167 mass versus time for pin cell with 1 fuel region and 8 fuel regions.

III.C. FLIP to LEU Fuel Comparison

Two full core MCNP input decks were written for the NSCR. One core consisted of 100% FLIP fuel and the other consisted of 100% 30/20 fuel. Monteburns was used to burn each of these reactor cores to determine the criticality as a function of time to determine the total possible operational time. It was assumed in this simulation that no fuel shuffling was performed. Thus, we have acquired a conservative estimate of the fuel lifetime. Various isotopes of interest were tabulated as well. These simulations were performed with and without a thermal column in place in the MCNP deck. A constant power of 1MW was used during the simulation.

Figure 34 contains the Monteburns calculated k_{eff} versus burnup for the FLIP and 30/20 fuels with the reactor away from the thermal column. Based off of these results the FLIP fuel has a core lifetime of 3500 MWd which agrees well with previous estimates.[15] Here, lifetime is assumed to be the amount of time the criticality is above one. According to these calculations the 30/20 fueled core has a slightly longer lifetime than the FLIP fuel (estimated 3700 MWd). Previous estimates of 30/20 core lifetime were 3000 MWd.[15] These simulations suggest a slightly higher core lifetime for the 30/20 fueled core.

The estimated burnup for the NSCR is approximately 198000 MW-days/TU. Given the amount of uranium in the FLIP fuel this equates to 3144 MWd. The Monteburns calculation for FLIP fuel suggests that the fuel will last for 3500 MWd as seen in Fig. 34. Since the FLIP fuel at the NSCR is nearly completely burned, there is confidence that the Monteburns calculation does an adequate job of predicting the lifetime of the fuels.

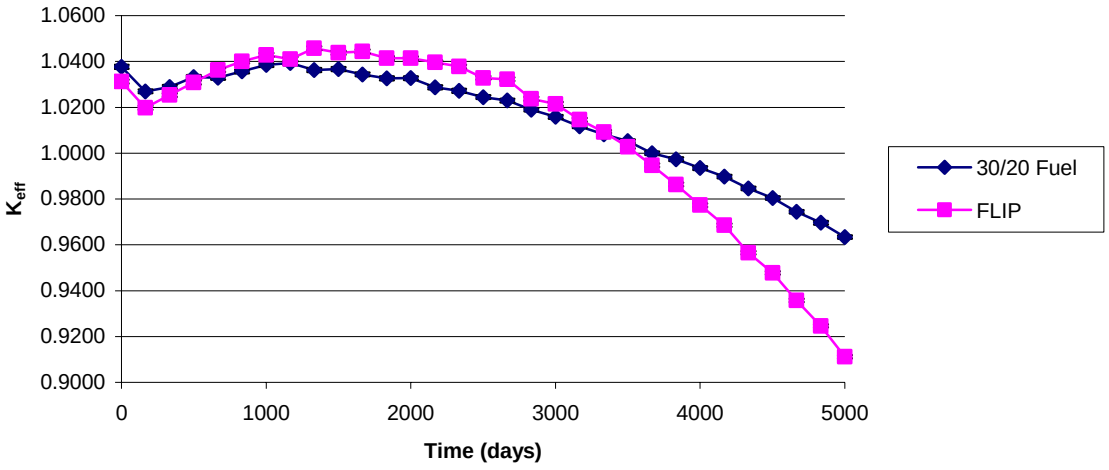

Fig. 34. k_{eff} versus time for the NSCR with FLIP and 30/20 fuel with no thermal column.

Figure 35 shows the Monteburns calculated k_{eff} versus core burnup for the FLIP and 30/20 fueled cores with the reactor against the thermal column. It is interesting to note that the addition of the thermal column increases the core lifetime by approximately 1000 MWd for the 30/20 fuel but only by 500 MWd for the FLIP fuel. Thus, with operation against the thermal column the 30/20 fuel significantly out performs the FLIP fuel.

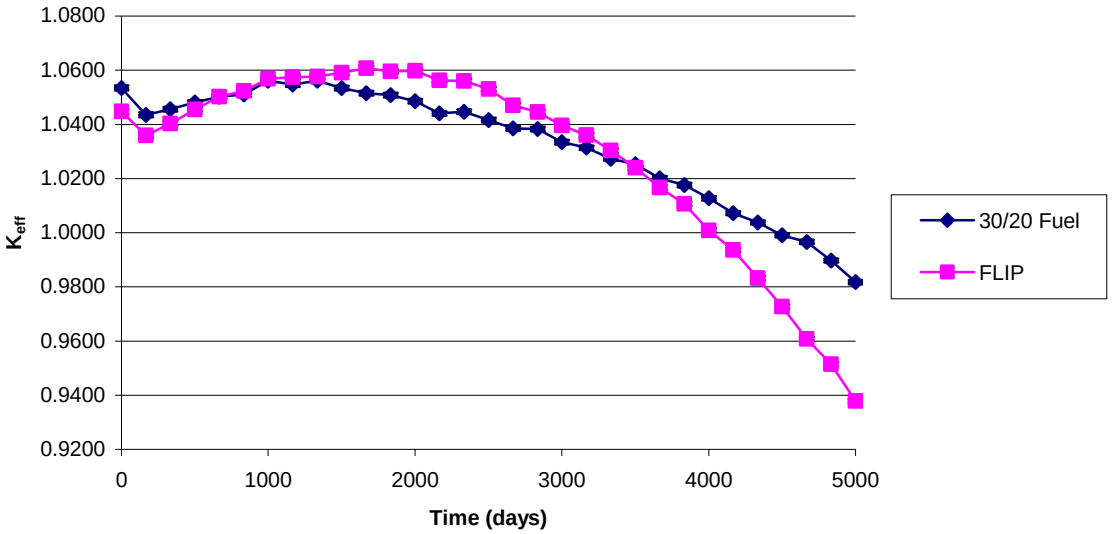

Fig. 35. k_{eff} versus time for the NSCR with FLIP and 30/20 fuel with thermal column.

The isotopic results are seen below in the figures on pages 53-59. Additional figures are found in Appendix B. The same graphs were generated for the simulation with a thermal column present. There is however little difference in the mass of each isotope produced and is therefore not included. An analysis of each plot is described below.

From Fig. 36 one will notice a greater mass of U-235 is present in the 30/20 fuel. Both fuels have a fairly linear decrease in mass over time and have nearly the same slope. Therefore, the depletion rate is nearly the same. From the previous analysis of the criticality versus time, the conclusion made was a longer lifetime could be expected

for the 30/20 fuel. The fact that there is more fissile material at the start of operation helps explain this conclusion.

Since the enrichment is less in the 30/20 fuel, there is considerably more U-238 (Fig. 37). Again, approximately the same depletion rates are seen for this isotope. Np-237 is created in the reactor by U-235 capturing a neutron to become U-236. U-236 then captures another neutron to become U-237. U-237 undergoes beta minus decay to become Np-237. Since the 30/20 fuel has more U-235 atoms than the FLIP fuel, it is expected that this new fuel will create more Np-237 (Fig. 38). The production rates of Np-237 are similar in both fuels. This is expected due to the similar depletion rates of U-235.

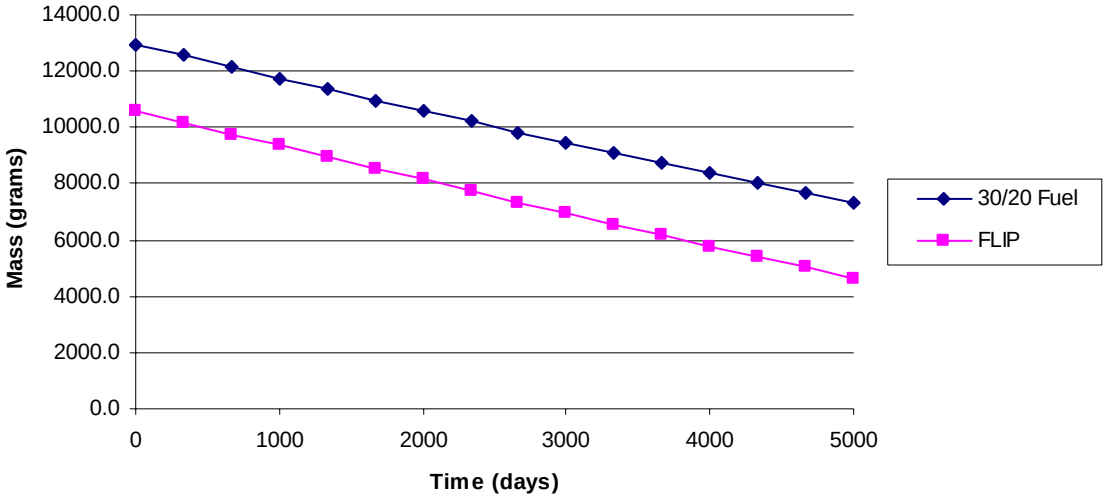

Fig. 36. U-235 mass versus time for the NSCR with FLIP and 30/20 fuel with no thermal column.

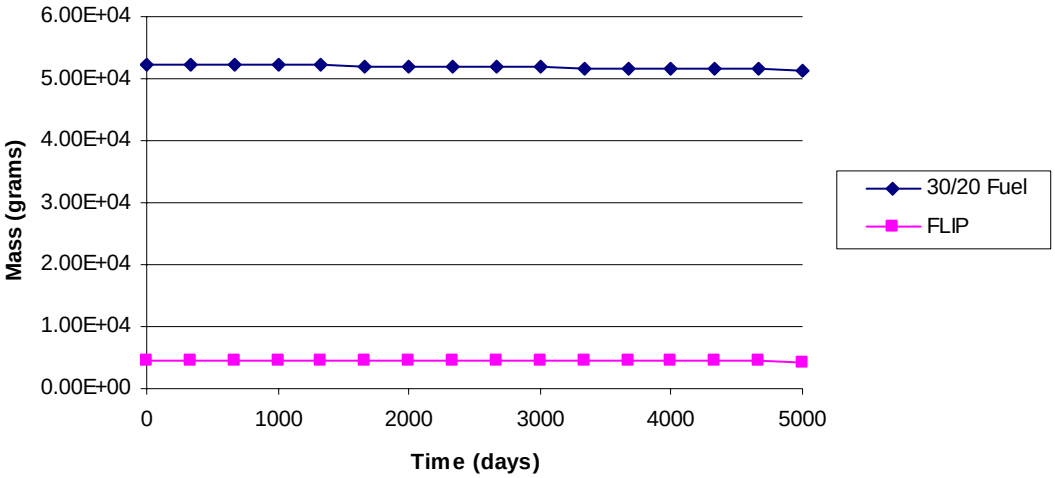

Fig. 37. U-238 mass versus time for the NSCR with FLIP and 30/20 fuel with no thermal column.

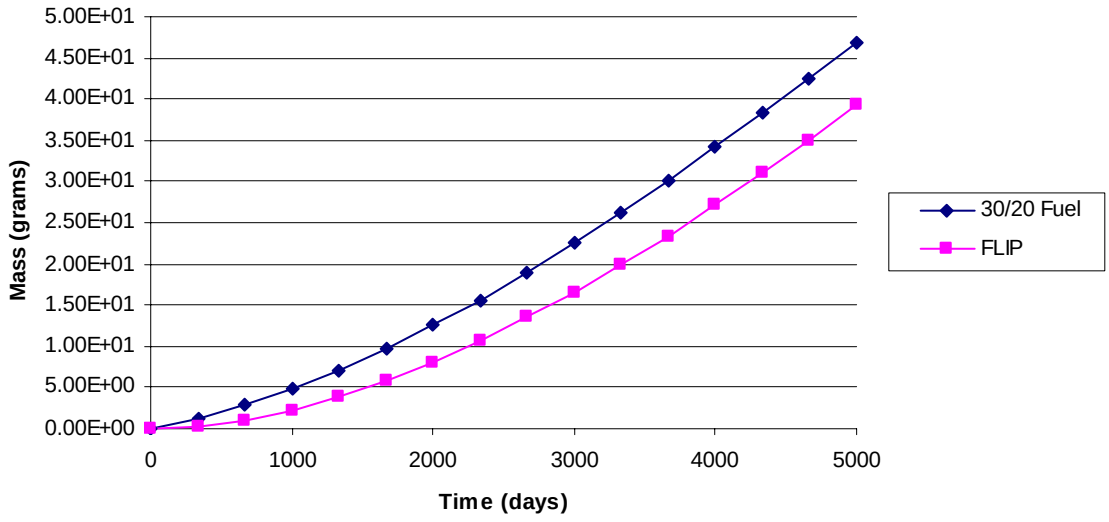

Fig. 38. Np-237 mass versus time for the NSCR with FLIP and 30/20 fuel with no thermal column.

Figs. 39 and 40 show the production of Pu-239 and Pu-240 in the reactor. Pu-239 is produced when U-238 captures a neutron to become U-239. U-239 beta minus decays into Np-239 and then Np-239 beta minus decays into Pu-239. Pu-239 can then capture a neutron to become Pu-240. The 30/20 fuel has a considerable higher amount of U-238. Therefore, more plutonium is produced with the new fuel. Pu-239 is also a fissile material. As the reactor operates, some of the power will come from fissions of Pu-239. This explains the concave curve in Fig. 39. This also helps explain the longer lifetime that is achieved with the 30/20 fuel.

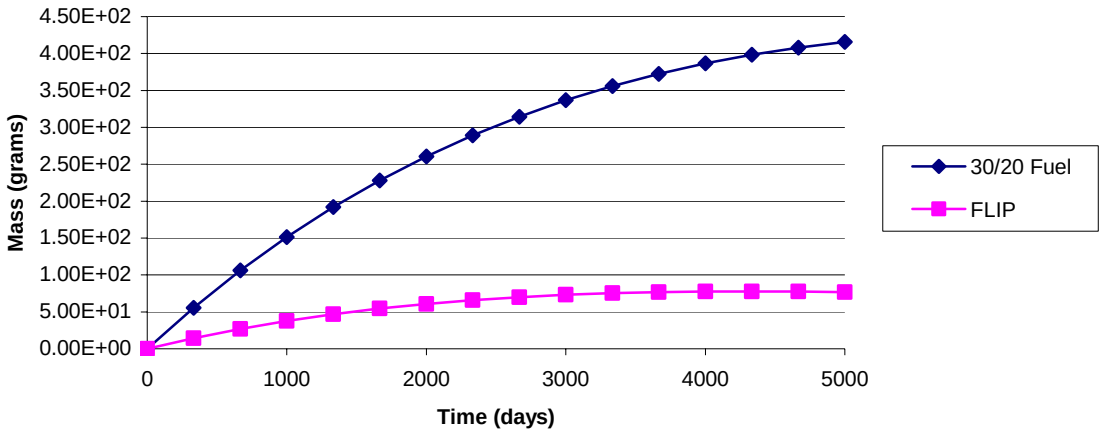

Fig. 39. Pu-239 mass versus time for the NSCR with FLIP and 30/20 fuel with no thermal column.

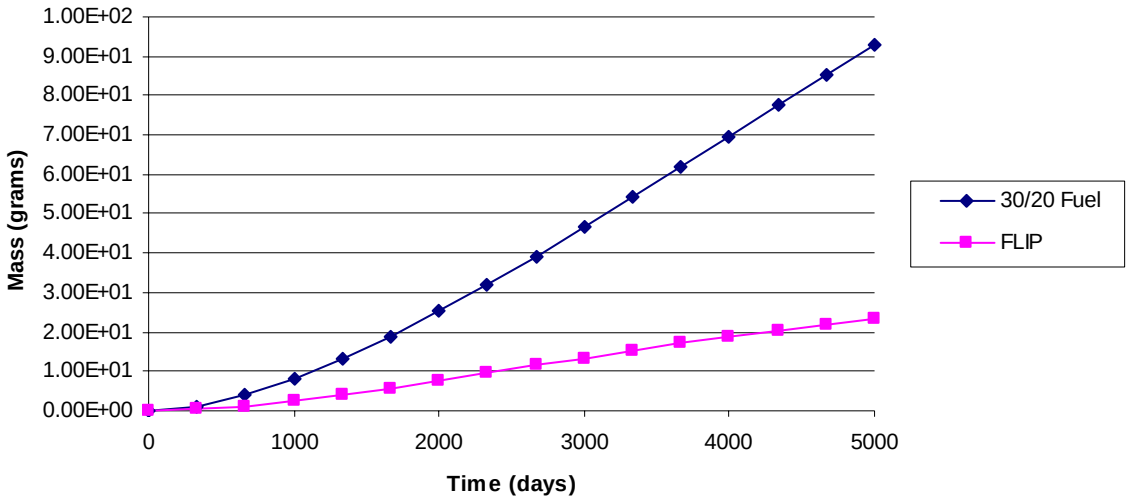

Fig. 40. Pu-240 mass versus time for the NSCR with FLIP and 30/20 fuel with no thermal column.

Am-241 is produced when Pu-240 captures a neutron to become Pu-241. Pu-241 then beta minus decays to produce Am-241. More U-238 in the 30/20 fuel leads to more plutonium which leads to more americium as seen in Figs. 41-43. Am-241 can capture a neutron to become Am-242 and Am-242 can capture a neutron to become Am-243. It is interesting to note that there is considerably more Am-243 than Am-242. This is because Am-242 is in a meta-stable state with a half-life of only 16 hours.

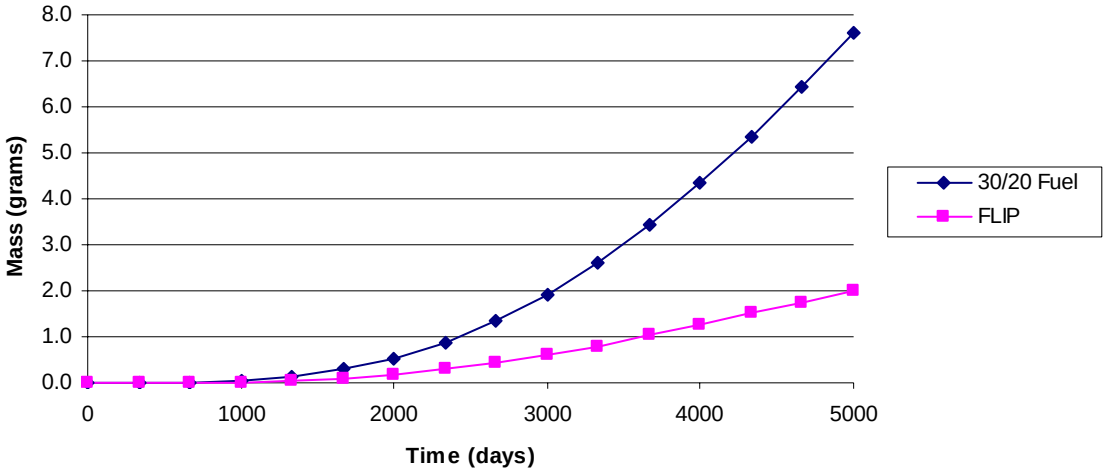

Fig. 41. Am-241 mass versus time for the NSCR with FLIP and 30/20 fuel with no thermal column.

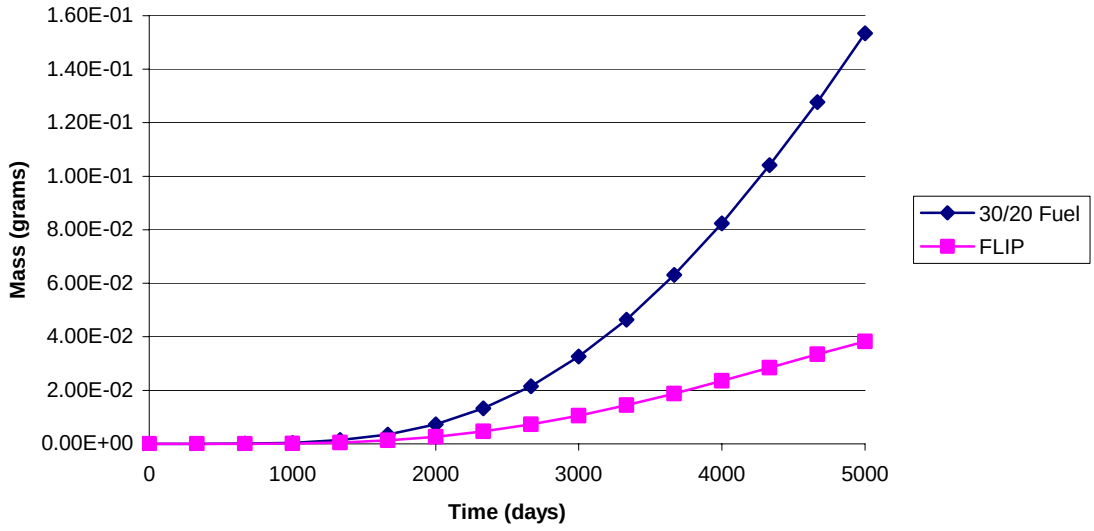

Fig. 42. Am-242 mass versus time for the NSCR with FLIP and 30/20 fuel with no thermal column.

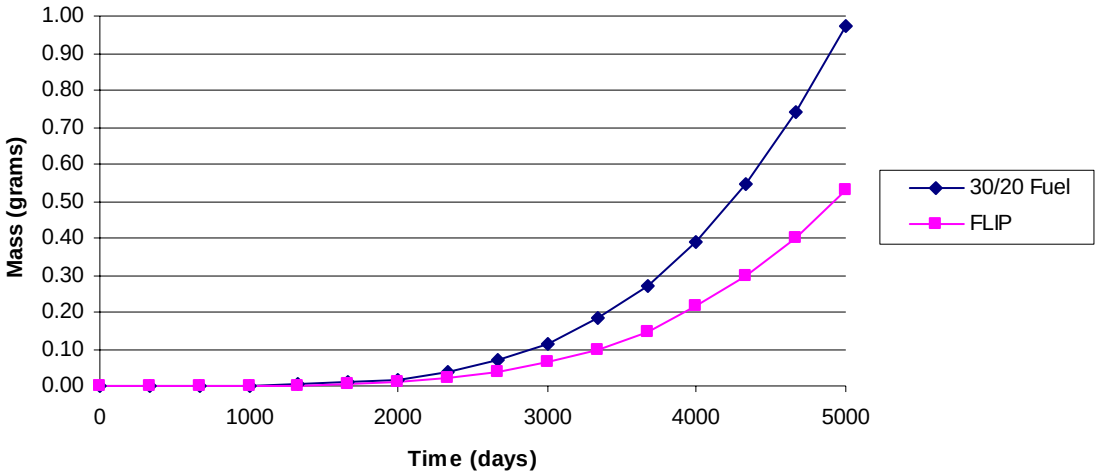

Fig. 43. Am-243 mass versus time for the NSCR with FLIP and 30/20 fuel with no thermal column.

Fig. 44 shows the Er-167 plot. As expected the amount of Er-167 decreases with time. The FLIP fuel has a natural erbium content of 1.5 wt% while the 30/20 fuel has a content of 0.9 wt%. It is interesting to note that the two fuels approach the same value in mass of Er-167 at a high burnup.

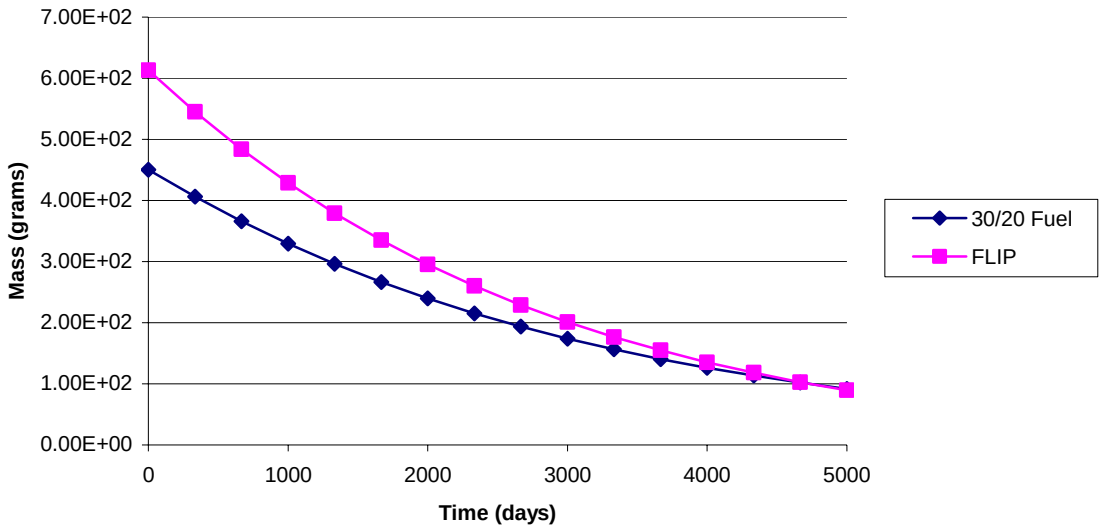

Fig. 44. Er-167 mass versus time for the NSCR with FLIP and 30/20 fuel with no thermal column.

The performance of this 30/20 fuel is quite good in comparison to the current FLIP fuel. A higher fuel lifetime can be achieved in the 30/20 fuel because there is more U-235 and U-238 atoms present. The U-235 is the main source of power in the reactor, but U-238 contributes as well since it produces Pu-239. The drawback to this higher performance is that this new fuel will produce more of the longer lived minor actinides (Np-237, Am-241, and Am-243).

III.D. Control Rod Worths

The worths of the control rods were also calculated. This was done by using MCNP to calculate the criticality of the reactor in several different configurations with and without the thermal column present. Tables IX and X show the results. In either case there is approximately $13-$14 worth of reactivity in the control rods. The last line in Tables IX and X shows the results for a simulation of the reactor in which the regulating rod and the shim safety rod with the most worth (shim safety rod #4, refer to Fig. 6 for location) are fully withdrawn from the core while the remaining four rods are inserted. This is the procedure used to calculate the minimum shutdown margin.[16] The required shutdown margin is -$0.25. In either simulation with and without the thermal column present, the shutdown margin is much more negative than -$0.25. This will provide enough negative reactivity to safely control the reactor.

The Safety Analysis Report for the NSCR also states that the maximum excess reactivity must be below 5.5% dk/k. This means the maximum value k_{eff} may be is 1.055. As one can see from Table X this requirement is met.

TABLE IX

Control Rod Worths without the Thermal Column

	k_{eff}	delta k/k	$
All Rods out	1.03833 +/- 0.000716		
Tran In	1.01199 +/- 0.000698	-0.0254 +/- 0.000964	-3.63 +/- 0.138
RR In	1.03171 +/- 0.000712	-0.0064 +/- 0.000973	-0.91 +/- 0.139
SS 1 In	1.01923 +/- 0.000744	-0.0184 +/- 0.000995	-2.63 +/- 0.142
SS 2 In	1.0253 +/- 0.000738	-0.0125 +/- 0.000991	-1.79 +/- 0.142
SS 3 In	1.02134 +/- 0.000684	-0.0164 +/- 0.000954	-2.34 +/- 0.136
SS 4 In	1.01068 +/- 0.000677	-0.0266 +/- 0.000950	-3.80 +/- 0.136
Total Worth		-0.1057 +/- 0.002379	-15.10 +/- 0.340
SS 4 and RR out	0.96703 +/- 0.000658	-0.0330 +/- 0.000658	-4.71 +/- 0.094

TABLE X

Control Rod Worths with the Thermal Column

	k_{eff}	delta k/k	$
All Rods out	1.05363 +/- 0.000727		
Tran In	1.03138 +/- 0.000660	-0.0211 +/- 0.000925	-3.01 +/- 0.132
RR In	1.04241 +/- 0.000730	-0.0106 +/- 0.000971	-1.51 +/- 0.139
SS 1 In	1.03469 +/- 0.000683	-0.0180 +/- 0.000939	-2.57 +/- 0.134
SS 2 In	1.04323 +/- 0.000709	-0.0099 +/- 0.000957	-1.41 +/- 0.137
SS 3 In	1.03998 +/- 0.000687	-0.0130 +/- 0.000942	-1.86 +/- 0.135
SS 4 In	1.02639 +/- 0.000677	-0.0259 +/- 0.000936	-3.70 +/- 0.134
Total Worth		-0.0984 +/- 0.0023	-14.06 +/- 0.329
SS 4 and RR out	0.99352 +/- 0.000665	-0.0065 +/- 0.000665	-0.93 +/- 0.095

The results from Tables IX and X were obtained by assuming the reactor was operating at normal operating temperatures (600K). The minimum shutdown margin and maximum excess reactivity requirements need to be met while the reactor is in a cold condition (300K). These technical specifications were not met when the reactor was in a configuration shown in Fig. 9. Fuel rods were removed from the core until these requirements were met. A configuration that will meet these requirements is shown in Fig. 45. Table XI shows the results for this configuration.

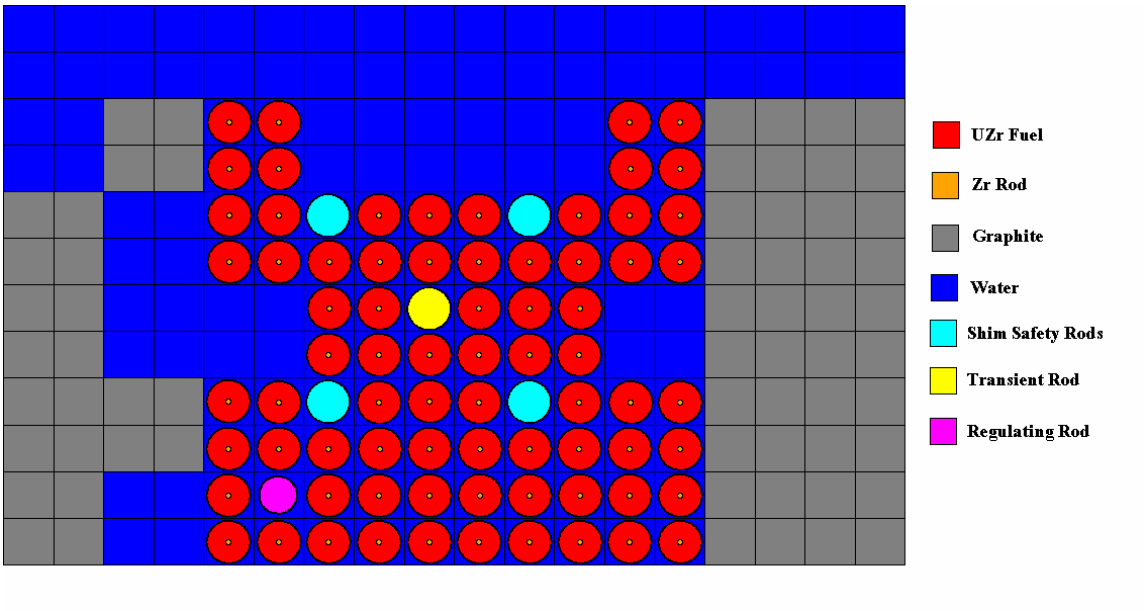

Fig. 45. Initial core configuration.

TABLE XI

Results for Initial Core Configuration

	keff	delta k/k	$
All Rods Out	1.04658 +/- 0.000691	0.0445 +/- 0.000661	6.36 +/- 0.094
All Rods In	0.94536 +/- 0.000614	-0.0578 +/- 0.000651	-8.26 +/- 0.093
SS 4 and RR Out	0.99427 +/- 0.000736	-0.0058 +/- 0.000740	-0.82 +/- 0.106

IV THERMAL ANLAYSIS

A steady-state thermal hydraulic analysis was performed to determine the temperature profile of the fuel as a function of time. To do this, an MCNP input deck was created that divided the reactor core into three regions as seen in Fig. 46. Each of these regions were divided into five axial sections. Each region and axial section was burned as a separate material. Therefore, there were 15 total materials burned using Monteburns. Monteburns burned this core over the course of the reactor's lifetime (3500 days). The MCNP and Monteburns input decks for these simulations can be found in Appendix C.

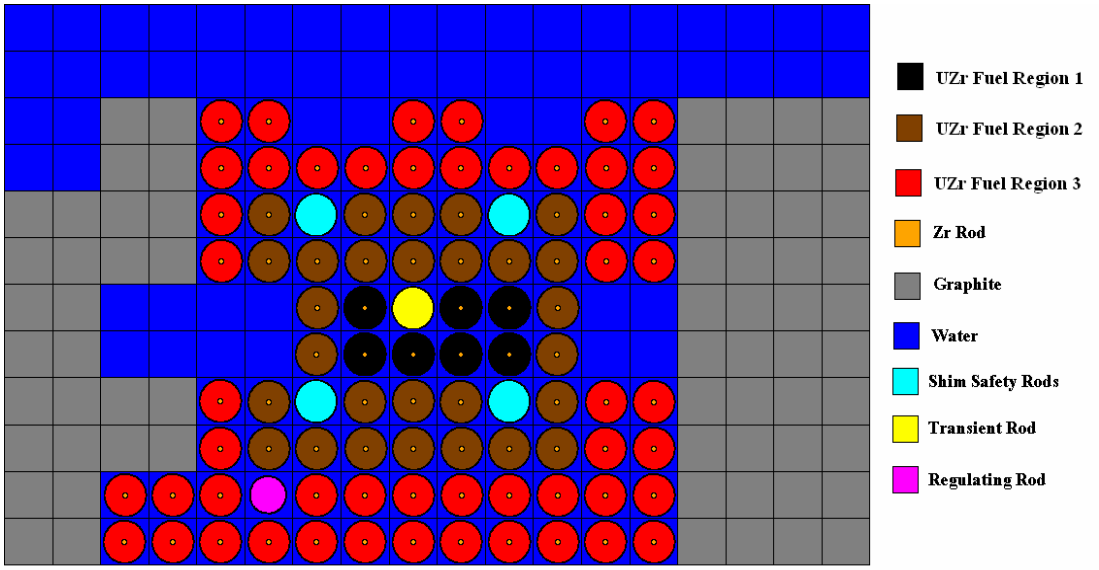

Fig. 46. Three region NSCR MCNP model.

After each burn step, Monteburns will create a MCNP deck with new isotopics for the desired materials to be burned. A new MCNP deck was written using the new isotopics. In this input deck, the same three regions were used but this time the fuel was divided into 15 axial locations instead of 5. The control rods were adjusted until a k_{eff} of 1.000 +/-0.0005 was achieved. Then an F7 tally was used to measure fission energy deposition in each of the 15 axial locations in all 86 fuel pins (1290 total tallies). A flow chart is provided to show the necessary process to achieve the desired results used in the input for the code PARET (Fig.47). Fig. 48 is provided to clarify the axial subzones created for each zone in each region. The MCNP input deck with the tallies is found in Appendix C. This analysis was performed at several burn steps. These steps were 0, 30, 300, 600, 1000, 2000, 2666, 3166, and 3500 days. A constant power of 1MW was assumed during the Monteburns simulation. This entire process was performed for the reactor core with and without the thermal column present.

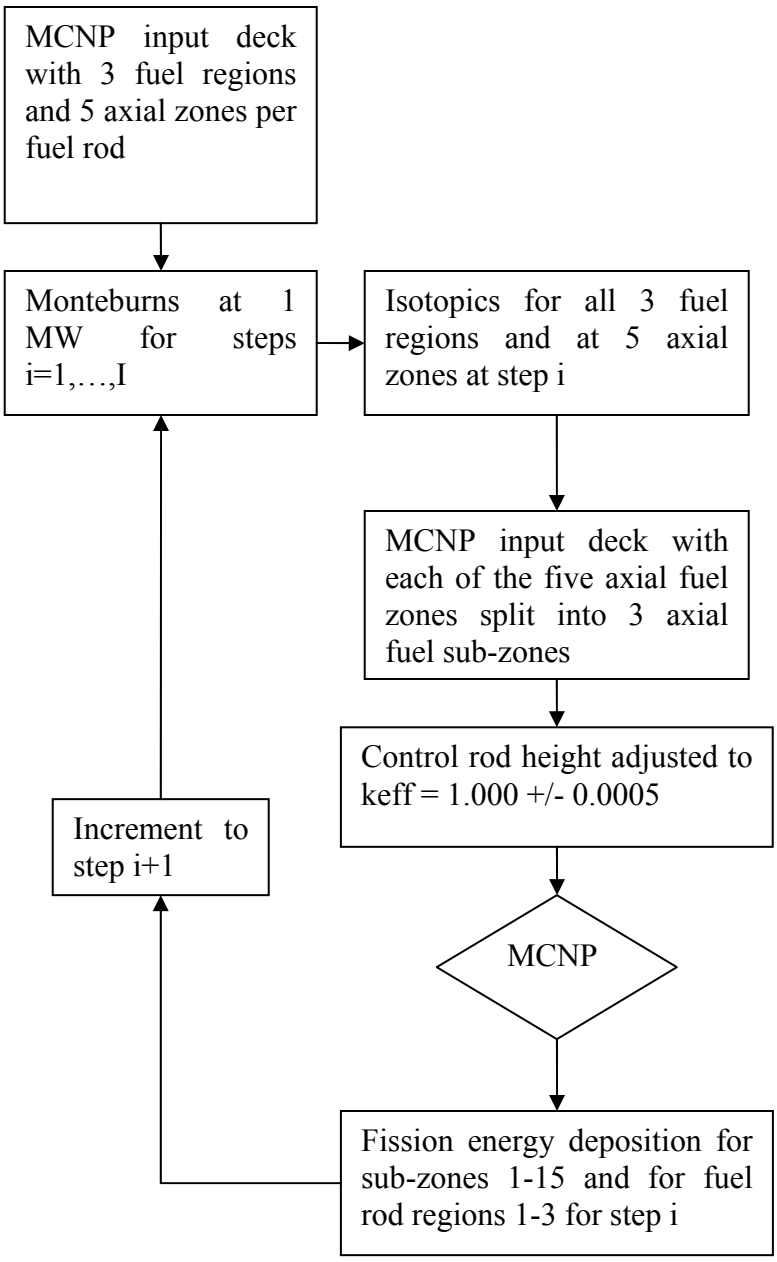

Fig. 47. Flowchart for determining input for PARET.

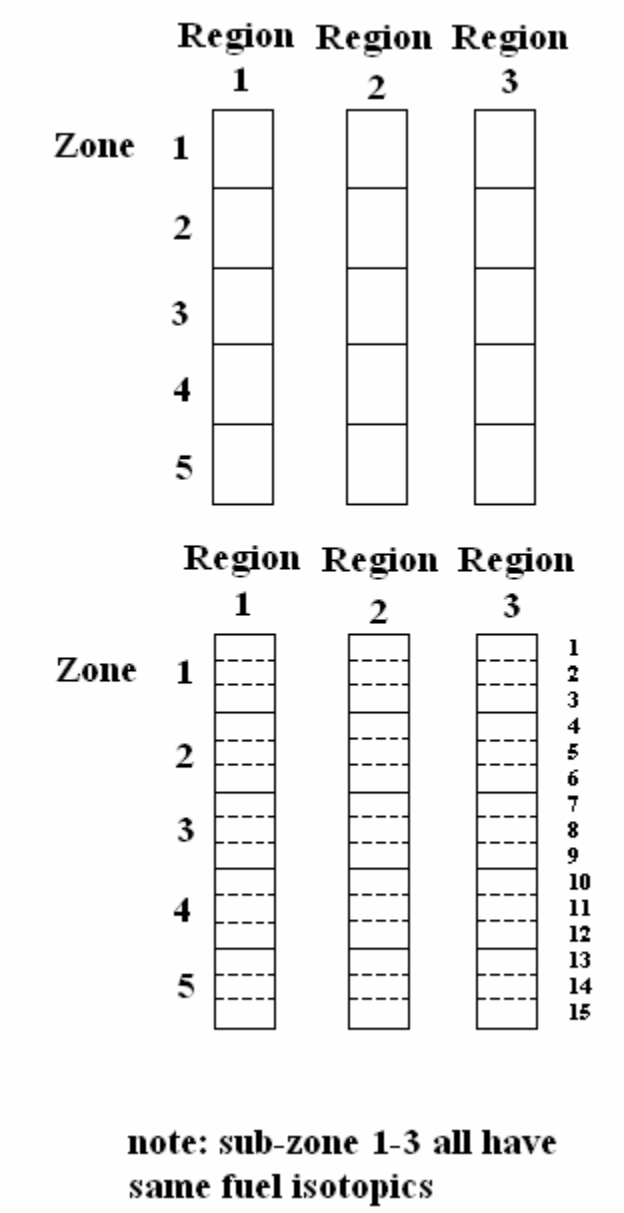

Fig. 48. Sub-zone description for Monteburns and MCNP input decks.

An F7 tally was used in MCNP to acquire the power profile. The F7 tally is a track length estimate of the fission energy deposition. Like most tallies in MCNP, the output of this tally is normalized per source particle. Therefore, the units are in MeV/g-source particle. The F7 tally includes the heating due to gamma rays in the fuel. In this calculation the gamma rays are assumed to deposit their energy locally in the fuel. This tally gives an accurate description of the heating of the fuel as long as photons from other sources are neglected. It was therefore decided that this tally would be appropriate to use for this simulation.

To model the power profile in PARET, the value assigned to each axial zone is the energy in that zone divided by the average zone energy. To do this, first an average of all F7 tallies were made. This means the axial energy for all 86 fuel pins each with 15 axial zones were averaged (1290 total tallies). Then each region was analyzed. For example, region 1 consists of seven fuel rods. For each axial location the energy was averaged among the seven fuel rods. Essentially an average channel was created to represent region 1. Each of these 15 energies was divided by the average axial zone energy found earlier to provide the proper input for PARET. PARET will calculate the fuel centerline, cladding, and coolant temperatures.

PARET requires a mass flow rate for these calculations. Since the reactor is cooled via natural convection a flow rate of 8.026 kg/s was used. This agrees with Brad Rearden's thesis[2] as well the measured mass flow rate found in the University of Texas at Austin's TRIGA reactor.[6] PARET also requires the thermal conductivity and heat

capacity for the fuel, gap, and cladding. The thermal conductivity was taken to be a constant with temperature. These values were 18.0 W/mK, 0.199 W/mK, and 16.8 W/mK for the fuel, gap, and cladding, respectively.[2] The value for the thermal conductivity in the fuel is independent of the uranium content for the range of weight percents between 8.5% and 45%.[15] These values also comply with the PARET sample input deck given with the manual.[5] The heat capacity for gap and cladding are 66.634 J/m^{3o}C and 3.975E6 J/m^{3o}C respectively. These values are also from the sample PARET input deck. The procedure for finding the heat capacity is the same used by Brad Rearden.[2] The heat capacities for $ZrH_{1.6}$ and uranium are found using Eqs. (3) and (4). The total heat capacity is found by applying the appropriate weight fractions seen in Eqs. (5) and (6). By multiplying by the density the final heat capacity used in PARET is found in Eq. (7). This is a similar value found for FLIP fuel.[2]

$$C_p(ZrH) = 0.7515T + 363.0938 \text{ J/kg}^{o}\text{C} \tag{3}$$

$$C_p(U) = 0.1305T + 109.4 \text{ J/kg}^{o}\text{C} \tag{4}$$

$$C_p(UZrH) = w(U)C_p(U) + w(ZrH)C_p(ZrH) \text{ J/kg}^{o}\text{C} \tag{5}$$

$$C_p(UZrH) = ((0.3)(C_p(U)) + (0.7)(C_p(ZrH)) \text{ J/kg}^{o}\text{C})\text{x}7183 \text{ kg/m}^3 \tag{6}$$

$$C_p(UZrH) = 0.4059E4T + 2.06E6 \text{ J/m}^{3o}\text{C} \tag{7}$$

The results are found in the figures on pages 71-82. Fig. 49 shows the fuel centerline temperatures in the hottest region, designated as region 1. The temperature profile remains quite consistent until a burnup of 2000 MWd is reached. After this burnup is reached, the temperature in the axial center of the fuel decreases significantly. This is more evident in Fig. 50. This is because neutrons distribute themselves in the core such that there are more in the axial center. This means that more of the fissile material (U-235) is depleted in the axial center. When this happens, more power must be supplied by the fuel in the top portion of the fuel since the power level is the same. Therefore, when the core is burned almost to the end of its life the temperature has a tendency to "flatten out" as seen in the curve of a burnup of 3500 MWd in Fig. 49. It is also interesting to note that the location of the highest temperature in the fuel rod tends to shift upward as a function of time. This is because the control rods were adjusted to achieve a criticality of one. As the fuel is depleted, positive reactivity insertion in the form of control rod withdrawal is needed to remain critical. This has a significant effect on region 1 since the control rods are in close proximity to these fuel rods. As the rods are withdrawn more fuel from the top portion of each fuel rod is exposed.

Another interesting aspect to note from Fig. 49 is that the temperature in the bottom most portion is larger than the next point. This is due to the fact that there are graphite reflectors above and below the fueled portion of each fuel rod. This is not seen in the top region in Fig. 49 because of the location of the control rods.

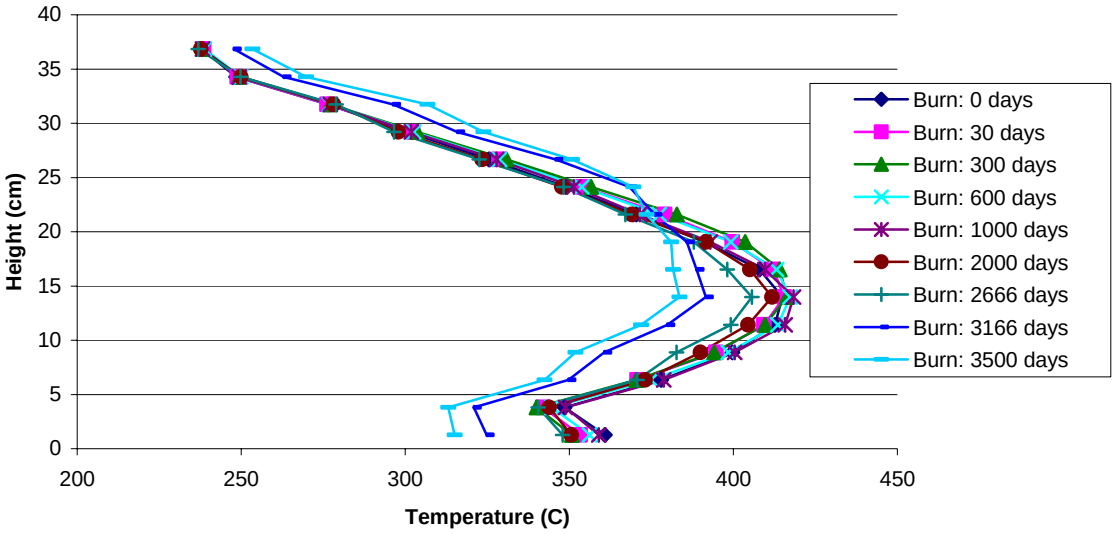

Fig. 49. Fuel centerline temperatures in region 1 without thermal column.

From Fig. 50 one can observe a steady rise in temperature until 1000 days. For the next 1000 days the temperature remains constant until suddenly it drops. When the reactor is in the beginning stages of operation, there is a production of plutonium. This plutonium provides additional fissile material that can provide power to the reactor. This means there is a positive reactivity insertion. To keep the criticality at one, control rods need to be inserted further. Therefore, less fuel is exposed to the neutron population. Since the overall power is constant the peak fuel temperature must rise. As mentioned earlier, when the core undergoes further burnup, the control rods need to be withdrawn and a flattening of the temperature profile is observed. Thus the peak fuel temperatures decrease after 2000 MWd as seen below.

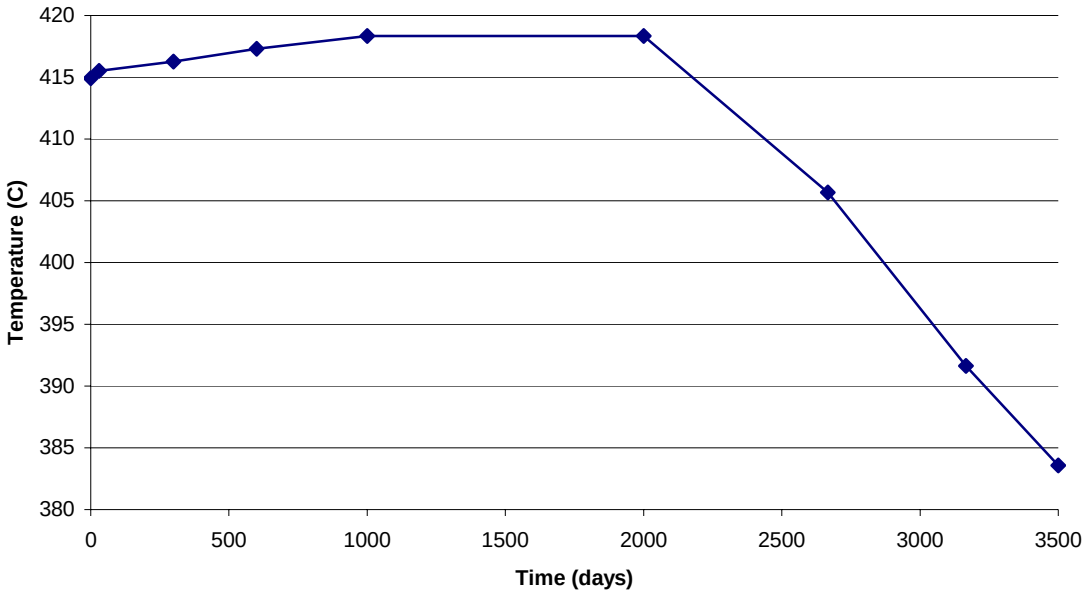

Fig. 50. Peak fuel temperatures in region 1 without thermal column.

Figs. 51 and 52 look similar to Figs. 49 and 50. Again the flattening of the temperature profile is observed for high burnups and the peak temperatures rise in the beginning of life, but then fall after 1000 days. The change in temperatures over time is not as drastic as in region 1 since this region is not as coupled to the control rods.

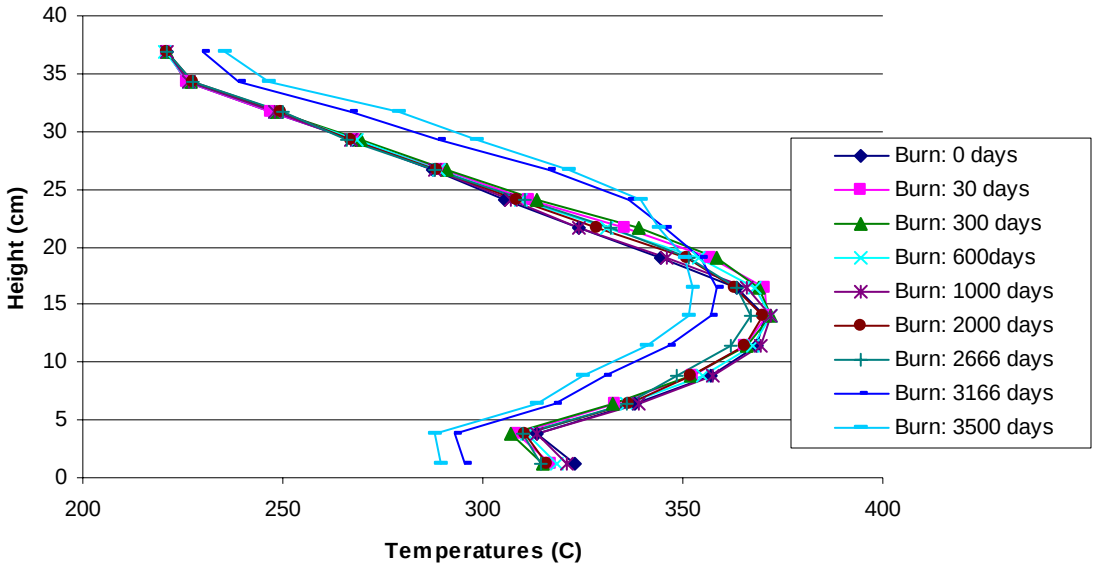

Fig. 51. Fuel centerline temperatures in region 2 without thermal column.

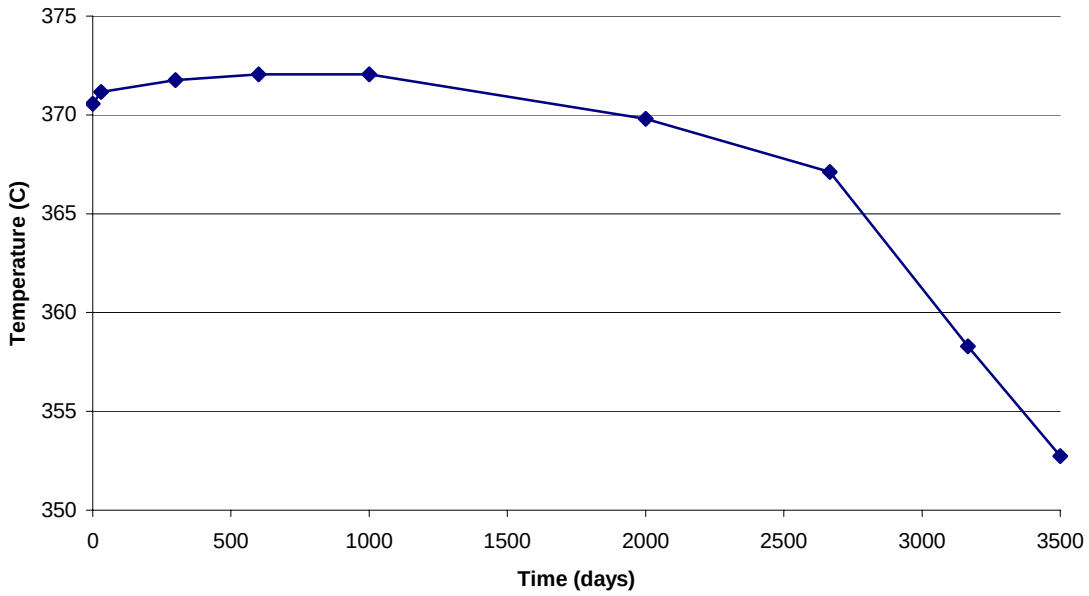

Fig. 52. Peak fuel temperatures in region 2 without thermal column.

Fig. 53 shows that region 3 behaves in a similar manner as regions 1 and 2. Since this region represents the fuel along the periphery of the reactor, the control rods have little effect on the neutron population here. This is also evident since the effects of the graphite reflectors on the top of the fueled region can be seen on the temperature profile in Fig. 53. This region does not see as large a neutron population as the other two regions. Therefore, more time is required for this region to deplete. This is seen by the fact that the peak temperatures do not significantly drop until a burnup of 3166 MWd as seen in Fig. 54. Fig. 54 still follows the basic shape as the other regions. Discrepancies are probably due to error associated with thermal hydraulic analysis.

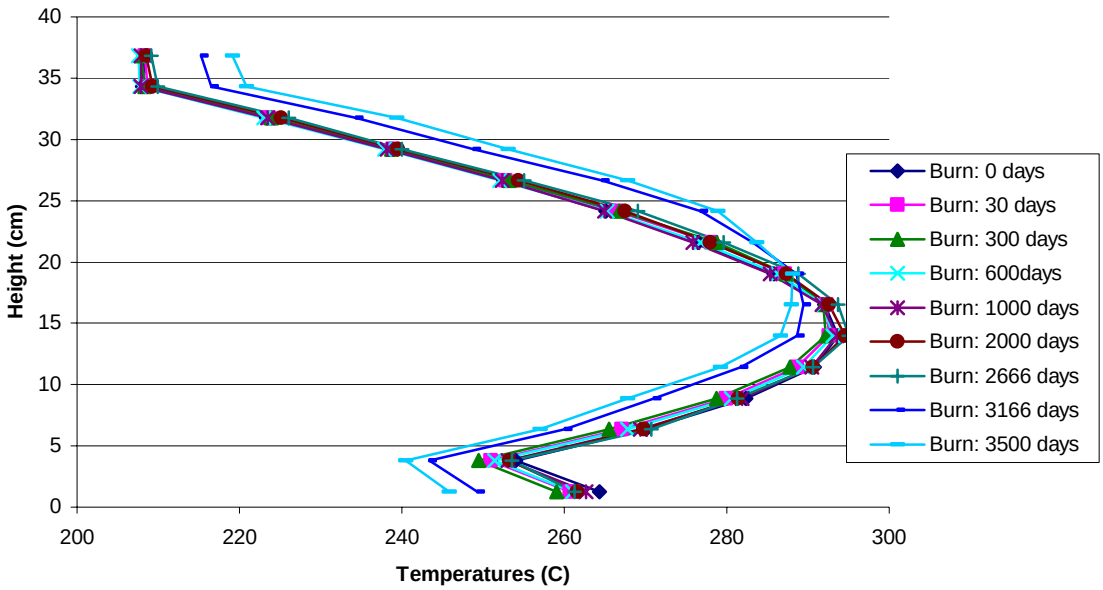

Fig. 53. Fuel centerline temperatures in region 3 without thermal column.

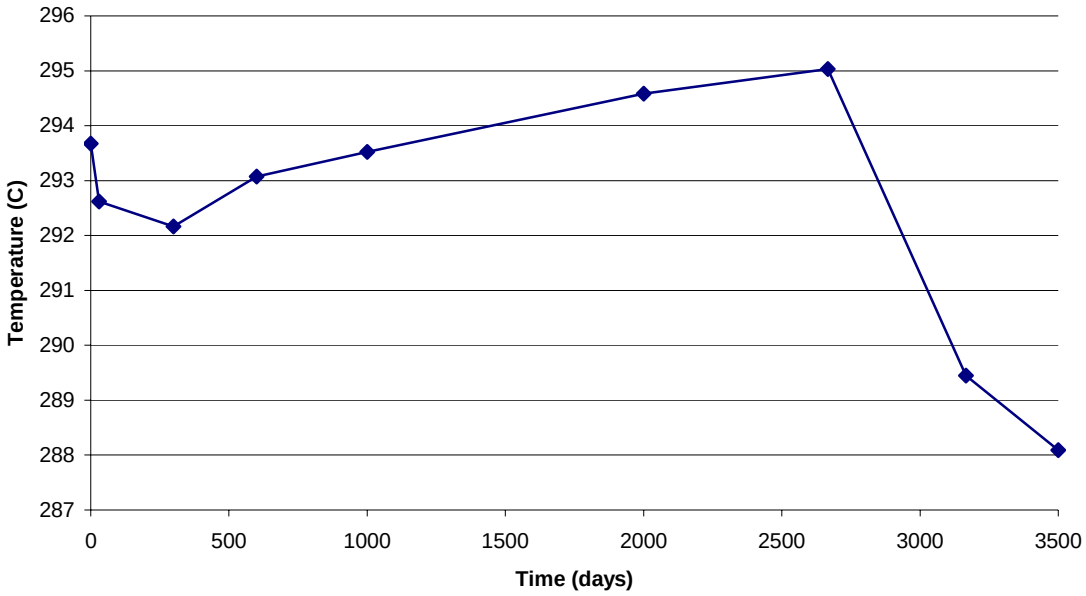

Fig. 54. Peak fuel temperatures in region 3 without thermal column.

An average region was also simulated. The shape of Figs. 55 and 56 are similar to the previous plots. The peak temperatures of 330^{o}C lies within the peak temperatures of 419^{o}C and 295^{o}C for regions 1 and 3 respectively.

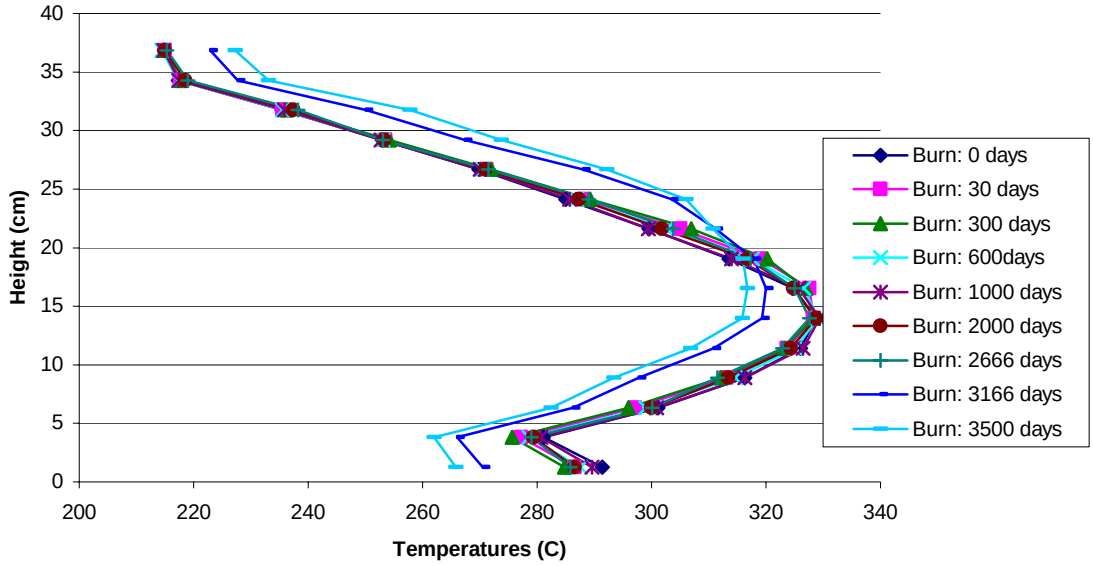

Fig. 55. Fuel centerline temperatures in average region without thermal column.

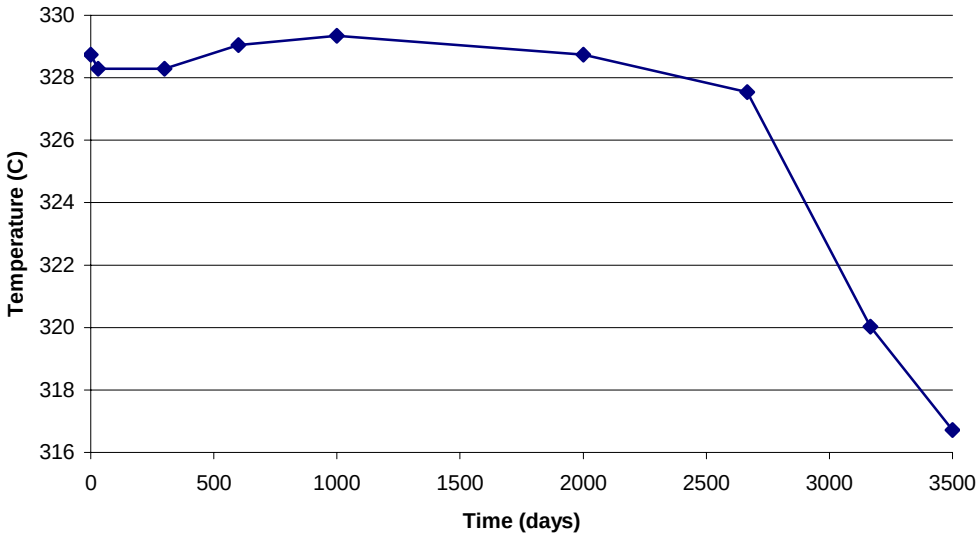

Fig. 56. Peak fuel temperatures in average region without thermal column.

The next sets of figures show the same temperature profiles as before except now a thermal column was used in the simulation. The thermal column acts like a large reflector for the entire east side of the reactor. This reflects more neutrons into the periphery of the core which inserts a positive reactivity. To keep the reactor critical, the rods are inserted more for these simulations. This insertion is not very large and has a minimal effect on the location of the peak temperature as seen with a comparison between Fig. 49 and Fig. 57. The peak temperature however drops from 419^{o}C to about 380^{o}C in region 1. This is because the thermal column introduces more neutrons to region 3 so more power can be delivered from this region, thus alleviating the temperatures in region 1. From a comparison between Figs. 51 and 59, the peak temperatures in region 2 with the thermal column present are lower (365^{o}C compared to 355^{o}C). Comparing Figs. 53 and 61 shows the peak temperature in region 3 is slightly higher with a thermal column present (293^{o}C to 300^{o}C). The peak temperature in the average region remains the same in either case at about 325^{o}C (Figs. 55 and 63).

It was found earlier in Section II that the addition of the thermal column will increase the core lifetime by approximately 1000 days for the 30/20 fuel. From the analysis of the core without the thermal column present, one can conclude that the "flattening out" effect is not seen until the fuel is nearly completely burned. This is why this effect is not as evident here. The temperatures in all regions are much more consistent. The addition of the thermal column also helps with the consistent fuel temperatures since the neutron population will flatten with respect to the radial direction

of the core. Figs. 58, 60, 62, and 64 do not take on the same shape as the previous analysis. This is again probably due to the lack of error assessment in the thermal hydraulic code. Also the differences in temperatures as a function of time are not nearly as great as in the analysis without the thermal column present.

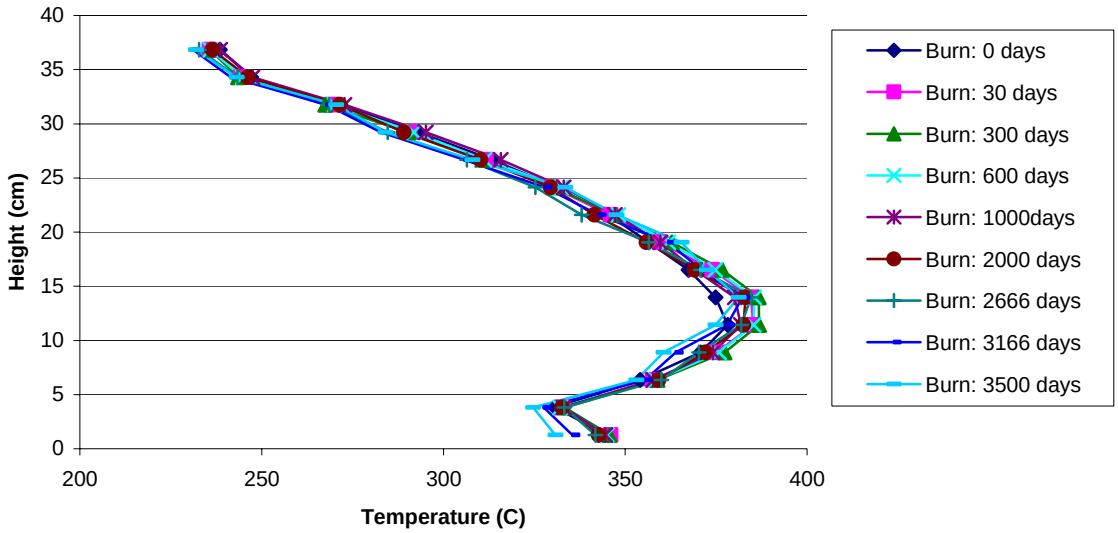

Fig. 57. Fuel centerline temperatures in region 1 with thermal column.

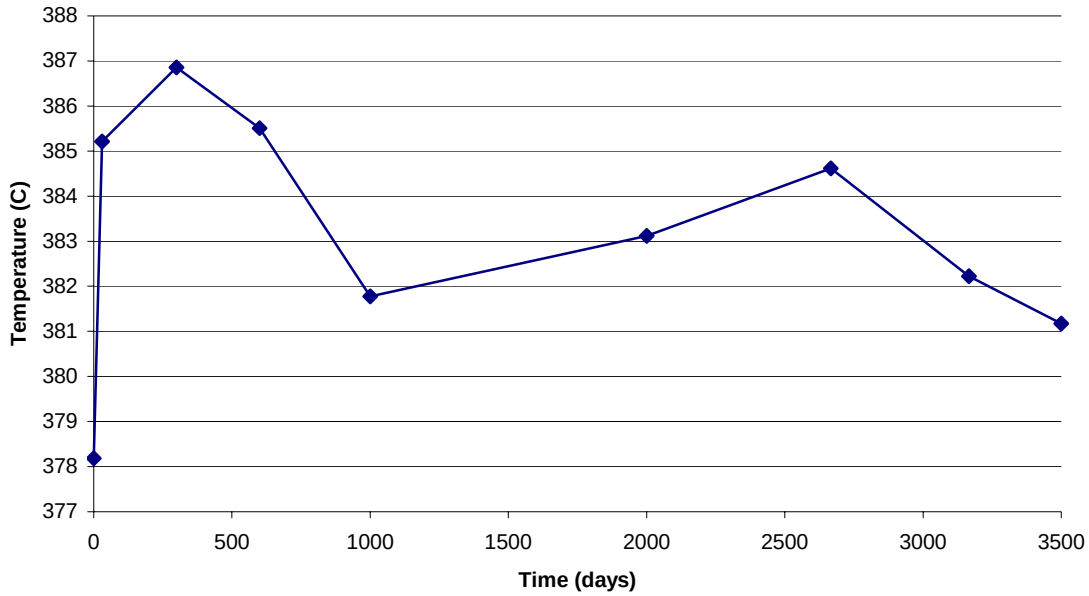

Fig. 58. Peak fuel temperatures in region 1 with thermal column.

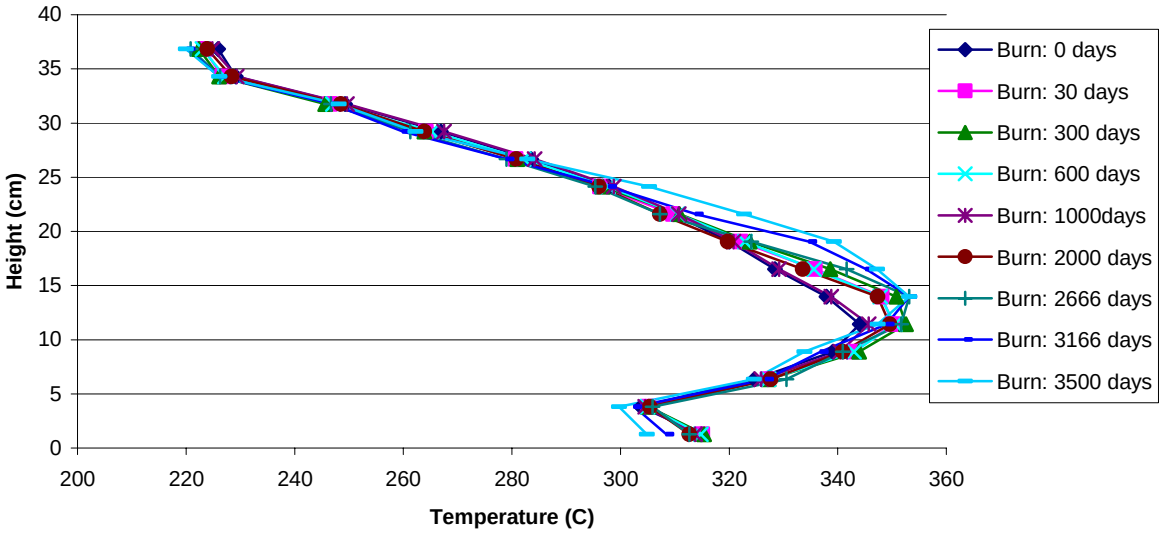

Fig. 59. Fuel centerline temperatures in region 2 with thermal column.

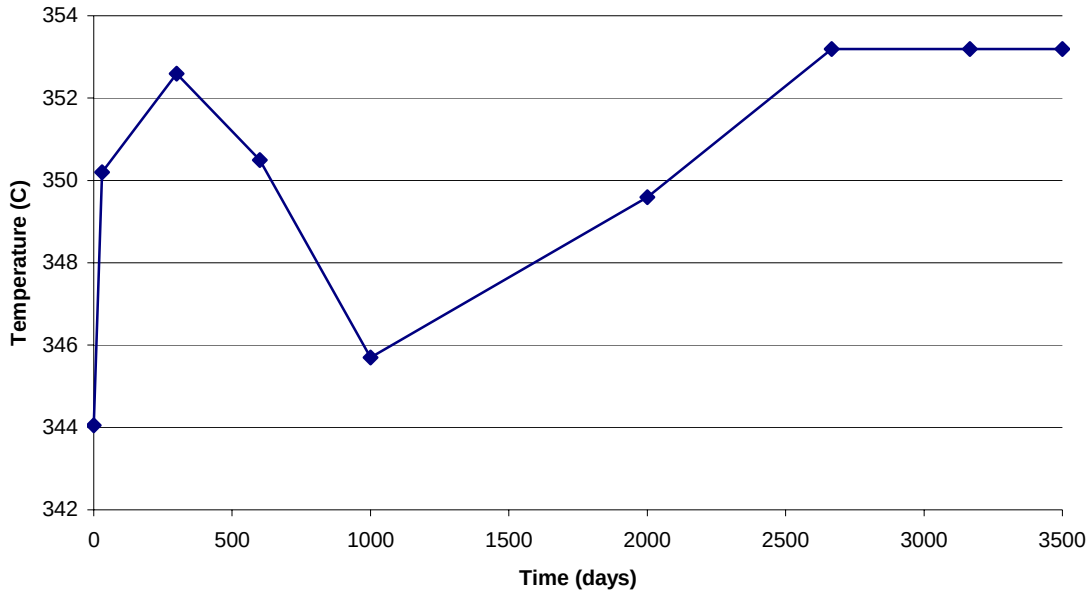

Fig. 60. Peak fuel temperatures in region 2 with thermal column.

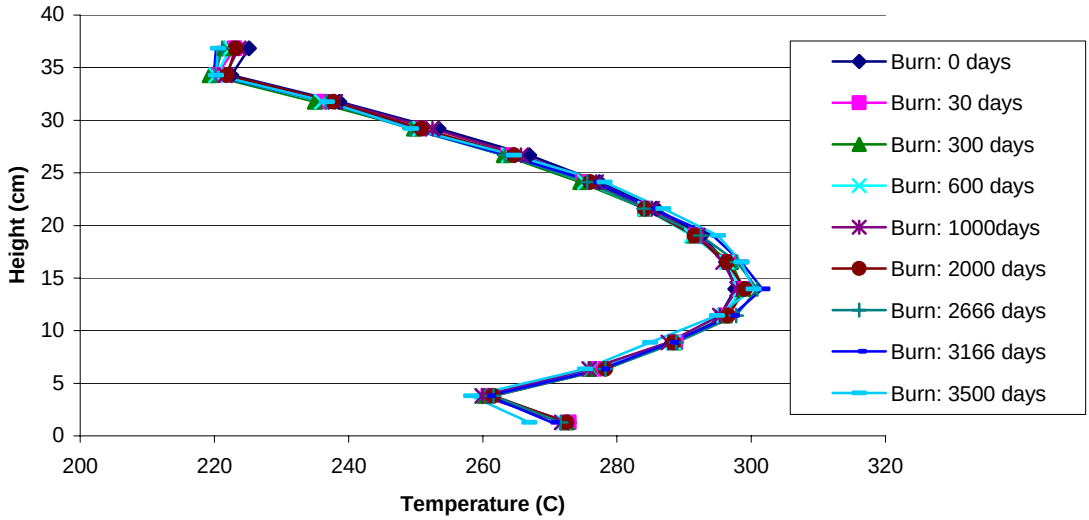

Fig. 61. Fuel centerline temperatures in region 3 with thermal column.

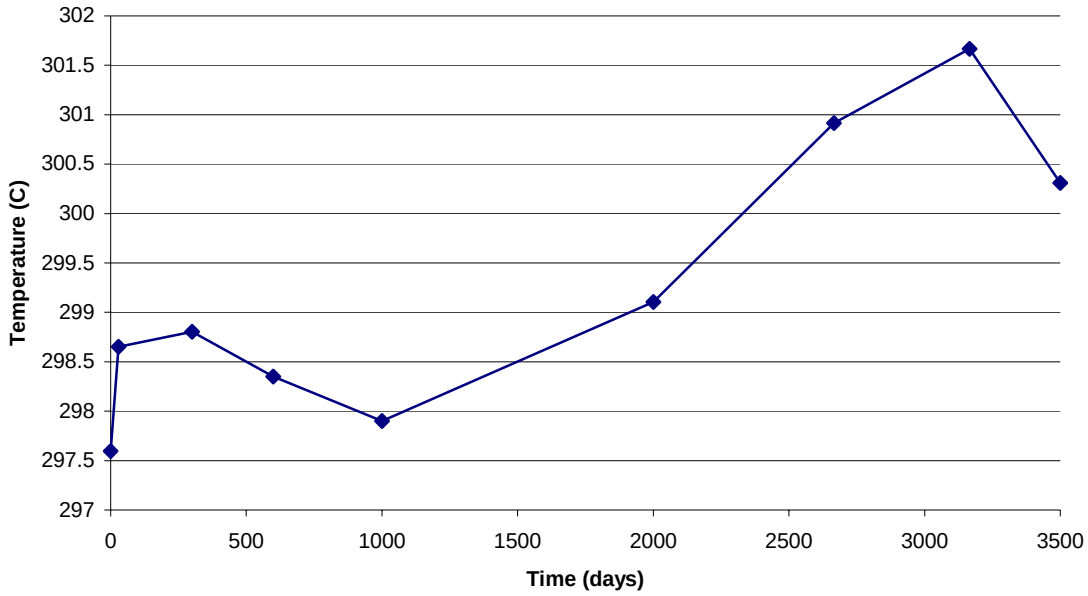

Fig. 62. Peak fuel temperatures in region 3 with thermal column.

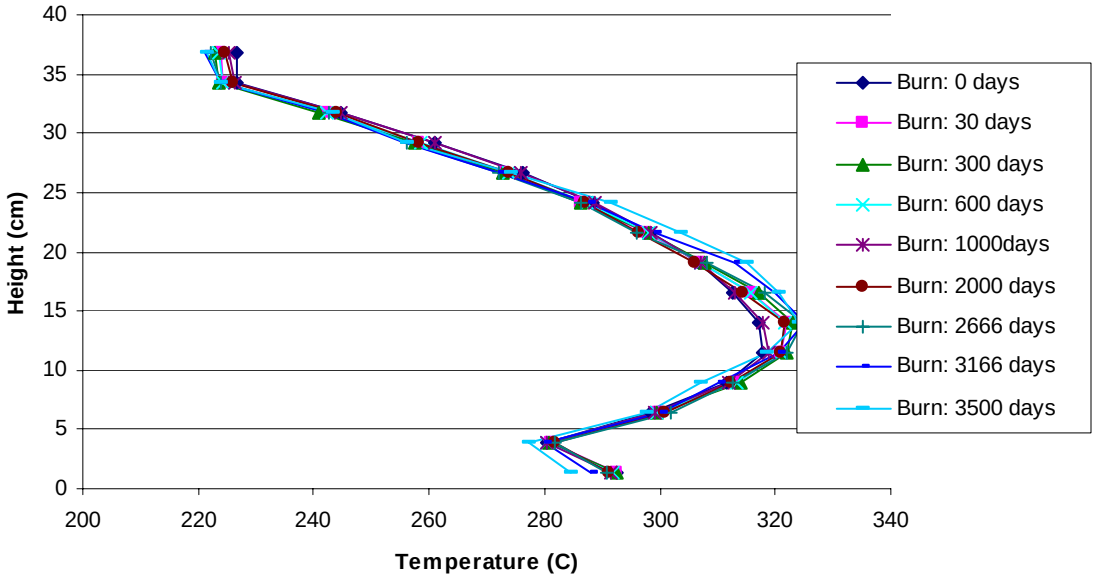

Fig. 63. Fuel centerline temperatures in average region with thermal column.

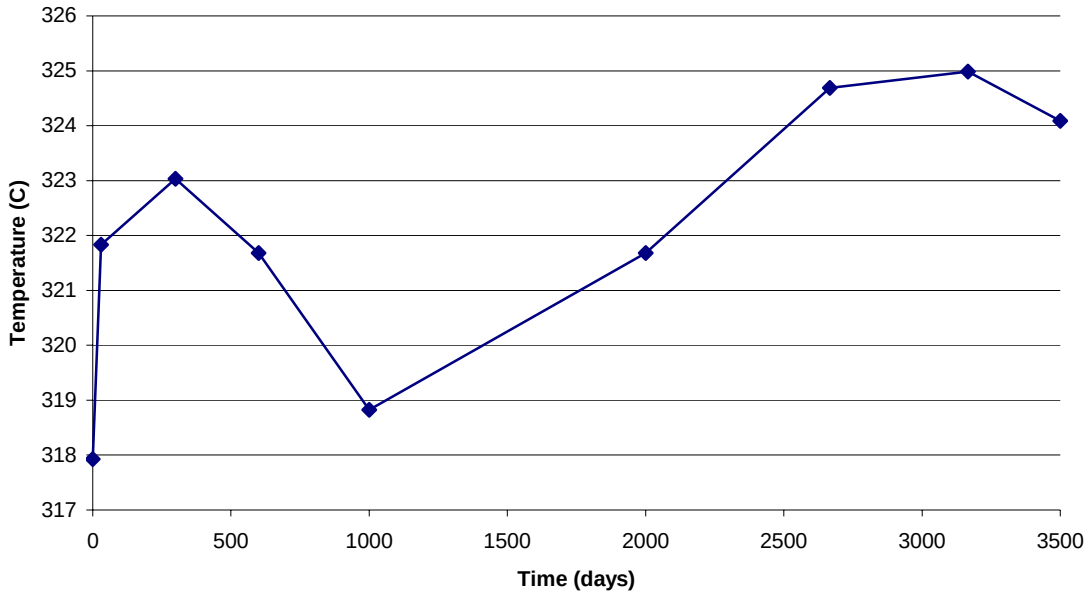

Fig. 64. Peak fuel temperatures in average region with thermal column.

The maximum fuel temperature in any simulation was 419°C while the maximum fuel surface temperature (and therefore a conservative measure for the maximum cladding temperature) was 179°C. These are both well within the limits of 950°C and 500°C for the fuel and cladding respectively.[15] In addition to increasing the core lifetime, the thermal column can reduce the peak fuel temperatures from 419°C to 380°C by providing a more even distribution of power to the periphery of the reactor.

V COEFFICIENT OF REACTIVITY OVER TIME

One of the key safety elements of TRIGA fuel is its strong negative temperature coefficient of reactivity. It is crucial that in the new 30/20 fuel the temperature coefficient of reactivity (α_T) remains highly negative throughout the lifetime of the reactor. α_T is defined as the change in criticality divided by criticality multiplied by the change in temperature as seen in Eq. (8). A negative coefficient of reactivity is an important feature all reactors must have to ensure stability during steady state operations.

$$\alpha_T = \frac{k_2 - k_1}{k_1 k_2 (T_2 - T_1)} \tag{8}$$

It is also the feature that allows for TRIGA reactors to be pulsed. During a pulsing experiment, the reactor will be in a critical configuration with a low power level and with the transient rod fully inserted. This rod is then pneumatically fired out of the core thus creating a supercritical configuration. This causes the power and temperature of the reactor to increase rapidly. It is therefore important that there is a large negative temperature coefficient of reactivity so that the reactor returns to a stable condition.

Outputs from previous Monteburns simulations were used for these calculations. These outputs are from the simulations used for the thermal analysis. At each burn step Monteburns will create an MCNP input deck that contains the updated isotopics for the fuel. Different cross sections at different temperatures were used at each time step and

the criticality was calculated using MCNP. The isotopes that were changed as a function of temperature were U-235, U-238, Pu-239, Er-166, Er-167 and the scattering cross sections for the ZrH. Since the data provided by Dr. Hawari can only be used to simulate the scattering effects at 600K, the cross section sets from 1999 were used in this simulation. The temperatures at which this analysis was performed were 300K, 600K, 800K, and 1200K. This was performed both with and without a thermal column present.

The figures on pages 85-94 show the results. Fig. 65 shows the criticality as a function of time in the NSCR. As expected, the thermal column provides a positive reactivity insertion since it acts as a large reflector to the east side of the reactor. It is interesting to note that the difference in criticality between the two systems remains approximately the same over time. In both cases a slight rise in k_{eff} is seen over the first 1000 days. This is due to the production of plutonium in the core which inserts positive reactivity. Beyond 1000 days the criticality drops as the fuel (primarily U-235 and Pu-239) in the core is depleted.

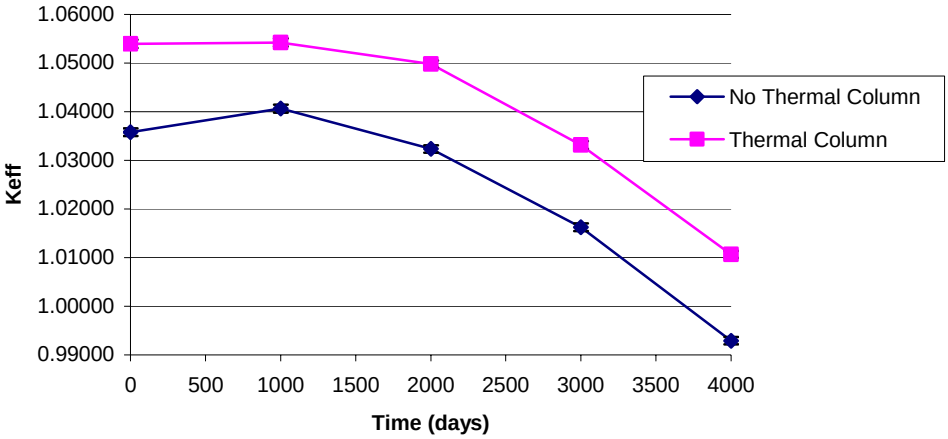

Fig. 65. Criticality versus time at 600K.

The criticality versus time assuming the reactor was operating at various temperatures is seen in Fig. 66. As the temperature rises the criticality decreases during all stages of burnup. This is a desirable feature since this means the coefficient of reactivity will be negative, thus adding an inherent safety feature to the reactor.

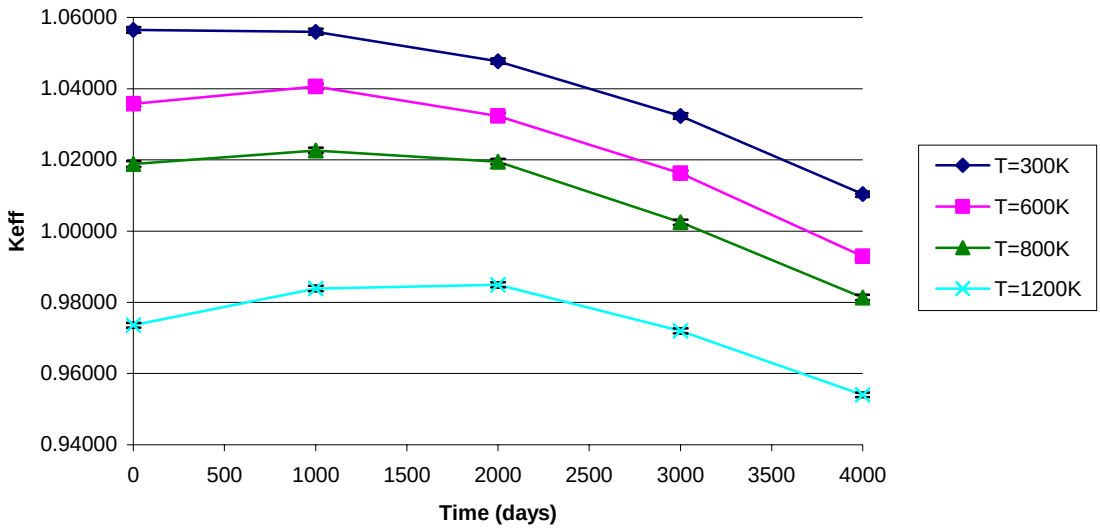

Fig. 66. Criticality versus time without thermal column.

Criticality versus temperature is plotted in Fig. 67. Criticality decreases as the temperature increases for all stages of burnup. Each curve also has the same approximate slope. Again, one can see that the criticality slightly increases from 0 to 1000 days of burnup, but then decreases after 1000 days.

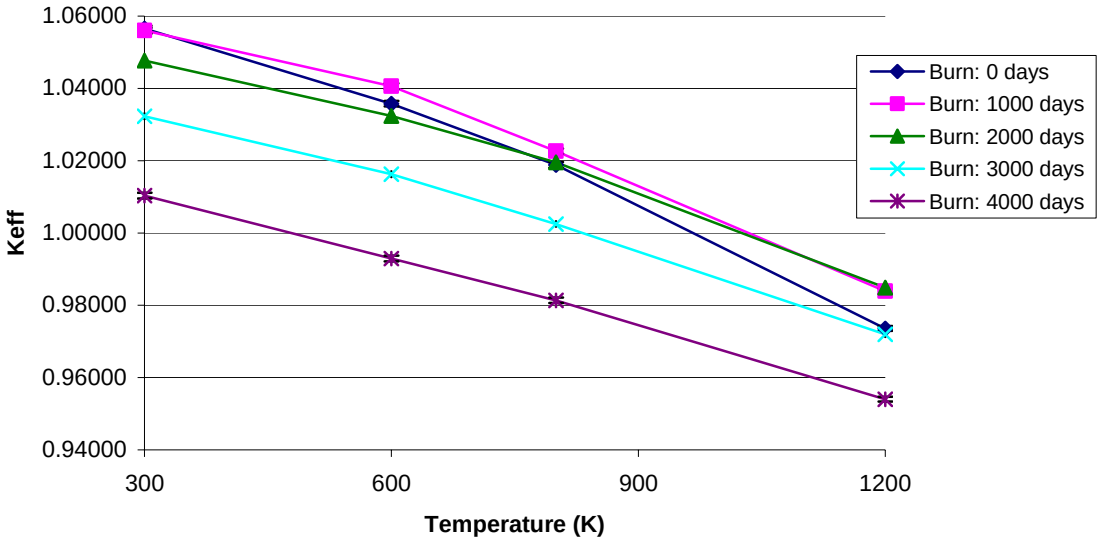

Fig. 67. Criticality versus temperature without thermal column.

Fig. 68 shows the temperature coefficient of reactivity as a function of temperature for different stages of burnup. In all stages of burnup, the temperature coefficient of reactivity becomes more negative as the temperature increases. This is because as the fuel heats up so will the ZrH moderator. The greater the temperature, the greater the energy at which the hydrogen in the ZrH lattice will oscillate. This increases the probability that a thermal neutron will gain energy and be absorbed in the Er-167 resonances. Thus, an increase in temperature will lead to a decrease in the temperature coefficient of reactivity. This is particularly important for pulsing experiment where the fuel temperatures are their largest in the operating lifetime of the reactor.

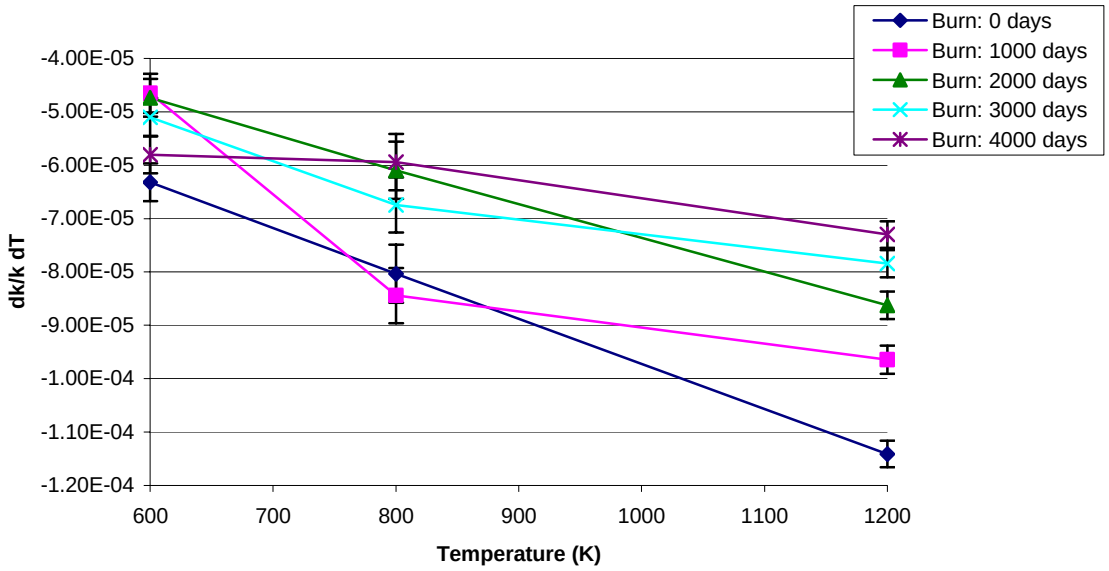

Fig. 68. dk/k dT versus temperature without thermal column.

To better illustrate the temperature coefficient of reactivity, Fig. 69 is shown. Again, higher temperatures yield a lower temperature coefficient of reactivity. The curve at 600 K is most relevant to the NSCR since this is approximately the operating temperature at 1 MW. It is seen here that α_T increases over the first 1000 days and then falls. This is because plutonium is being produced in the core causing a positive reactivity insertion. With time however, the reactor becomes more dependant on the plutonium for a source of power and the plutonium becomes depleted. With less fissile material to absorb neutrons, the α_T decreases. The curves for 800 K and 1200 K do not show this turning over effect. This may be because the ZrH effect is so dependent on the temperature. An increase in temperature could lead to a much more rapid depletion rate

for Er-167. Without Er-167 the ZrH effect will not contribute as much to the temperature coefficient of reactivity.

Figs. 70 and 71 show essentially the same plots as Figs. 68 and 69 but the units for α_T are in \$/K. The unit of a dollar is found by simply dividing the temperature coefficient of reactivity by the portion of delayed neutrons that cause fission (β_{eff}). A beta-effective of 0.007 was used.

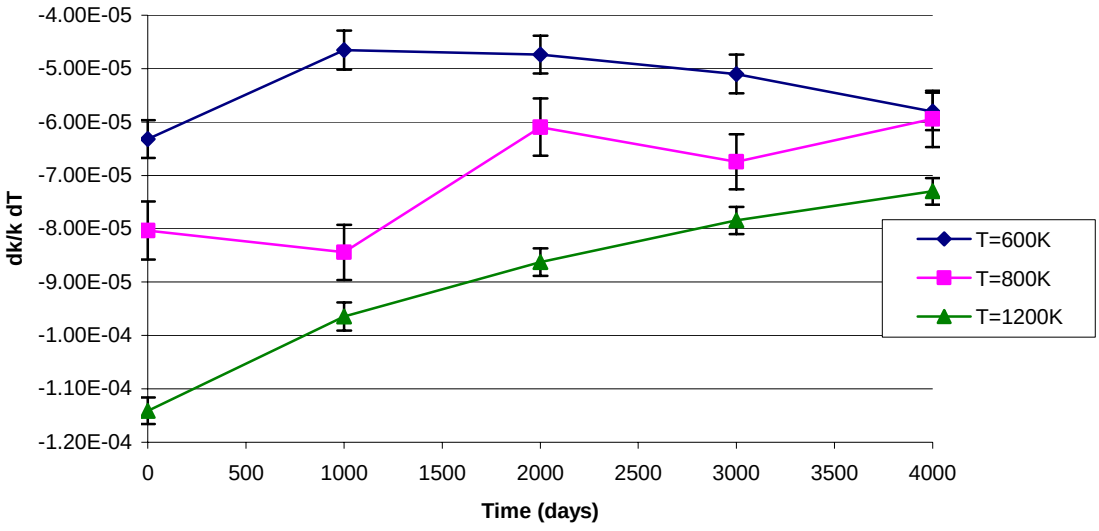

Fig. 69. dk/k dT versus time without thermal column.

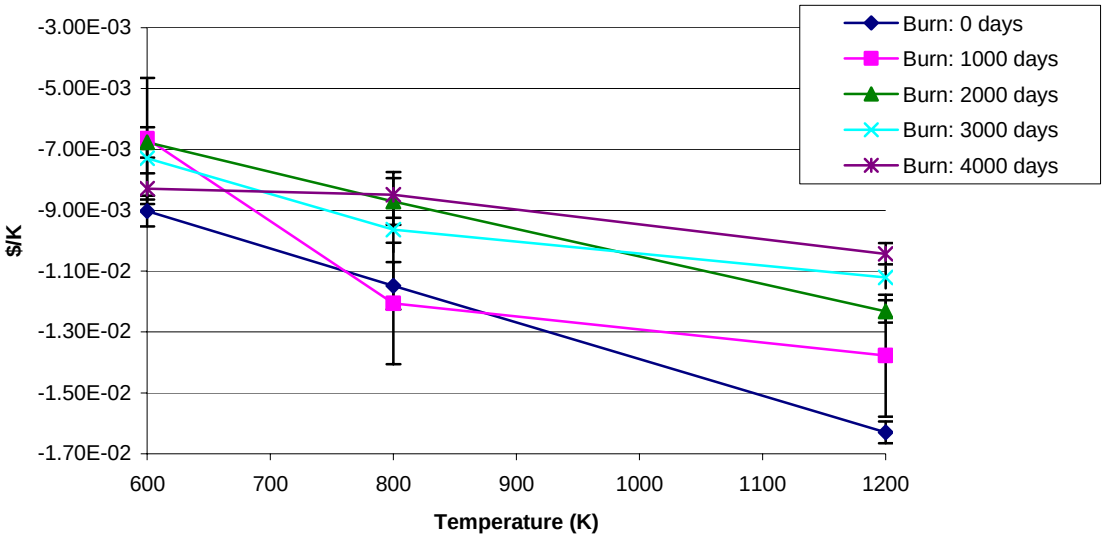

Fig. 70. $/K versus temperature without thermal column.

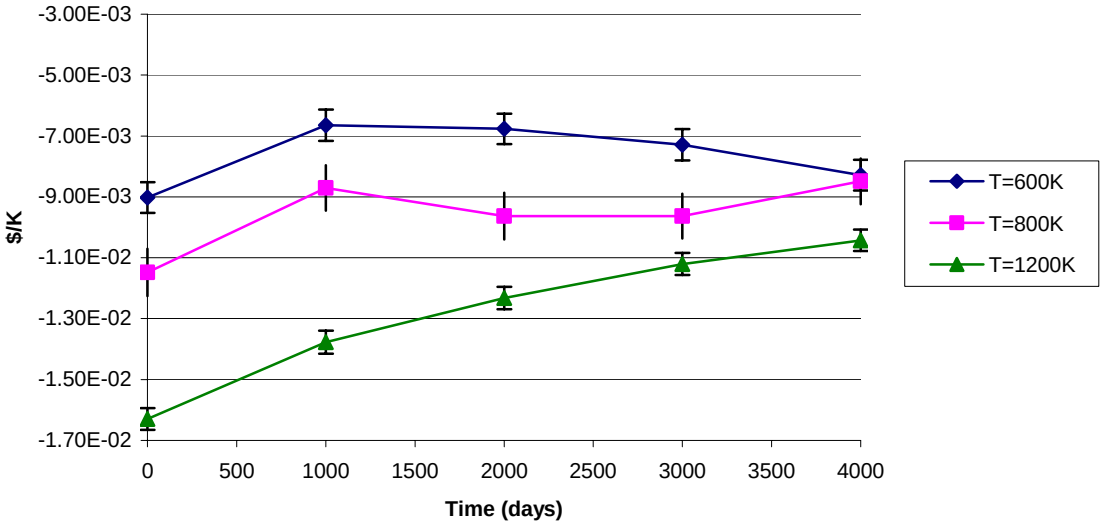

Fig. 71. $/K versus time without thermal column.

Figs. 72-77 show the same basic results obtained earlier for the simulations without a thermal column present. As expected, for Figs. 72 and 73 the values for criticality are higher, but the shape is essentially the same as those found in Figs. 66 and 67. Figs. 74 and 75 have the same shape as Figs. 68 and 69. Again, one can observe a turning over effect for the curve at 600 K in Fig. 75 as seen before in Fig. 69. This turning over effect does not occur until 2000 days instead of 1000 days. This may be because the addition of the thermal column extends the fuel lifetime by approximately 1000 days. Therefore, this turning over characteristic is "delayed".

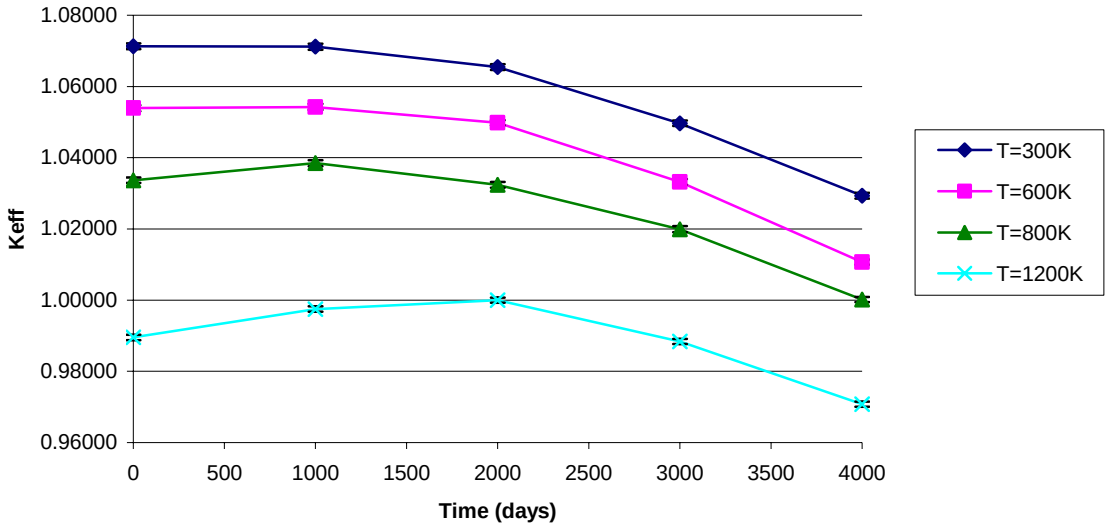

Fig. 72. Criticality versus time with thermal column.

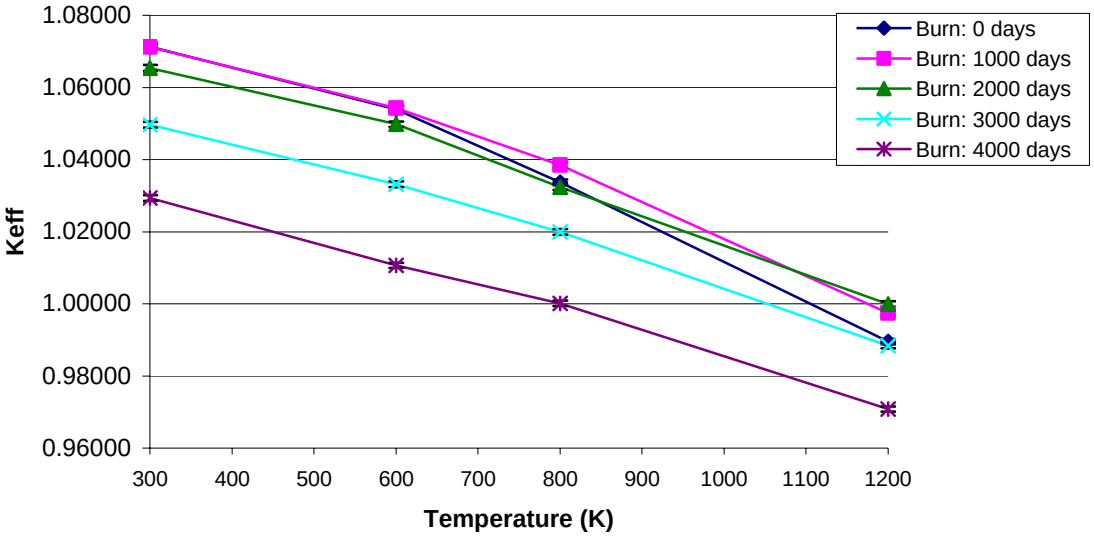

Fig. 73. Criticality versus temperature with thermal column.

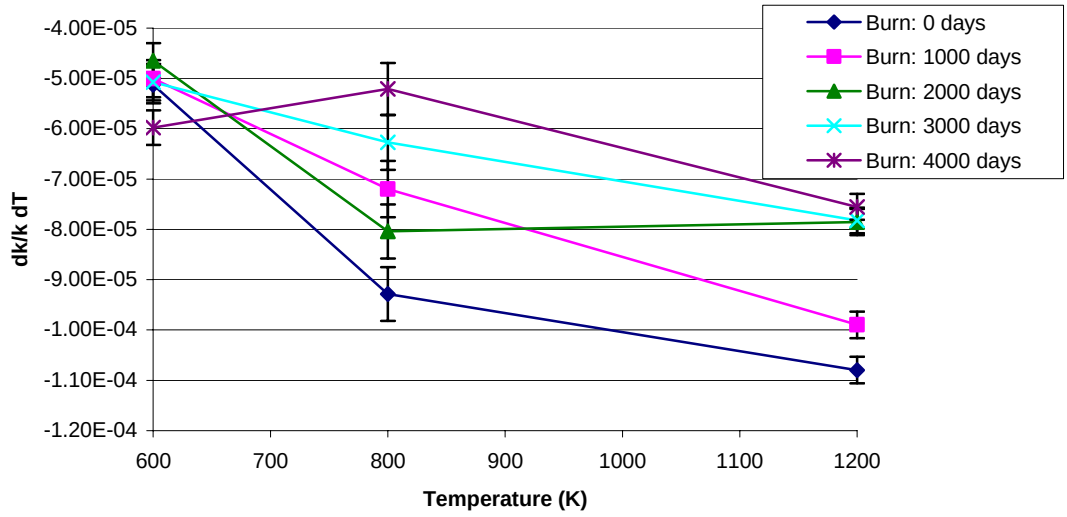

Fig. 74. dk/k dT versus temperature with thermal column.

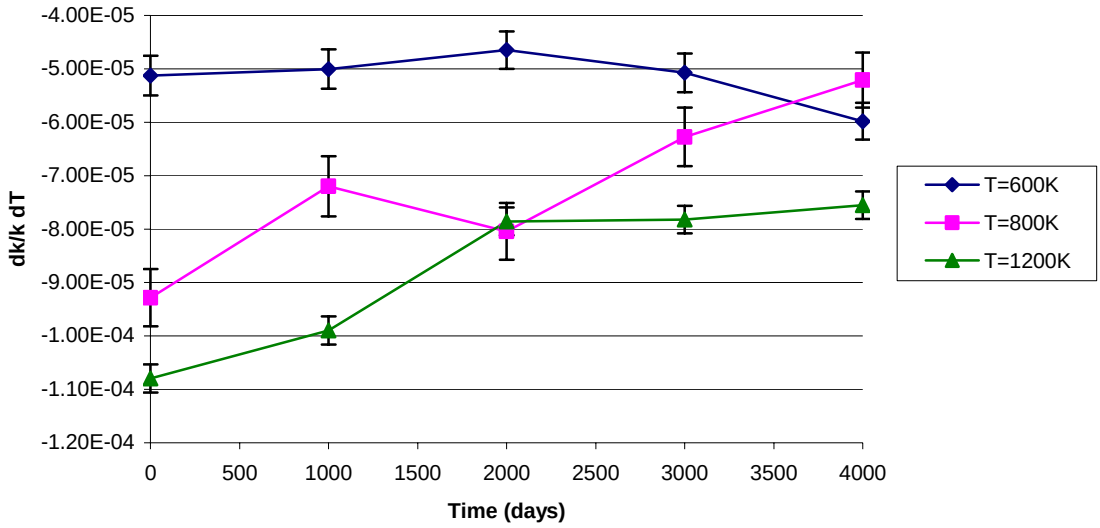

Fig. 75. dk/k dT versus time with thermal column.

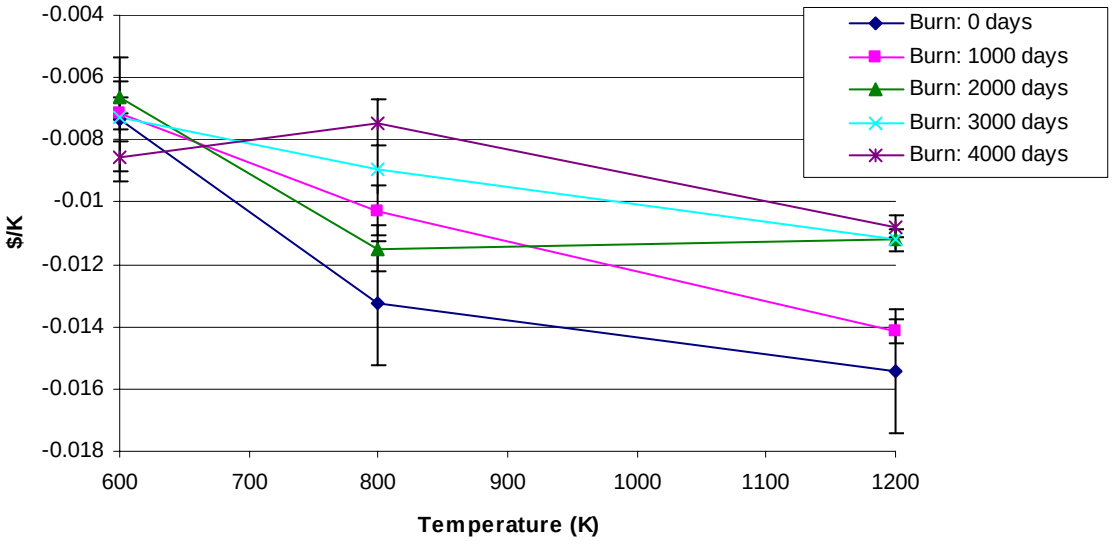

Fig. 76. $/K versus temperature with thermal column.

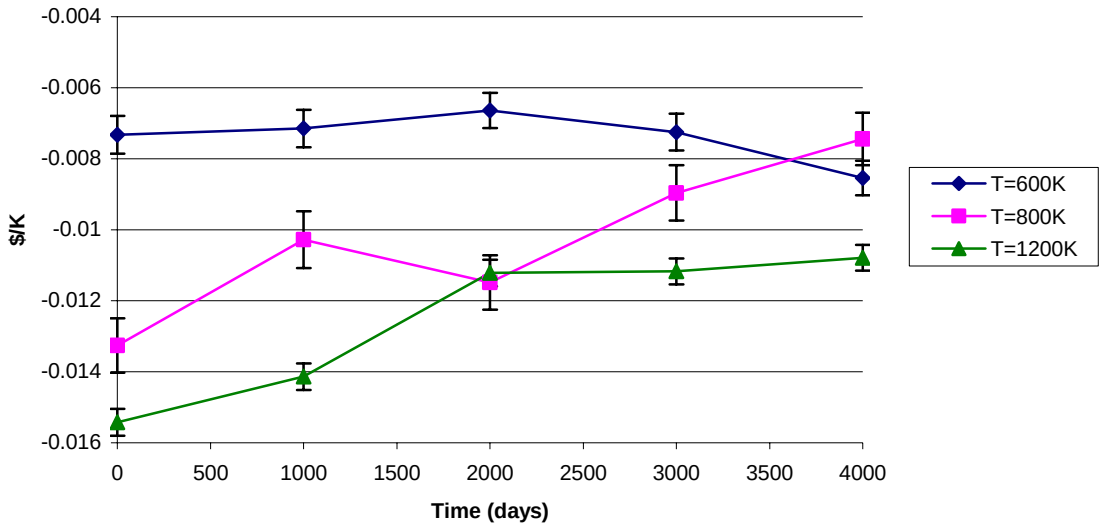

Fig. 77. $/K versus time with thermal column.

Fig. 78 is provided to show the temperature coefficient of reactivity characteristics for FLIP fuel.[17] The values on the y-axis are actually negative. Therefore, as the temperature increases the temperature coefficient of reactivity becomes more negative. This characteristic is seen in Figs. 68 and 74. Also α_T is at its most negative values during the beginning of life and increases as a function of time (Fig. 78). Figs. 68 and 74 show this behavior as well. The values for α_T in the FLIP fuel range from approximately -3E-5 to -26E-5 dk/k-dT for a temperature range of 0°C to 1000°C.

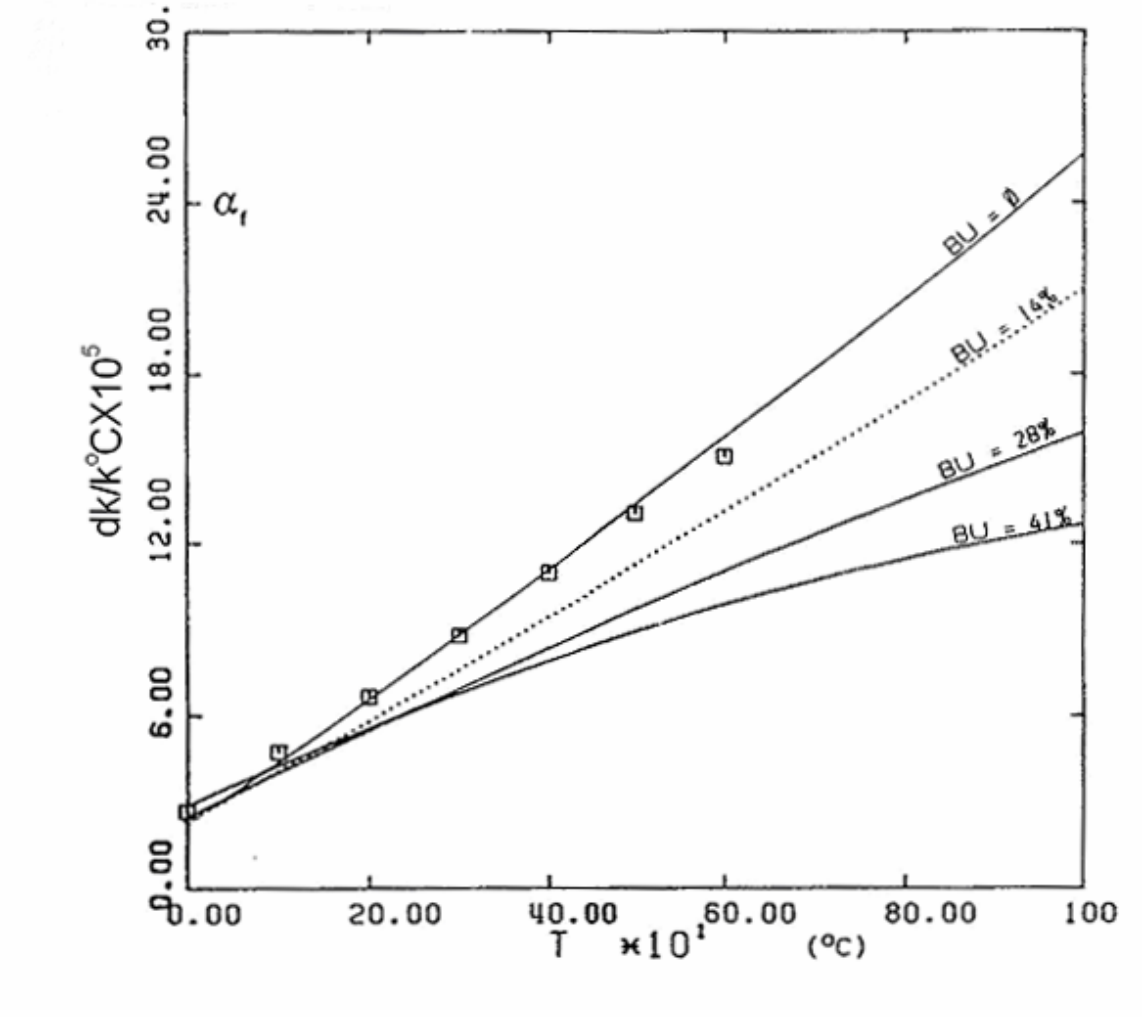

Fig. 78. Temperature coefficient of reactivity for FLIP fuel.

As can be seen, the temperature coefficient of reactivity always remains negative regardless of the burnup or configuration of the reactor. This is desired since it will make the reactor inherently safe. The coefficient of reactivity remained below -4E-5 dk/k-dT at all times regardless of whether a thermal column was present or not. It should be noted that the temperature coefficient of reactivity versus temperature has a

similar shape to that seen for FLIP fuel. The FLIP fuel however has a more negative α_T than for the 30/20 fuel according to Fig. 78. According to the Safety Analysis Report for the NSCR[16], α_T ranges from -8E-5 to -17E-5 dk/k-^oC for the temperature range of 600 K and 1000 K for beginning of life FLIP fuel. From Fig. 68, the 30/20 fuel ranges from -6.5E-5 to -9.5E-5 dk/k-^oC between 600 K and 1000 K. This implies that the 30/20 will not be able to perform as large of pulsing experiments as before. The temperature coefficient of reactivity for the 30/20 fuel may be enhanced and be closer to the values found for FLIP fuel if a higher weight percentage of erbium is used. Further analysis needs to be made to determine the magnitude of pulsing experiments that this new fuel can handle.

VI RACE

The RACE program uses a neutron source driving a subcritical configuration. The neutron source is produced by bombarding a heavy metal target with high energy electrons. The electrons produce Bremsstrahlung photons while slowing down and the photons produce fast neutrons via photonuclear reactions. These neutrons are then multiplied through a subcritical lattice. The RACE program originally was designed to make use of the FLIP core; however, since the fuel at the NSC will be changed to the 30/20 fuel, an analysis must be performed to confirm that the RACE experiments are still capable with the new fuel. It is of interest to know whether or not this experiment will produce enough heat in the reactor so that temperature feedback mechanisms are observed. This section describes a feasibility test for this reactor in relation to the RACE project.

VI.A. Target Optimization

The first step in designing the RACE experiments is to optimize the shape of the target for neutron production. It is already assumed that a solid right circular cylindrical target will be used. Therefore, it is desired to know what the height and radius should be to produce the maximum amount of neutrons. A target that is too small may have too many photons exiting the target without producing neutrons. A target that is too large however may absorb these neutrons that are produced before they exit the target. It was assumed that a tungsten target would be used. MCNP simulations were run with the

radius being constant while the height was adjusted. A height of 4 cm was chosen and the radius was adjusted. The neutron fluxes on each of the surfaces of the cylindrical target were tallied in MCNP (Fig. 79). As one can see most of the neutrons exit the top of the cylinder. Since in the actual experiment there will be a vacuum above the target for the accelerator, these neutrons will have little affect on the heat production in the reactor. It would be beneficial to conduct further studies to optimize this target so that the neutron flux on the top portion of the target is minimized while increasing the flux on the sides. This work is not conducted in this thesis project since it was already assumed that the target would be a simple cylinder of tungsten.

It was therefore decided to optimize the neutron current from the sides of the target. Fig. 80 shows the exiting neutron current from the target as a function of target height. As one can see after about four centimeters, the height is optimized and increasing the height has essentially no effect. Next the radius was optimized by assuming a constant height of four centimeters. Fig. 81 shows the exiting neutron current from the target as a function of target radius. The optimal radius found here is about 3 cm.

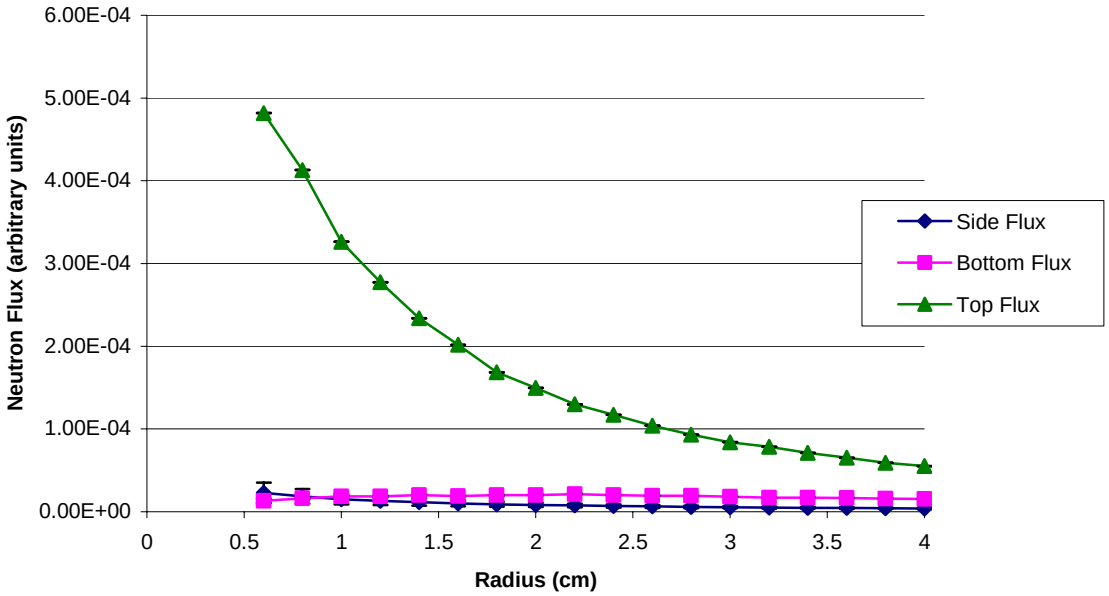

Fig. 79. Neutron flux exiting various surfaces of the tungsten target as a function of radius at a height set to 4 cm.

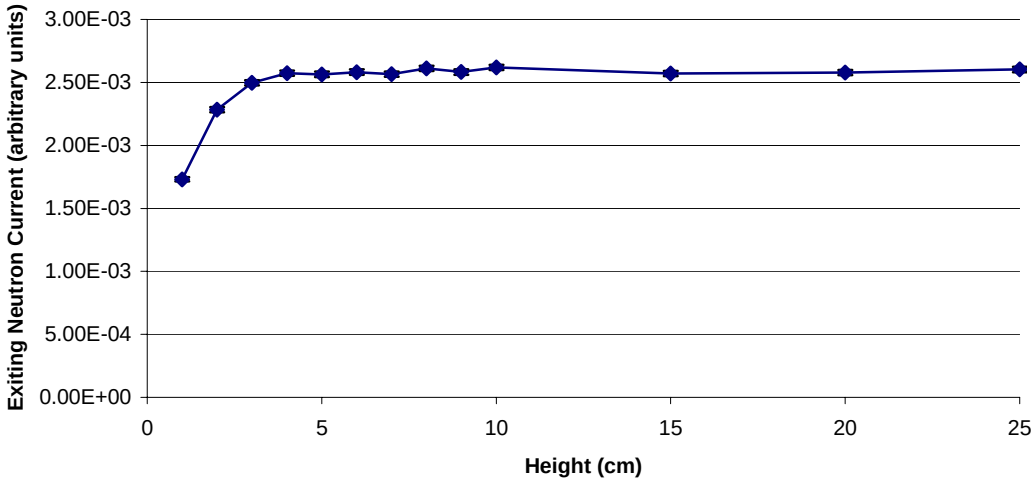

Fig. 80. Neutron current versus target height for tungsten target with a radius of 3cm.

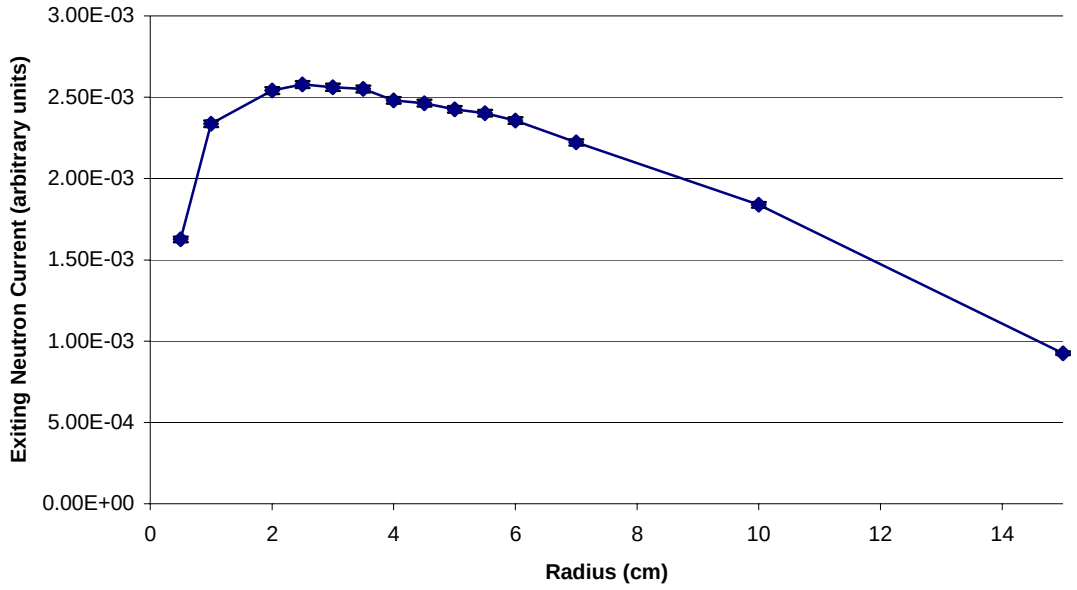

Fig. 81. Neutron current versus target radius for tungsten target with a height of 4 cm.

VI.B. RACE Simulations

Two locations were chosen for the target in the NSCR: the D7 and D2 locations. These locations can be seen in Fig. 6. The D7 location will be highly coupled with the core while the D2 will not be as coupled. The target was chosen to be tungsten with a radius of 3.55 cm and a height of 10 cm. The D7 and D2 positions consist of a rectangular opening that is 8.1 X 7.7 cm. A target radius of 3.55 cm was chosen so that the target would be close to the fuel to improve the fuel heating while still maintaining a clearance of over 3 mm on either side. The height of the target is irrelevant after about 4 centimeters so there is no harm in extending the height to 10 centimeters. The tungsten target was set in the D7 or D2 position such that the top of the target was 3 cm above the

vertical centerline of the core. This was done since the majority of the neutrons will be produced within the first 3 to 4 centimeters of the top portion of the target. Therefore, the maximum neutron current coming from the sides of the target is at a location that is in the center of the core.

First a criticality simulation was performed. The shim safety rods were inserted until a keff of 0.9800 +/- 0.0005 was achieved. Then the source driven simulation was run to determine heat production in the core. The MCNP input deck for this simulation is found in Appendix D. Figs. 82-87 show these results for the D7 position. The D7 position occupies (13, S8), (14, S8), (13, S7), and (14, S7) seen in Fig. 83. From Fig. 82 and 83 one will notice that the photons deposit their energy locally. Only the fuel rods in the close vicinity are significantly heated.

Figs. 84 and 85 show a more uniform heating of the reactor. As expected the neutron heating is higher in the portions of the reactor close to the target and less in the periphery. The regulating rod and transient rod can be clearly identified in Fig. 85 in positions (6, S4) and (9, S8) respectively. These two rods are actually fully withdrawn from the core in this simulation. The voids seen in Fig. 85 at positions (6, S4) and (9, S8) are because no heating tally was made for those positions. The shim safety rods are in positions (7, S10), (11, S10), (11, S6), and (7, S6). The effect of the shim safety rods is more prevalent in the (11, S10) and (11, S6) positions. These control rods lower the amount of heating in their vicinity, particularly for the fuel rod located in position (11,

S8). This causes a peak in the heating on both sides of this fuel rod in positions (10, S8) and (12, S8).

Figs. 86 and 87 show the total heating for the D7 position. This is merely the sum of the photon and neutron heating found earlier. As expected, the greatest heating is found close to the target. It would be more desirable to obtain a more constant heating throughout the core. For this reason, the target was moved to the D2 position in hopes that the photon heating would not produce as large a spike in the heating.

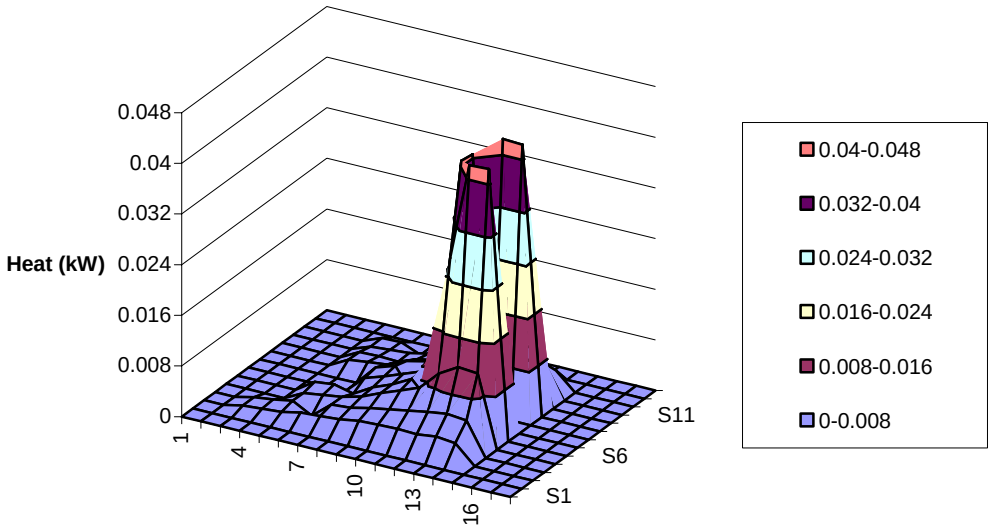

Fig. 82. Photon energy deposition in D7 position.

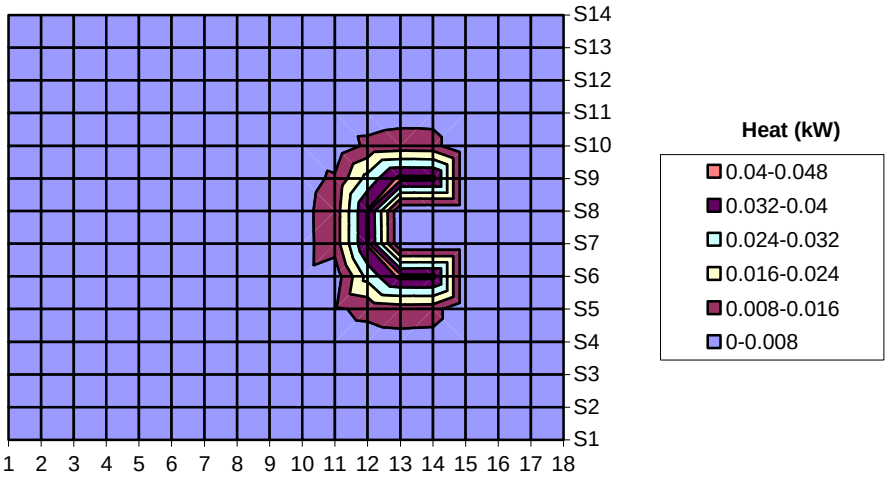

Fig. 83. Top view of photon energy deposition in D7 position.

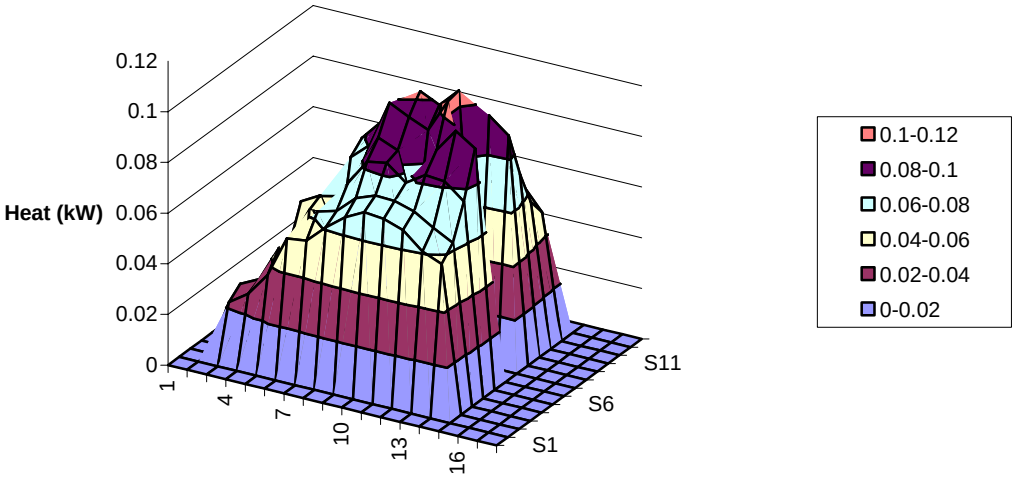

Fig. 84. Neutron energy deposition in D7 position.

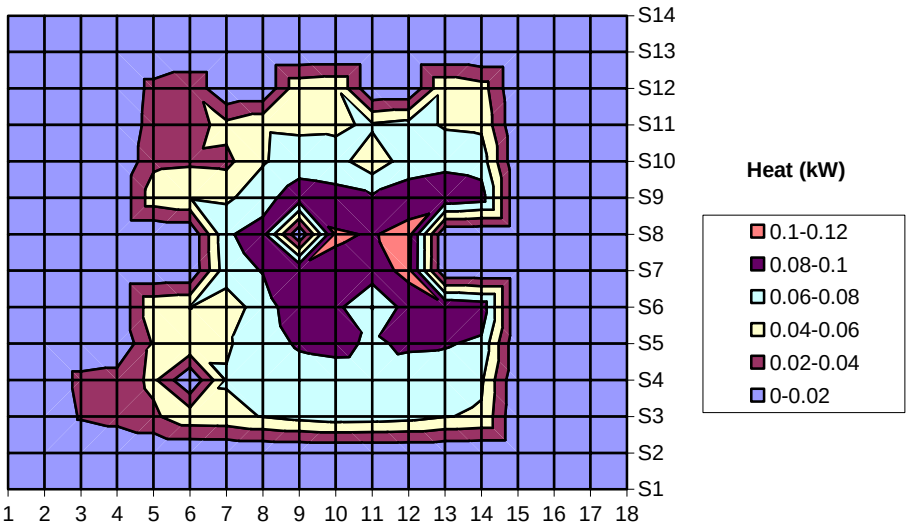

Fig. 85. Top view of neutron energy deposition in D7 position.

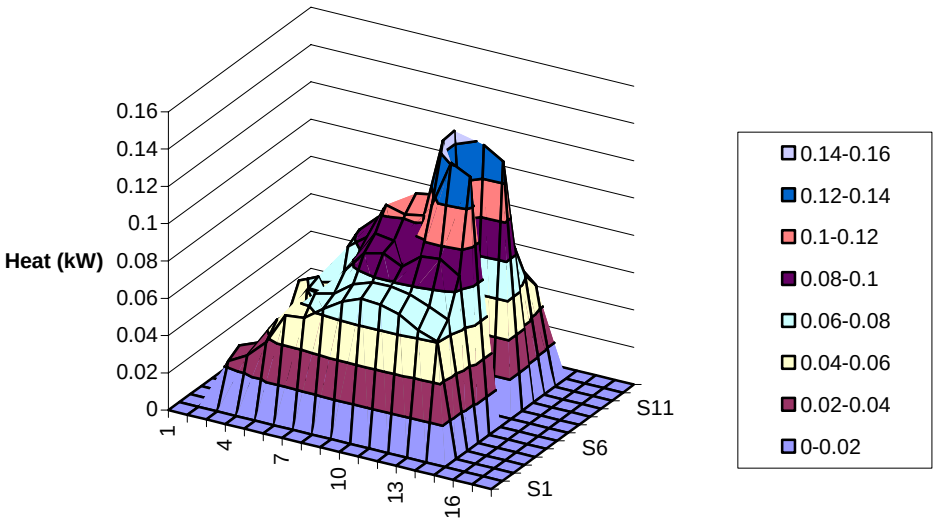

Fig. 86. Total energy deposition in D7 position.

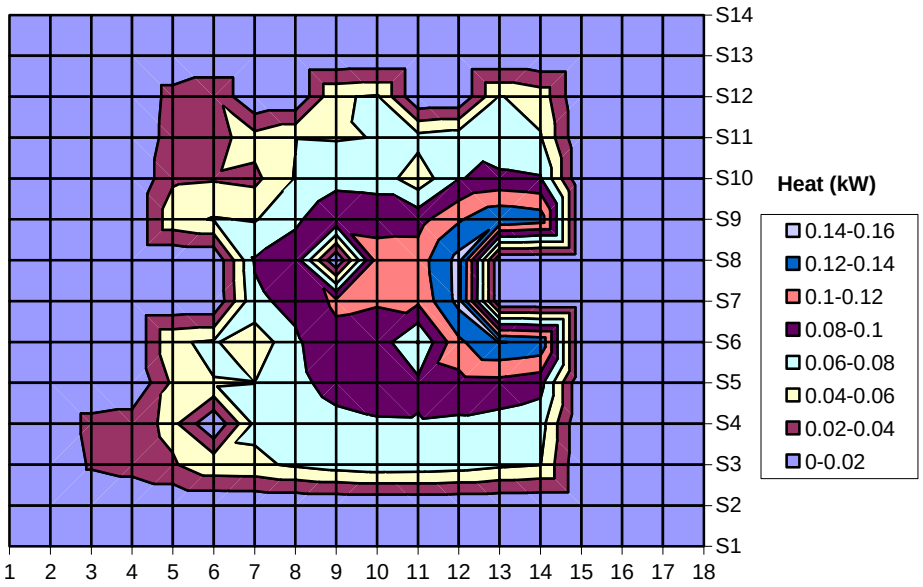

Fig. 87. Top view of total energy deposition in D7 position.

Figs. 88 and 89 show the photon heating from the tungsten target in the D2 position. Again the photons deposit their energies locally. Essentially only the two fuel rods closest to the target experience a significant amount of heat in relation to the other fuel rods. Figs. 90 and 91 show the neutron heating. As in the photon heating, the same two fuel rods at positions (5, S6) and (5, S9) experience the most heat. This time the effects of shim safety control rods located at positions (7, S10) and (7, S6) can be seen. These two rods seem to "squeeze" the heat more towards the center of the core as seen in Fig. 91. The total energy distribution is seen in Fig. 92 and 93. With the exception of the fuel rods located at (5, S6) and (5, S9), there is a more uniform heating distribution.

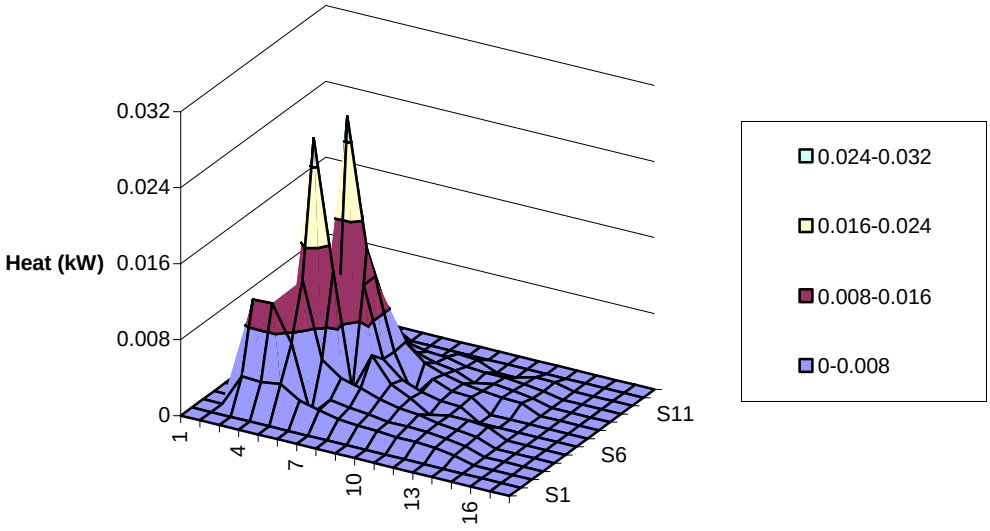

Fig. 88. Photon energy deposition in D2 position.

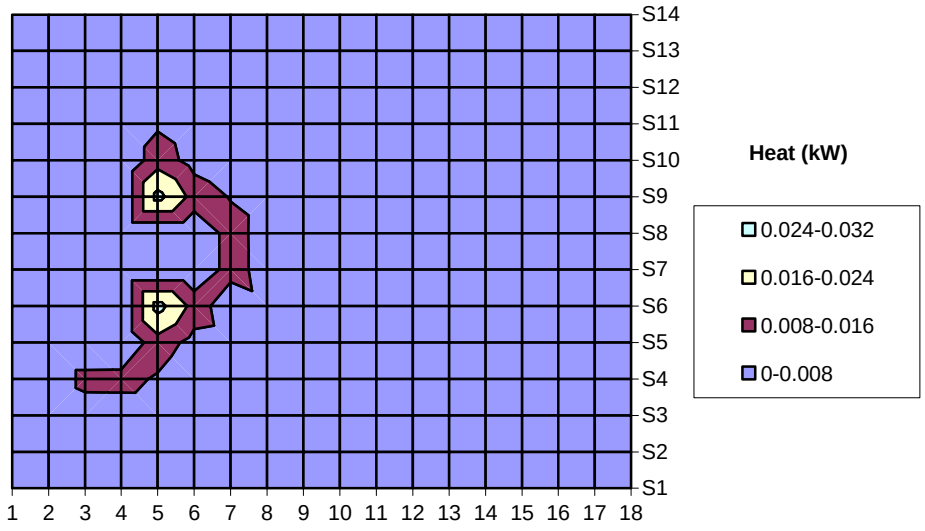

Fig. 89. Top view of photon energy deposition in D2 position.

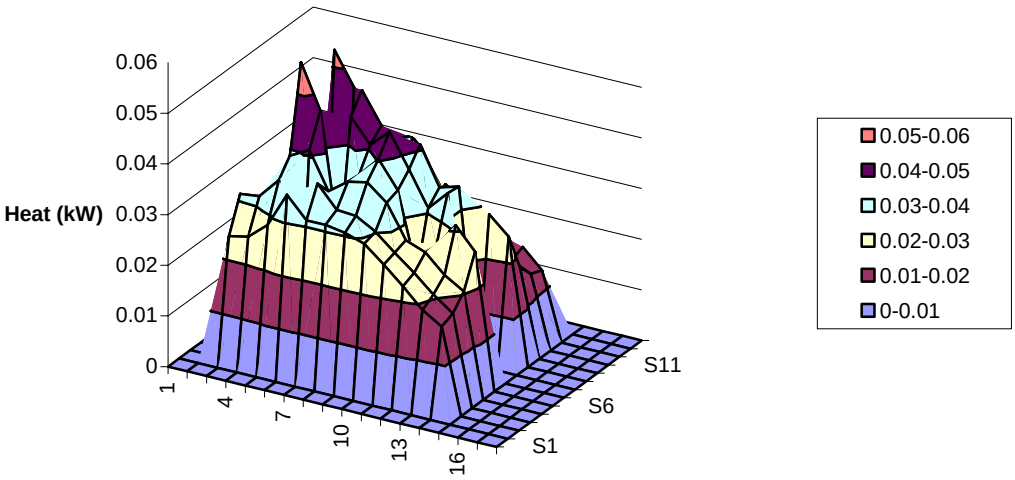

Fig. 90. Neutron energy deposition in D2 position.

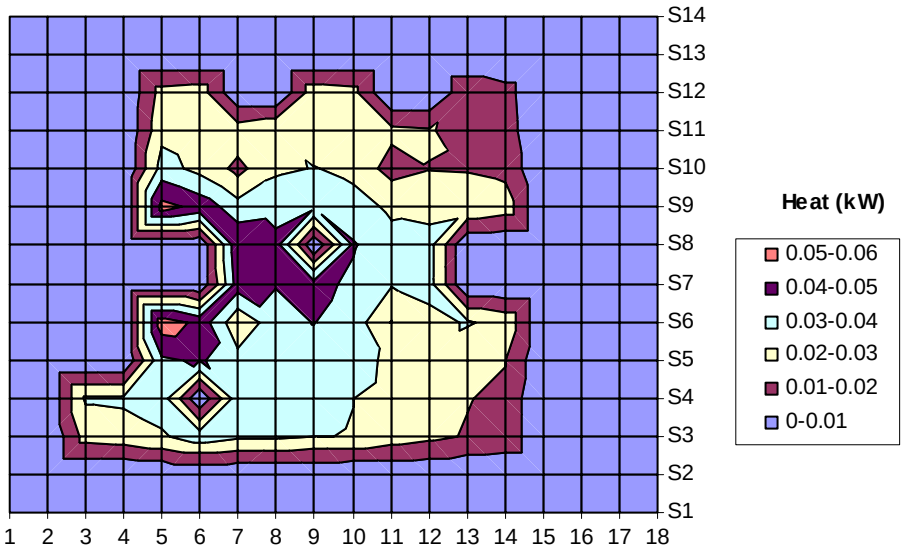

Fig. 91. Top view of neutron energy deposition in D2 position.

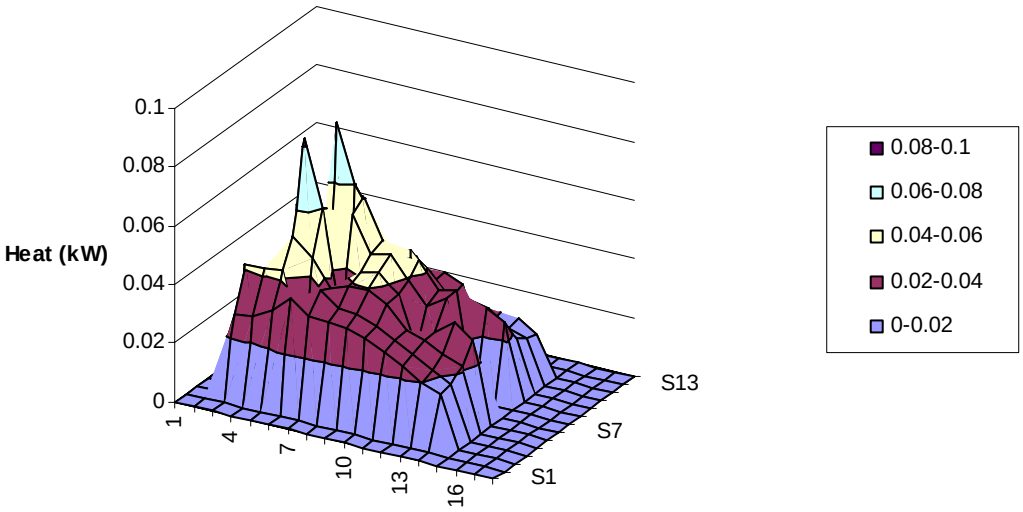

Fig. 92. Total energy deposition in D2 position.

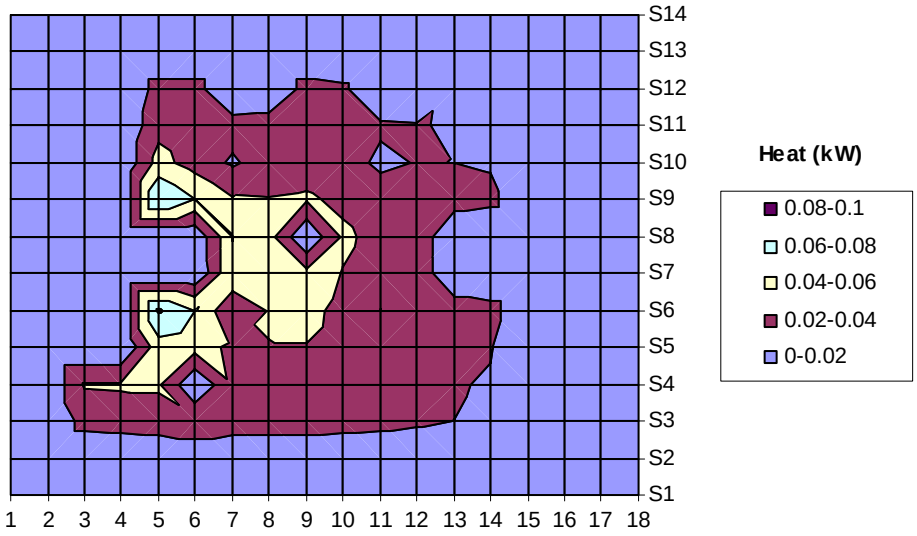

Fig. 93. Top view of total energy deposition in D2 position.

It was desired to achieve a total power greater than 1 kW in the core, so that the temperature feedback effects could be observed. The D7 position yielded a power of 6.54 kW +/- 0.0171 kW and the D2 had a power of 2.98 kW +/- 0.00918 kW. In either case the photon heating accounted for approximately 10% of the total heating. This total power was calculated assuming that the electron accelerator was operating at 1 mA and that the electrons were at 20 MeV. It was also desired that no single fuel element exceeds a power of 35 kW. All fuel elements stay well below this limit. Since this criterion is met and the reactor produces a power in excess of 1 kW at a reasonable criticality, the RACE project is feasible for this reactor.

VII CONCLUSIONS

The purpose of this thesis was to perform neutronic and thermal hydraulic analyses to confirm that the new 30/20 fuel to be used at the Nuclear Science Center Reactor located at Texas A&M University allows the reactor to conform to its technical specifications and to show its capability as an experimental facility. These analyses were performed by using improved ZrH cross sections that were provided by Dr. Ayman Hawari from North Carolina State University.

The first step in the analysis was to compare the new ZrH cross sections with existing cross sections from the MCNP library. The results show fairly consistent agreement among the cross sections and the new cross sections may better predict the criticality of the reactor.

Buildup and depletion calculations were made with the program Monteburns to compare the criticality and isotopics between FLIP and the new 30/20 fuel. These simulations were performed with and without a thermal column present. One conclusion that can be drawn from this is that the thermal column increases the lifetime of the core from 3500 MW-days to 4500 MW-days. Also the lifetime of the reactor is slightly higher with the 30/20 fuel.

The control rod worths were calculated and compared to technical specifications. It was determined that fuel rods would need to be removed from the typical core configuration during the initial loading so that the minimum shutdown margin and maximum excess reactivity specifications will be met.

The code PARET was utilized to determine the fuel centerline and cladding temperatures. Plots were made of the fuel centerline temperature versus height for various regions in the reactor over different periods of time. As expected the temperature profile flattens as a function of time. These plots were generated with and without a thermal column present. The thermal column better distributes the power to the periphery of the reactor thus decreasing the maximum temperature. For this steady state analysis the maximum fuel and cladding temperatures were 419^{o}C and 179^{o}C; well below their thermal limits of 950^{o}C and 500^{o}C.

The temperature coefficient of reactivity remains negative at all times during the operation of the reactor. This value is maintained below -4E-5 dk/k-dT. The 30/20 exhibits the same characteristics as the FLIP fuel in regards to the temperature coefficient of reactivity. The FLIP fuel however is more negative than the 30/20 fuel. This means that the new fuel will not be able to support as large of pulsing experiments as before. The difference in the temperature coefficient of reactivity between the two fuels may be because FLIP fuel has a higher weight percentage of erbium. A higher percentage of erbium would be desirable for the 30/20 fuel so that the value for the maximum pulse would be the same as seen for FLIP fuel. Additional analysis is required to determine what the maximum pulse is for this fuel.

RACE simulations were performed. This involves placing a cylindrical tungsten target near the core and bombarding the target with electrons. These electrons produce high energy photons which in turn produce high energy neutrons from photonuclear

reactions. The target was determined to have a height of 10cm and a radius of 3.55cm after an optimization study was performed. Two locations were simulated; at the D7 and D2 positions. It was desired to obtain a total power generated in the reactor in excess of 1 kW so that temperature feedback effects could be seen. Assuming that an accelerator with 1 mA and 20 MeV electrons would be provided, the two positions yielded powers of 6.54 kW and 2.98 kW. Therefore, it would seem that the RACE project is feasible for the NSCR with the 30/20 fuel.

The 30/20 fuel performs well in comparison to the FLIP fuel. Since there is both more U-235 and U-238 atoms present in the 30/20 fuel, the fuel lifetime of this core exceeds the FLIP fuel. The control rod worths will provide enough excess reactivity to properly control the reactor. Steady-state temperatures generated in this fuel are well within the thermal limits. Additional tests will need to be conducted to determine the maximum pulsing experiments for this new fuel.

REFERENCES

1. T. A. PARISH, “Nuclear Safety Analyses and Core Design Calculations to Convert the Texas A&M University Nuclear Science Center Reactor to Low Enriched Uranium Fuel,” Nuclear Engineering Department, Texas A&M University, College Station, TX (1995).

2. B. T. REARDEN, “Engineering Analysis of a Power Upgrade for the Texas A&M Nuclear Science Center Reactor,” Nuclear Engineering Department, Texas A&M University, College Station, TX (1995).

3. X-5 MONTE CARLO TEAM, “MCNP-A General Monte Carlo N-Particle Transport Code, Version 5,” LA-UR-03-1987, Los Alamos National Laboratory, Los Alamos, NM (2003).

4. D. L. POSTON and H. R. TRELLUE, “User’s Manual, Version 2.0 for MONTEBURNS Version 1.0,” LA-UR-99-4999, Los Alamos National Laboratory, Los Alamos, NM (1999).

5. W. L. WOODRUFF and R. S. SMITH, “A Users Guide for the ANL Version of the PARET Code, PARET/ANL (2001 Rev.),” ANL/RERTR/TM-16, Argonne National Laboratory, Argonne, Illinois (2001).

6. TRIGA Reactor Facility, Nuclear Engineering Teaching Laboratory, The Univeristy of Texas at Austin, "Safety Analysis Report," (1991).

7. M. BADEA et al., "Improved S(α, β) Tables for TRIGA Criticality and Reactivity Feedback Calculations," Institute for Reactor Safety, Forschungszentrum Karlsruhe, Germany (2005).

8. W. M. STACEY, "Nuclear Reactor Physics," John Wiley & Sons, Inc, New York, NY (2001).

9. Advanced Fuel Cycle Initiative (AFCI) website (2003): http://afci.lanl.gov/aboutaaa.html, accessed on May 2006.

10. D. E. BELLER, "Draft Program Plan, AFCI Reactor-Accelerator Coupling Experiments (RACE) Project" Idaho State University-Idaho Accelerator Center, Pocatello, ID (2004).

11. T. WODDI, "Reactor Accelerator Coupling Experiments: A Feasibility Study," Nuclear Engineering Department, Texas A&M University, College Station, TX (2005).

12. A. G. CROFF, "A User's Manual for the Origen2 Computer Code," ORNL/TM-7175, Oak Ridge National Laboratory, Oak Ridge, TN (1980).

13. A. HAWARI, Personal Communication, North Carolina State University, (September 2005).

14. W. WHITTEMORE, Personal Communication, General Atomic, (October 2005).

15. Safety Evaluation Report on High-Uranium Content, Low-Enriched Uranium-Zirconium Hydride Fuels for TRIGA Reactors, NUREG-1282, U.S. Nuclear Regulatory Commission (1987).

16. Safety Analysis Report for the Nuclear Science Center Reactor, Texas A&M University, Texas Engineering Experiment Station (2003).

17. M. RAVNIK, "Nuclear Safety Parameters of Mixed TRIGA Cores," World Scientific, (1991).

APPENDIX A

ONE TO EIGHT RADIAL REGION COMPARISON

A.1. MCNP Input Deck for One Radial Region

```
3D Pin Cell from NSC Reactor
c
c        Cell Cards
1     1  0.04297569   -1 +8 -9            imp:n=1
2     2  0.0887799    -2 +1 +8 -9         imp:n=1
3     3  0.083848     -3 +2 +8 -9         imp:n=1
4     4  0.100040    -6 +7 -4 +5 +3 +8 -9 imp:n=1
99    0              +6 -7 +4 -5 +9 -8    imp:n=0

c        Surface cards
1     cz  0.2280
c    -  Interior Cells -
c    10    cz 0.4171375
c    11    cz 0.606275
c    12    cz 0.7954125
c    13    cz 0.98455
c    14    cz 1.1736875
c    15    cz 1.362825
c    16    cz 1.5519625
c
2     cz  1.7411
3     cz  1.7920
*4    px  1.9431
*5    px -1.9431
*6    py  1.9431
*7    py -1.9431
*8    pz -19.05
*9    pz  19.05

c        Material cards
kcode 3000 1.0 30 400
ksrc  0.2 0.2 0.0
c
c        Zirconiun
m1    40000.60c 4.29757e-2
c        U-ZrH Fuel
m2     1001.53c  4.91576e-2
       6000.66c  1.78701e-3
      40000.58c  3.22796e-2
      68166.34c  7.71700e-5
      68167.34c  5.29900e-5
      92234.66c  8.23000e-6
```

```
      92235.14c  1.08197e-3
      92236.66c  1.21000e-5
      92238.14c  4.32127e-3
      72000.60c  1.93677e-6
      94238.60c  1.0e-30
      94239.14c  1.0e-30
      94240.60c  1.0e-30
      94241.60c  1.0e-30
      94242.60c  1.0e-30
mt2    H/Zr2.05t
       Zr/H2.05t
c        SS304
m3    24000.50c  1.7482e-2
      26000.50c  5.6730e-2
      28000.50c  7.9390e-3
      25055.66c  1.6970e-3
m4     1001.66c  6.6691E-2
       8016.66c  3.3346E-2 $ Light water
mt4    lwtr.60t
```

A.2. MCNP Input Deck for Eight Radial Regions

```
3D Pin Cell from NSC Reactor
c
c        Cell Cards
1     1  0.04297569   -1 +8 -9             imp:n=1
c       - Interior cylinders -
11    11  0.0887799    1 -10 8 -9           imp:n=1
12    12  0.0887799    10 -11 8 -9          imp:n=1
13    13  0.0887799    11 -12 8 -9          imp:n=1
14    14  0.0887799    12 -13 8 -9          imp:n=1
15    15  0.0887799    13 -14 8 -9          imp:n=1
16    16  0.0887799    14 -15 8 -9          imp:n=1
17    17  0.0887799    15 -16 8 -9          imp:n=1
c
2     18  0.0887799    -2 +16 +8 -9         imp:n=1
3     3  0.083848     -3 +2 +8 -9           imp:n=1
4     4  0.100040    -6 +7 -4 +5 +3 +8 -9 imp:n=1
99    0              +6 -7 +4 -5 +9 -8    imp:n=0

c        Surface cards
1     cz  0.228
c    -  Interior Cells -
10    cz 0.4171375
11    cz 0.606275
12    cz 0.7954125
13    cz 0.98455
14    cz 1.1736875
15    cz 1.362825
16    cz 1.5519625
c
2     cz  1.7411
3     cz  1.7920
*4    px  1.9431
*5    px -1.9431
*6    py  1.9431
*7    py -1.9431
*8    pz -19.05
*9    pz  19.05

c        Material cards
kcode 3000 1.0 30 100
ksrc  0.2 0.2 0.0
c
c        Zirconiun
m1    40000.60c 4.29757e-2
c        U-ZrH Fuel
m11     1001.53c  4.91576e-2
       6000.66c  1.78701e-3
      40000.58c  3.22796e-2
      68166.34c  7.71700e-5
```

```
      68167.34c  5.29900e-5
      92234.66c  8.23000e-6
      92235.14c  1.08197e-3
      92236.66c  1.21000e-5
      92238.14c  4.32127e-3
      72000.60c  1.93677e-6
      94238.60c  1.0e-30
      94239.14c  1.0e-30
      94240.60c  1.0e-30
      94241.60c  1.0e-30
      94242.60c  1.0e-30
mt11    H/Zr2.05t
       Zr/H2.05t
c       U-ZrH Fuel
m12     1001.53c  4.91576e-2
       6000.66c  1.78701e-3
      40000.58c  3.22796e-2
      68166.34c  7.71700e-5
      68167.34c  5.29900e-5
      92234.66c  8.23000e-6
      92235.14c  1.08197e-3
      92236.66c  1.21000e-5
      92238.14c  4.32127e-3
      72000.60c  1.93677e-6
      94238.60c  1.0e-30
      94239.14c  1.0e-30
      94240.60c  1.0e-30
      94241.60c  1.0e-30
      94242.60c  1.0e-30
mt12    H/Zr2.05t
       Zr/H2.05t
c       U-ZrH Fuel
m13     1001.53c  4.91576e-2
       6000.66c  1.78701e-3
      40000.58c  3.22796e-2
      68166.34c  7.71700e-5
      68167.34c  5.29900e-5
      92234.66c  8.23000e-6
      92235.14c  1.08197e-3
      92236.66c  1.21000e-5
      92238.14c  4.32127e-3
      72000.60c  1.93677e-6
      94238.60c  1.0e-30
      94239.14c  1.0e-30
      94240.60c  1.0e-30
      94241.60c  1.0e-30
      94242.60c  1.0e-30
mt13    H/Zr2.05t
       Zr/H2.05t
c       U-ZrH Fuel
m14     1001.53c  4.91576e-2
```

```
       6000.66c  1.78701e-3
      40000.58c  3.22796e-2
      68166.34c  7.71700e-5
      68167.34c  5.29900e-5
      92234.66c  8.23000e-6
      92235.14c  1.08197e-3
      92236.66c  1.21000e-5
      92238.14c  4.32127e-3
      72000.60c  1.93677e-6
      94238.60c  1.0e-30
      94239.14c  1.0e-30
      94240.60c  1.0e-30
      94241.60c  1.0e-30
      94242.60c  1.0e-30
mt14    H/Zr2.05t
       Zr/H2.05t
c        U-ZrH Fuel
m15     1001.53c  4.91576e-2
       6000.66c  1.78701e-3
      40000.58c  3.22796e-2
      68166.34c  7.71700e-5
      68167.34c  5.29900e-5
      92234.66c  8.23000e-6
      92235.14c  1.08197e-3
      92236.66c  1.21000e-5
      92238.14c  4.32127e-3
      72000.60c  1.93677e-6
      94238.60c  1.0e-30
      94239.14c  1.0e-30
      94240.60c  1.0e-30
      94241.60c  1.0e-30
      94242.60c  1.0e-30
mt15    H/Zr2.05t
       Zr/H2.05t
c        U-ZrH Fuel
m16     1001.53c  4.91576e-2
       6000.66c  1.78701e-3
      40000.58c  3.22796e-2
      68166.34c  7.71700e-5
      68167.34c  5.29900e-5
      92234.66c  8.23000e-6
      92235.14c  1.08197e-3
      92236.66c  1.21000e-5
      92238.14c  4.32127e-3
      72000.60c  1.93677e-6
      94238.60c  1.0e-30
      94239.14c  1.0e-30
      94240.60c  1.0e-30
      94241.60c  1.0e-30
      94242.60c  1.0e-30
mt16    H/Zr2.05t
```

```
       Zr/H2.05t
c        U-ZrH Fuel
m17     1001.53c  4.91576e-2
       6000.66c  1.78701e-3
      40000.58c  3.22796e-2
      68166.34c  7.71700e-5
      68167.34c  5.29900e-5
      92234.66c  8.23000e-6
      92235.14c  1.08197e-3
      92236.66c  1.21000e-5
      92238.14c  4.32127e-3
      72000.60c  1.93677e-6
      94238.60c  1.0e-30
      94239.14c  1.0e-30
      94240.60c  1.0e-30
      94241.60c  1.0e-30
      94242.60c  1.0e-30
mt17    H/Zr2.05t
       Zr/H2.05t
c        U-ZrH Fuel
m18     1001.53c  4.91576e-2
       6000.66c  1.78701e-3
      40000.58c  3.22796e-2
      68166.34c  7.71700e-5
      68167.34c  5.29900e-5
      92234.66c  8.23000e-6
      92235.14c  1.08197e-3
      92236.66c  1.21000e-5
      92238.14c  4.32127e-3
      72000.60c  1.93677e-6
      94238.60c  1.0e-30
      94239.14c  1.0e-30
      94240.60c  1.0e-30
      94241.60c  1.0e-30
      94242.60c  1.0e-30
mt18    H/Zr2.05t
       Zr/H2.05t
c        SS304
m3    24000.50c  1.7482e-2
      26000.50c  5.6730e-2
      28000.50c  7.9390e-3
      25055.66c  1.6970e-3
m4     1001.66c  6.6691E-2
       8016.66c  3.3346E-2 $ Light water
mt4    lwtr.60t
```

A.3. Monteburns Input for Eight Radial Regions

```
DPRK Rod Irradiation
PC
8                     !Number of MCNP Materials to Burn
11                    !MCNP Material "m" Numbers
12
13
14
15
16
17
18
14.60511             !Volume of Cells Containing the Materials
23.16878
31.73246
40.29613
48.8598
57.42348
65.98715
74.55083
0.0116279             !Power in MWt
-196.0                !Q-value for Fission
5000.0                !Total Number of Days Burned
2                     !Number of Outer Burn Steps
1                     !Number of Inner Burn Steps
1                     !Number of Predictor Steps
0                     !Step to Restart After
candunau              !ORIGEN2 Library
/packages/origen/origen22/libs  !Location of ORIGEN2 Library
0.005                 !Fractional Importance Limit
1                     !Flag for Intermediate keff Calculations
24                     !Number of Automatic Tally Isotopes
92234.66c
92235.14c
92236.66c
92237.50c
92238.14c
92239.35c
93237.60c
94238.60c
94239.14c
94240.60c
94241.60c
94242.60c
95241.60c
95242.66c
95243.60c
62149.66c
62150.50c
62152.50c
```

```
40000.58c
1001.53c
68166.34c
68167.34c
6000.66c
72000.60c
24                    !Number of Automatic Tally Isotopes
92234.66c
92235.14c
92236.66c
92237.50c
92238.14c
92239.35c
93237.60c
94238.60c
94239.14c
94240.60c
94241.60c
94242.60c
95241.60c
95242.66c
95243.60c
62149.66c
62150.50c
62152.50c
40000.58c
1001.53c
68166.34c
68167.34c
6000.66c
72000.60c
24                    !Number of Automatic Tally Isotopes
92234.66c
92235.14c
92236.66c
92237.50c
92238.14c
92239.35c
93237.60c
94238.60c
94239.14c
94240.60c
94241.60c
94242.60c
95241.60c
95242.66c
95243.60c
62149.66c
62150.50c
62152.50c
40000.58c
```

```
1001.53c
68166.34c
68167.34c
6000.66c
72000.60c
24                    !Number of Automatic Tally Isotopes
92234.66c
92235.14c
92236.66c
92237.50c
92238.14c
92239.35c
93237.60c
94238.60c
94239.14c
94240.60c
94241.60c
94242.60c
95241.60c
95242.66c
95243.60c
62149.66c
62150.50c
62152.50c
40000.58c
1001.53c
68166.34c
68167.34c
6000.66c
72000.60c
24                    !Number of Automatic Tally Isotopes
92234.66c
92235.14c
92236.66c
92237.50c
92238.14c
92239.35c
93237.60c
94238.60c
94239.14c
94240.60c
94241.60c
94242.60c
95241.60c
95242.66c
95243.60c
62149.66c
62150.50c
62152.50c
40000.58c
1001.53c
```

```
68166.34c
68167.34c
6000.66c
72000.60c
24                    !Number of Automatic Tally Isotopes
92234.66c
92235.14c
92236.66c
92237.50c
92238.14c
92239.35c
93237.60c
94238.60c
94239.14c
94240.60c
94241.60c
94242.60c
95241.60c
95242.66c
95243.60c
62149.66c
62150.50c
62152.50c
40000.58c
1001.53c
68166.34c
68167.34c
6000.66c
72000.60c
24                    !Number of Automatic Tally Isotopes
92234.66c
92235.14c
92236.66c
92237.50c
92238.14c
92239.35c
93237.60c
94238.60c
94239.14c
94240.60c
94241.60c
94242.60c
95241.60c
95242.66c
95243.60c
62149.66c
62150.50c
62152.50c
40000.58c
1001.53c
68166.34c
```

```
68167.34c
6000.66c
72000.60c
24                    !Number of Automatic Tally Isotopes
92234.66c
92235.14c
92236.66c
92237.50c
92238.14c
92239.35c
93237.60c
94238.60c
94239.14c
94240.60c
94241.60c
94242.60c
95241.60c
95242.66c
95243.60c
62149.66c
62150.50c
62152.50c
40000.58c
1001.53c
68166.34c
68167.34c
6000.66c
72000.60c
```

APPENDIX B

ADDITIONAL FLIP TO LEU COMPARISON FIGURES

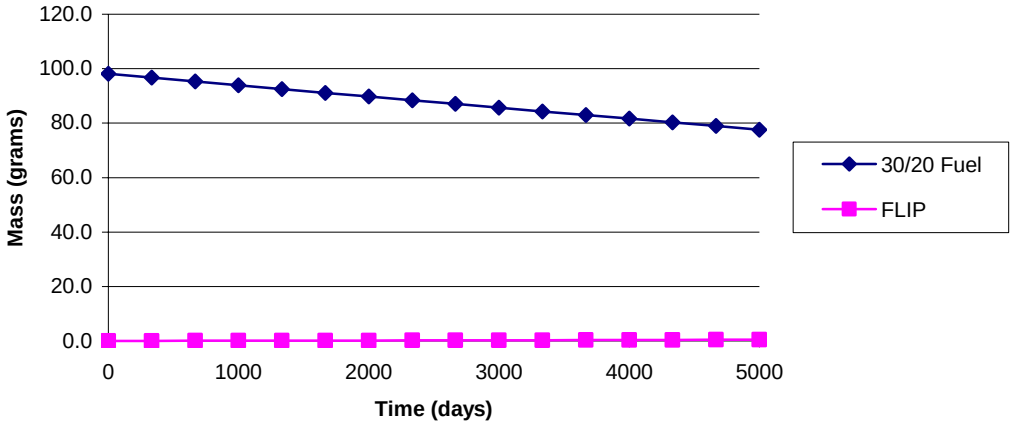

B-1. FLIP to LEU comparison: U-234 versus time with no thermal column.

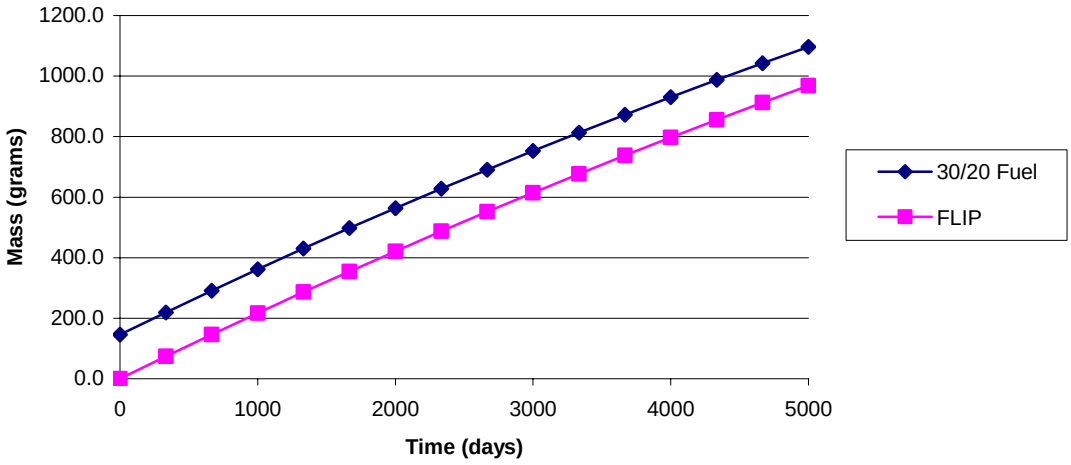

B-2. FLIP to LEU comparison: U-236 versus time with no thermal column.

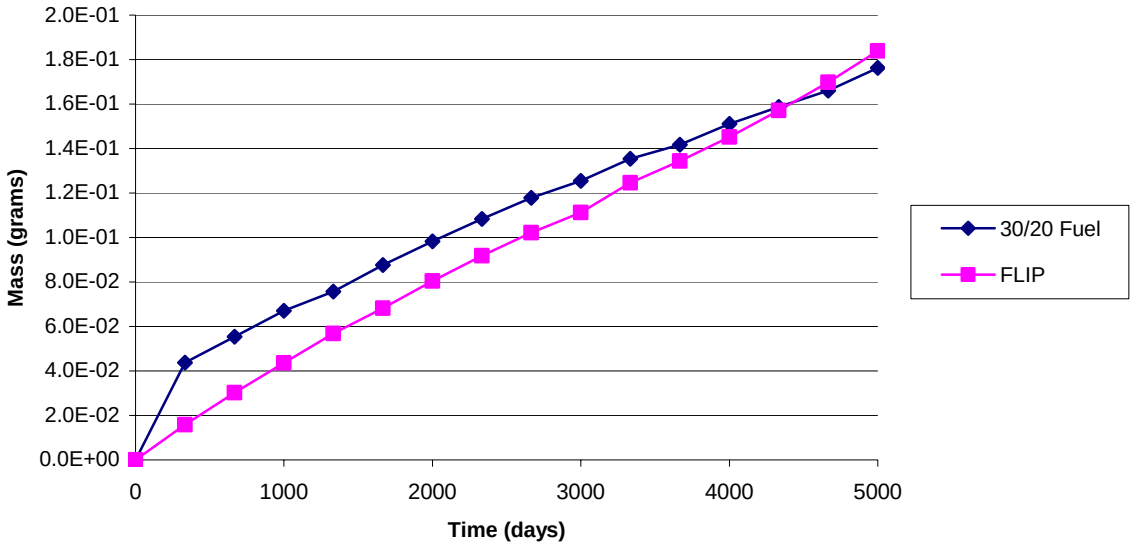

B-3. FLIP to LEU comparison: U-237 versus time with no thermal column.

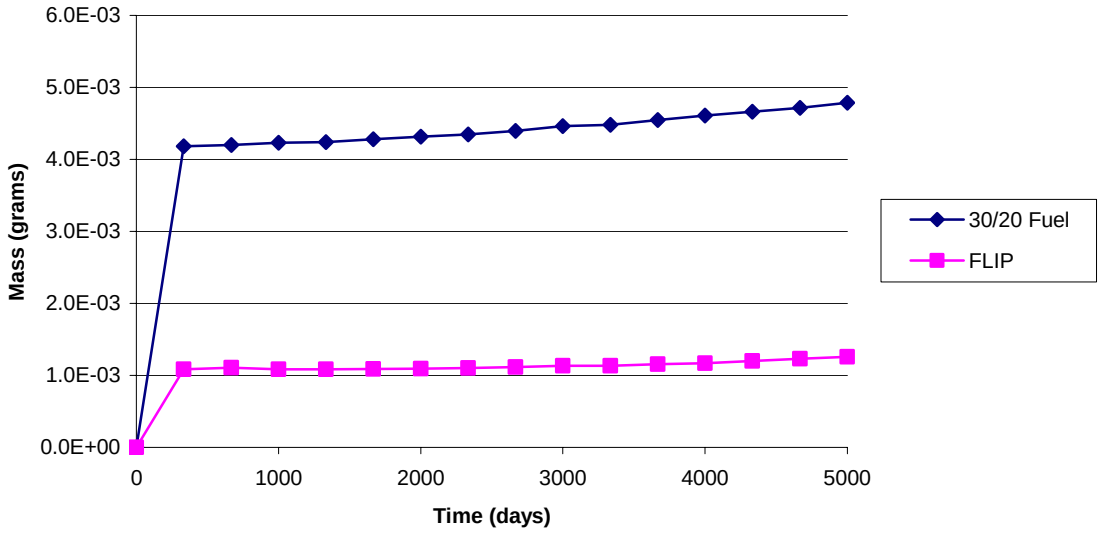

B-4. FLIP to LEU comparison: U-239 versus time with no thermal column.

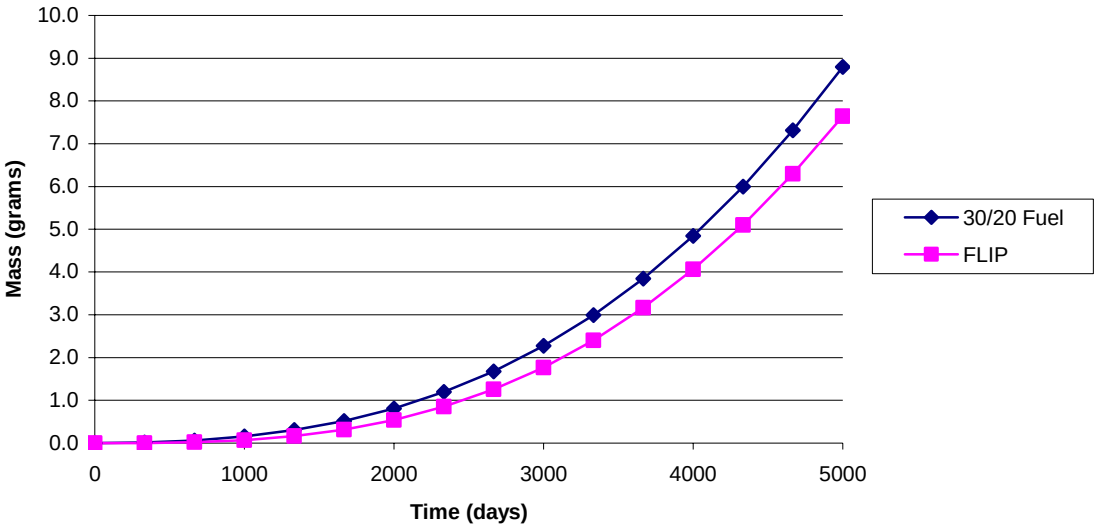

B-5. FLIP to LEU comparison: Pu-238 versus time with no thermal column.

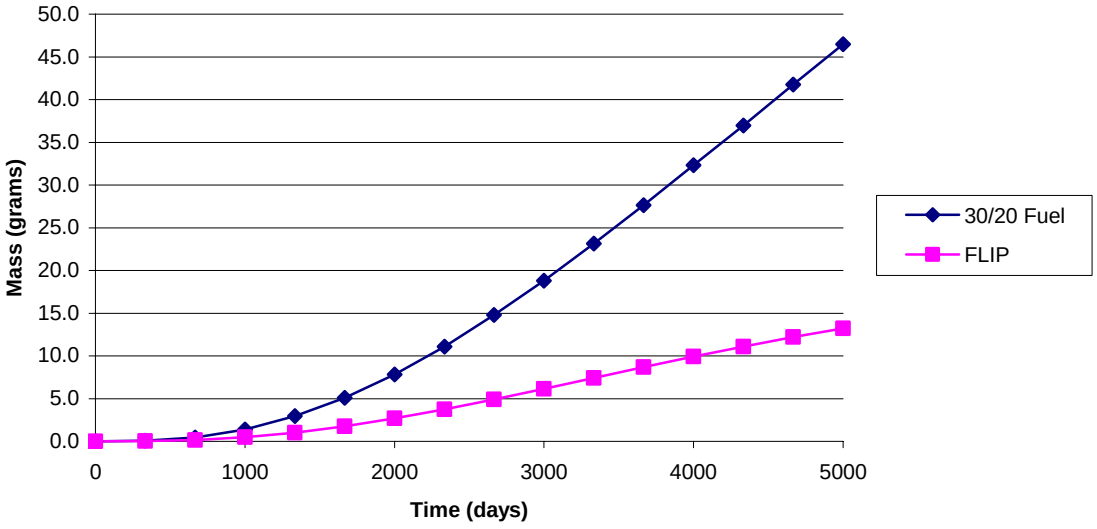

B-6. FLIP to LEU comparison: Pu-241 versus time with no thermal column.

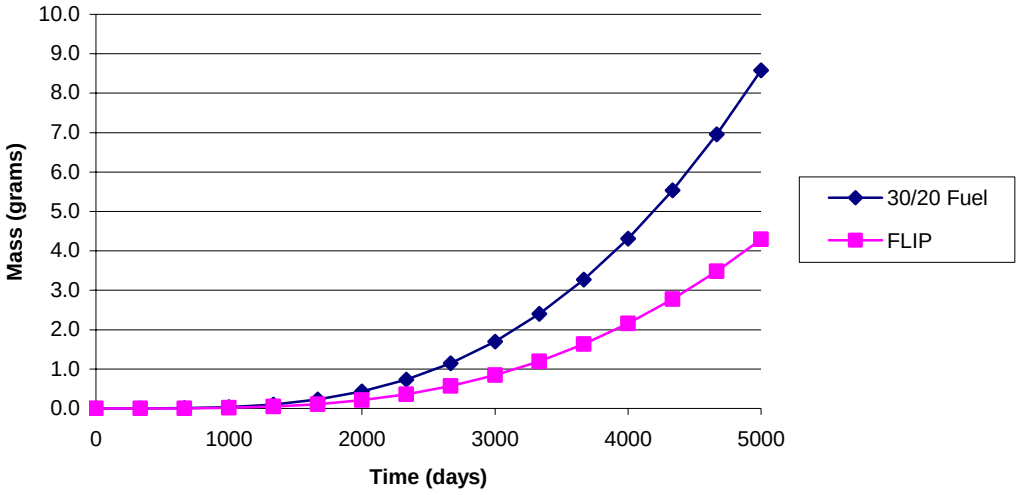

B-7. FLIP to LEU comparison: Pu-242 versus time with no thermal column.

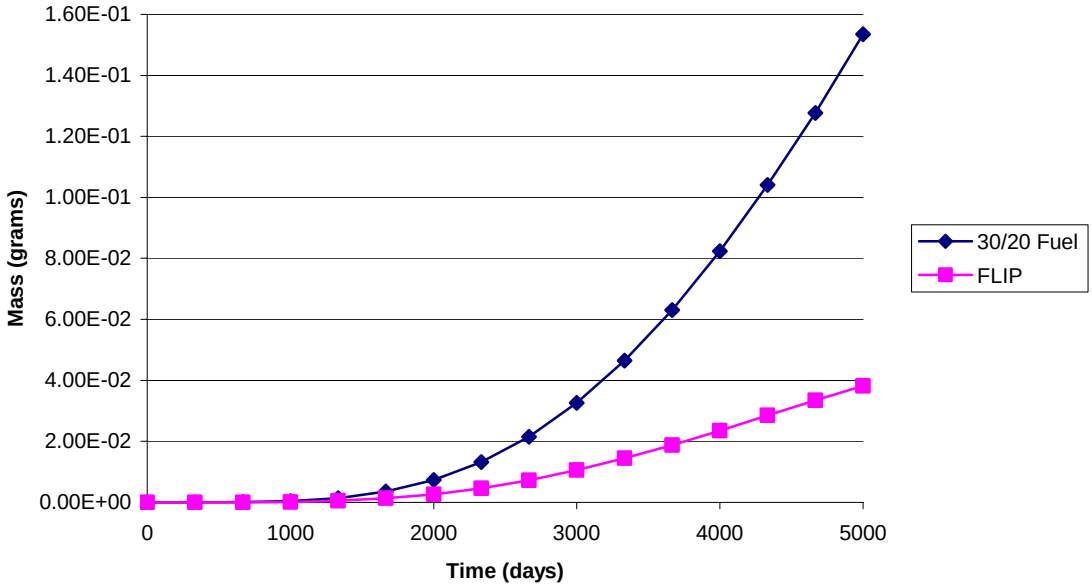

B-8. FLIP to LEU comparison: Am-242 versus time with no thermal column.

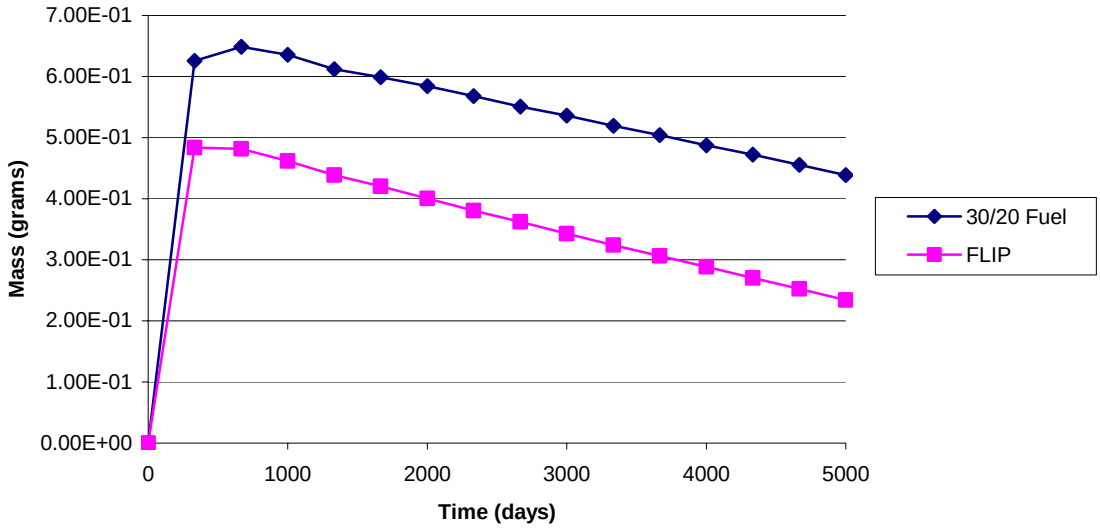

B-9. FLIP to LEU comparison: Sm-149 versus time with no thermal column.

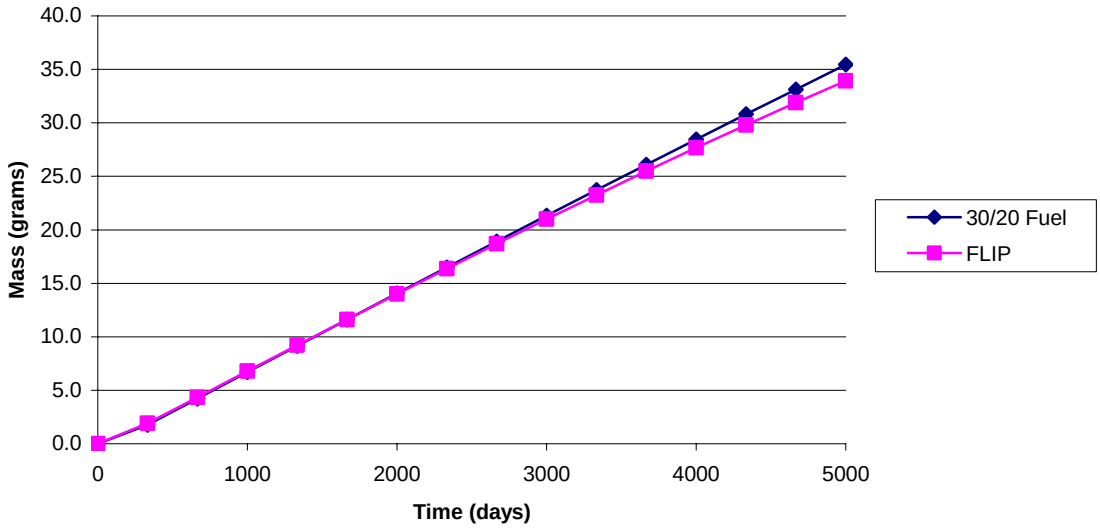

B-10. FLIP to LEU comparison: Sm-150 versus time with no thermal column.

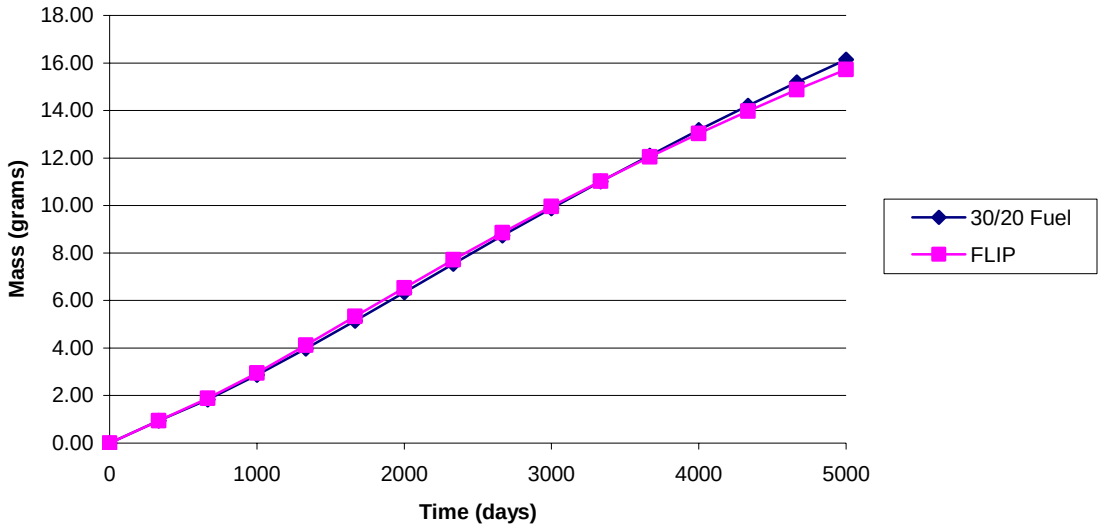

B-11. FLIP to LEU comparison: Sm-152 versus time with no thermal column.

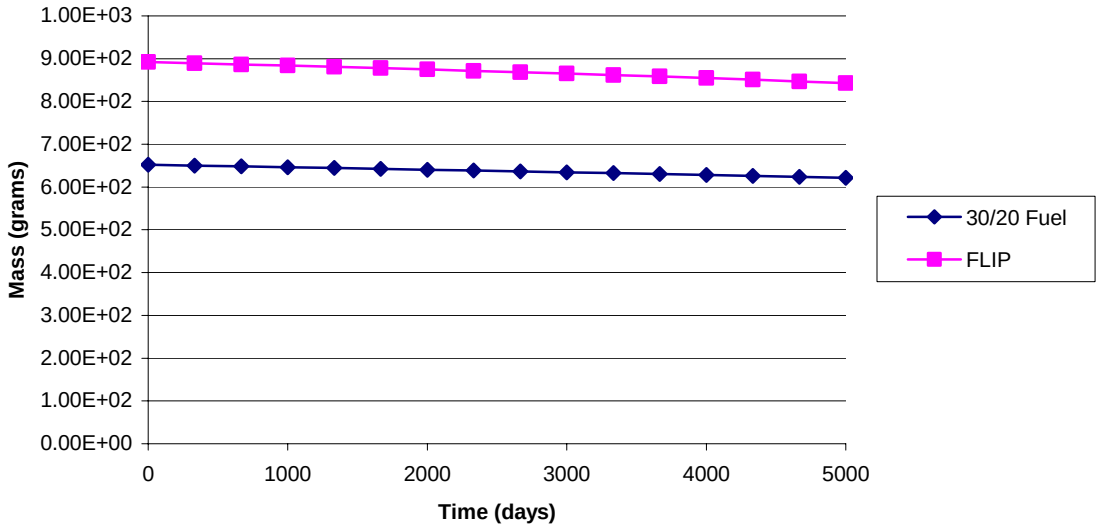

B-12. FLIP to LEU comparison: Er-166 versus time with no thermal column.

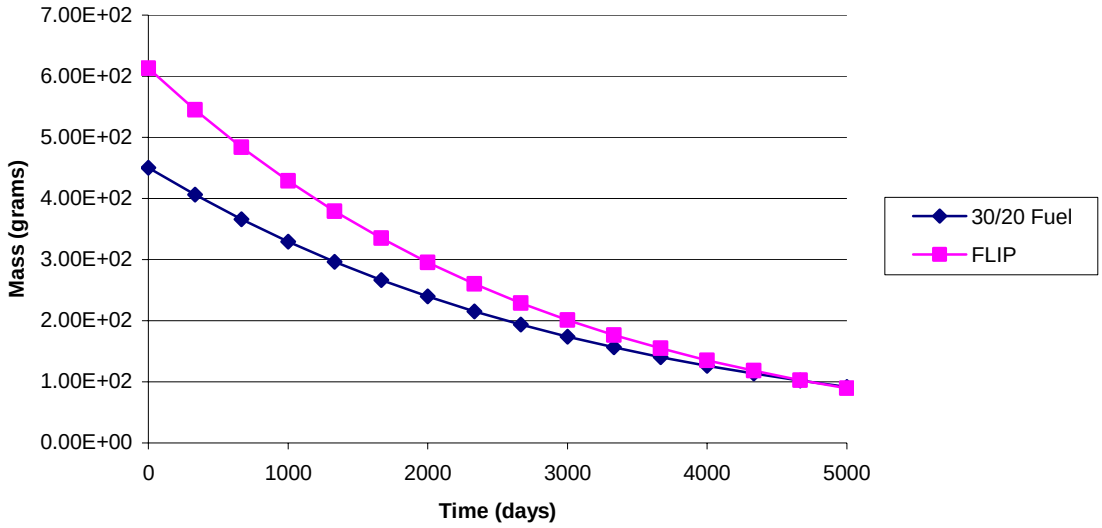

B-13. FLIP to LEU comparison: Er-167 versus time with no thermal column.

APPENDIX C

THERMAL ANALYSIS

C.1. MCNP Input Deck for NSCR with 15 Materials

```
TRIGA Reactor 3D Core Lattice (no thermal column)
c
c   - Description -
c
c        This deck includes a full core simulation for the
c        TAMU NSC TRIGA. Rod-to-rod spacing is rod averages
c        in x- and y-dimensions. Spacing is rectangular (not
c        square).  Fuel and clad materials are from Rearden
c        Thesis (August 1995).  The grid plate is included as
c        a solid aluminum section beneath the core. Support
c        structure for the grid plate was not included. Also,
c        the beam ports and thermal column were not included.
c        Since the pool is essentially infinitely large, the
c        tank and tank liner were ignored.
c
c        Shim safety rods must be moved in bank using surfaces
c        200, 201, and 202. The transient rod can be moved using
c        surfaces 302, 303, 304, and 305.  The Regulating rod can
c        be moved using surfaces 402 and 403.  Fuel and rod
c        materials are all fresh.  Erbium cross sections are
c        from Charlton-3xc-library, all other cross sections
c        are ENDF/B-VI standard MCNP cross sections.
c
c        Modified for 30/20 fuel.
c
c     -- Cell Cards --
c
c         - Fuel Pin -
09    1  0.04297569  -100 +111 -112      u=9 imp:n=1
101   11  0.0887799  +100 -101 +111 -1000 u=9 imp:n=1
102   12  0.0887799  +100 -101 +1000 -1001 u=9 imp:n=1
103   13  0.0887799  +100 -101 +1001 -1002 u=9 imp:n=1
104   14  0.0887799  +100 -101 +1002 -1003 u=9 imp:n=1
105   15  0.0887799  +100 -101 +1003 -112 u=9 imp:n=1
11    3  0.083848  +101 -102 +110 -113   u=9 imp:n=1
12    7  0.0878229  -101 +110 -111     u=9 imp:n=1
13    7  0.0878229  -101 +112 -113     u=9 imp:n=1
14    8  0.089452  -102 +113 -114        u=9 imp:n=1
15    9  0.095482  -102 -110 +109        u=9 imp:n=1
16   10  0.060220  -109 +108            u=9 imp:n=1
17    4  0.100040  +102 +109            u=9 imp:n=1
18    4  0.100040  -108                 u=9 imp:n=1
```

```
19    4  0.100040  -102 +114             u=9 imp:n=1
c
c         - Fuel Pin -
209    1  0.04297569  -100 +111 -112      u=10 imp:n=1
2101   16  0.0887799  +100 -101 +111 -1000 u=10 imp:n=1
2102   17  0.0887799  +100 -101 +1000 -1001 u=10 imp:n=1
2103   18  0.0887799  +100 -101 +1001 -1002 u=10 imp:n=1
2104   19  0.0887799  +100 -101 +1002 -1003 u=10 imp:n=1
2105   20  0.0887799  +100 -101 +1003 -112 u=10 imp:n=1
211    3  0.083848  +101 -102 +110 -113   u=10 imp:n=1
212    7  0.0878229  -101 +110 -111     u=10 imp:n=1
213    7  0.0878229  -101 +112 -113     u=10 imp:n=1
214    8  0.089452  -102 +113 -114        u=10 imp:n=1
215    9  0.095482  -102 -110 +109        u=10 imp:n=1
216   10  0.060220  -109 +108            u=10 imp:n=1
217    4  0.100040  +102 +109            u=10 imp:n=1
218    4  0.100040  -108                 u=10 imp:n=1
219    4  0.100040  -102 +114            u=10 imp:n=1
c
c         - Fuel Pin -
309    1  0.04297569  -100 +111 -112      u=11 imp:n=1
3101   21  0.0887799  +100 -101 +111 -1000 u=11 imp:n=1
3102   22  0.0887799  +100 -101 +1000 -1001 u=11 imp:n=1
3103   23  0.0887799  +100 -101 +1001 -1002 u=11 imp:n=1
3104   24  0.0887799  +100 -101 +1002 -1003 u=11 imp:n=1
3105   25  0.0887799  +100 -101 +1003 -112 u=11 imp:n=1
311    3  0.083848  +101 -102 +110 -113   u=11 imp:n=1
312    7  0.0878229  -101 +110 -111     u=11 imp:n=1
313    7  0.0878229  -101 +112 -113     u=11 imp:n=1
314    8  0.089452  -102 +113 -114        u=11 imp:n=1
315    9  0.095482  -102 -110 +109        u=11 imp:n=1
316   10  0.060220  -109 +108            u=11 imp:n=1
317    4  0.100040  +102 +109            u=11 imp:n=1
318    4  0.100040  -108                 u=11 imp:n=1
319    4  0.100040  -102 +114            u=11 imp:n=1
c
c
c         - Shim Safety Control Rod -
20    5  0.135143  -101 +201 -202        u=2 imp:n=1
21    3  0.083848  +101 -102 +200 -202   u=2 imp:n=1
22    1  0.04297569  -100 +200 -201      u=2 imp:n=1
23    2  0.0887779  +100 -101 +200 -201  u=2 imp:n=1
24    4  0.100040  +102 +109            u=2 imp:n=1
25    4  0.100040  -102 -200            u=2 imp:n=1
26    4  0.100040  -102 +202            u=2 imp:n=1
27   10  0.060220  +102 -109 +108        u=2 imp:n=1
28    4  0.100040  +102 -108            u=2 imp:n=1
c
c         - Transient Control Rod -
30    5  0.135143  -300 +303 -304        u=3 imp:n=1
31    3  0.083848  +300 -301 +302 -305   u=3 imp:n=1
```

```
32    0            -300 +302 -303        u=3 imp:n=1
33    4  0.100040  +301 +109             u=3 imp:n=1
34    4  0.100040  -301 -302             u=3 imp:n=1
35    0            -300 +304 -305        u=3 imp:n=1
36    4  0.100040  -301 +305             u=3 imp:n=1
37   10  0.060220  +301 -109 +108        u=3 imp:n=1
38    4  0.100040  +301 -108             u=3 imp:n=1
c
c         - Regulating Control Rod -
40    6  0.127794  -400 +402 -403        u=4 imp:n=1
41    3  0.083848  +400 -401 +402 -403   u=4 imp:n=1
42    4  0.100040  +401 +109             u=4 imp:n=1
43    4  0.100040  -401 -402             u=4 imp:n=1
44    4  0.100040  -401 +403             u=4 imp:n=1
45   10  0.060220  +401 -109 +108        u=4 imp:n=1
46    4  0.100040  +401 -108             u=4 imp:n=1
c
c         - Graphite Element -
50    7  0.0878229  -500 +109 -502     u=5 imp:n=1
51    7  0.0878229  +500 +109 -502     u=5 imp:n=1
52   10  0.060220  -500 -109 +108        u=5 imp:n=1
53    4  0.100040  -108                  u=5 imp:n=1
54    4  0.100040  +502                  u=5 imp:n=1
c
c         - Water Hole -
60    4  0.100040  -500 +109             u=6 imp:n=1
61    4  0.100040  +500                  u=6 imp:n=1
62   10  0.060220  -500 -109 +108        u=6 imp:n=1
63    4  0.100040  -500 -108             u=6 imp:n=1
c
c         - Water Hole with Tally Element -
70    4  0.100040  -500 +600 -601        u=7 imp:n=1 vol=156.1064 $
Tally vol in water
71    4  0.100040  -500 -600 +109        u=7 imp:n=1
72    4  0.100040  -500 +601             u=7 imp:n=1
73    4  0.100040  +500                  u=7 imp:n=1
74   10  0.060220  -500 -109 +108        u=7 imp:n=1
75    4  0.100040  -500 -108             u=7 imp:n=1
c
c         - Fuel Assembly  Lattice -
700   0        -702 +701 -704 +703 lat=1 u=8 fill=0:17 0:11 0:0
      5 5 11 11 11 11 11 11 11 11 11 11 11 5 5 5 5
      5 5 11 11 11 4 11 11 11 11 11 11 11 5 5 5 5
      5 5 5 5 11 10 10 10 10 10 10 10 11 11 5 5 5 5
      5 5 5 5 11 10 2 10 10 10 2 10 11 11 5 5 5 5
      5 5 6 6 7 7 10 9 9 9 9 10 6 6 5 5 5 5
      5 5 6 6 7 7 10 9 3 9 9 10 6 6 5 5 5 5
      5 5 5 5 11 10 10 10 10 10 10 10 11 11 5 5 5 5
      5 5 5 5 11 10 2 10 10 10 2 10 11 11 5 5 5 5
      7 7 5 5 11 11 11 11 11 11 11 11 11 11 5 5 5 5
      7 7 5 5 11 11 6 6 11 11 6 6 11 11 5 5 5 5
```

```
      6 6 6 6 6 6 6 6 6 6 6 6 6 6 6 6 6 6
      6 6 6 6 6 6 6 6 6 6 6 6 6 6 6 6 6 6    imp:n=1
801   0        +800 -801 +802 -803 +804 -805 fill=8  imp:n=1
c         - Thermal Colunm
80    7  8.1299E-2 -80 +81 -82 -83 -84 -85     imp:n=1
c
c         - Universe -
900   4  0.10004   #801 #80 -900 imp:n=1
999   0            +900                       imp:n=0

c
c     -- Surface Cards --
c
c         - Fuel Pin Surfaces -
100   c/z   2.025015 1.927225 0.2280
101   c/z   2.025015 1.927225 1.7411
102   c/z   2.025015 1.927225 1.7920
108   pz  -30.48
109   pz  -17.78
110   pz   -8.89
111   pz    0.00
112   pz   38.10
113   pz   46.99
114   pz   58.42
c     -- Inner fuel surfaces --
1000  pz 7.62
1001  pz 15.24
1002  pz 22.86
1003  pz 30.48
c
c         - Shim Safety Rod Surfaces -
200   pz   0.00 $(0.00 for full removal)
201   pz   38.10 $(38.10 for full removal)
202   pz   73.66 $(73.66 for full removal)
c
c         - Transient Rod Surfaces -
300   c/z   2.025015 1.927225 1.5164
301   c/z   2.025015 1.927225 1.5876
302   pz   -8.89
303   pz   38.10 $(38.10 for full removal)
304   pz   76.20 $(76.20 for full removal)
305   pz   80.00
c
c         -Regulating Rod Surfaces -
400   c/z   2.025015 1.927225 1.5164
401   c/z   2.025015 1.927225 1.5876
402   pz   38.10 $(38.10 for full removal)
403   pz   76.20 $(76.20 for full removal)
c
c         - Water Hole and Graphite Element Surfaces -
500   c/z   2.025015 1.927225 7.0000
```

```
501   pz   -8.89
502   pz   46.99
c
c         - Tally Element Surfaces -
600   pz   14.00
601   pz   24.00
c
c         - Pin Cell Surfaces -
701   px   0.00
702   px   4.05003
703   py   0.00
704   py   3.85445
c
c         - Core Surfaces -
800   px   0.0001
801   px  72.90053
802   py   0.0001
803   py  46.2533
804   pz -100.0
805   pz  100.0
c
c         - Thermal Colunm -
c     -  y-Planes that define the front and back
80     py    -1.2705
81     py -306.0705
c     -  Inclined planes, each plane is defined by 3 points
82     P -9.269735 -0.0005 41.91  82.170265 -0.0005 41.91
          97.410265 -304.8005 80.01                          $ Top
Plane
83     P 82.170265 -0.0005 41.91  97.410265 -304.8005 80.01
         82.170265 -0.0005 -3.81                           $ Right
Plane
84     P -9.269735 -0.0005 41.91  -9.269735 -0.0005 -3.81
         -24.509735 -304.8005 -41.91                        $ Left
Plane
85     P -9.269735 -0.0005 -3.81  82.170265 -0.0005 -3.81
          97.410265 -304.8005 -41.91                        $ Bottom
Plane
c
c         - Reflector and Universe Cells -
900   cz 1000.00

c
c     -- Data Cards --
c
mode  n
kcode 3000 1.0 20 400
ksrc  37.0 22.0 19.0
m1    40000.60c 4.29757e-2
c        U-ZrH Fuel
m2     1001.53c  4.91576e-2
```

```
       6000.66c  1.78701e-3
      40000.58c  3.22796e-2
      68166.34c  7.71700e-5
      68167.34c  5.29900e-5
      92234.66c  8.23000e-6
      92235.14c  1.08197e-3
      92236.66c  1.21000e-5
      92238.14c  4.32127e-3
      72000.60c  1.93677e-6
      94238.60c  1.0e-30
      94239.14c  1.0e-30
      94240.60c  1.0e-30
      94241.60c  1.0e-30
      94242.60c  1.0e-30
mt2    H/Zr2.05t
       Zr/H2.05t
m11    1001.53c  4.91576e-2
       6000.66c  1.78701e-3
      40000.58c  3.22796e-2
      68166.34c  7.71700e-5
      68167.34c  5.29900e-5
      92234.66c  8.23000e-6
      92235.14c  1.08197e-3
      92236.66c  1.21000e-5
      92238.14c  4.32127e-3
      72000.60c  1.93677e-6
      94238.60c  1.0e-30
      94239.14c  1.0e-30
      94240.60c  1.0e-30
      94241.60c  1.0e-30
      94242.60c  1.0e-30
mt11    H/Zr2.05t
       Zr/H2.05t
m12    1001.53c  4.91576e-2
       6000.66c  1.78701e-3
      40000.58c  3.22796e-2
      68166.34c  7.71700e-5
      68167.34c  5.29900e-5
      92234.66c  8.23000e-6
      92235.14c  1.08197e-3
      92236.66c  1.21000e-5
      92238.14c  4.32127e-3
      72000.60c  1.93677e-6
      94238.60c  1.0e-30
      94239.14c  1.0e-30
      94240.60c  1.0e-30
      94241.60c  1.0e-30
      94242.60c  1.0e-30
mt12    H/Zr2.05t
       Zr/H2.05t
m13     1001.53c  4.91576e-2
```

```
       6000.66c  1.78701e-3
      40000.58c  3.22796e-2
      68166.34c  7.71700e-5
      68167.34c  5.29900e-5
      92234.66c  8.23000e-6
      92235.14c  1.08197e-3
      92236.66c  1.21000e-5
      92238.14c  4.32127e-3
      72000.60c  1.93677e-6
      94238.60c  1.0e-30
      94239.14c  1.0e-30
      94240.60c  1.0e-30
      94241.60c  1.0e-30
      94242.60c  1.0e-30
mt13    H/Zr2.05t
       Zr/H2.05t
m14     1001.53c  4.91576e-2
       6000.66c  1.78701e-3
      40000.58c  3.22796e-2
      68166.34c  7.71700e-5
      68167.34c  5.29900e-5
      92234.66c  8.23000e-6
      92235.14c  1.08197e-3
      92236.66c  1.21000e-5
      92238.14c  4.32127e-3
      72000.60c  1.93677e-6
      94238.60c  1.0e-30
      94239.14c  1.0e-30
      94240.60c  1.0e-30
      94241.60c  1.0e-30
      94242.60c  1.0e-30
mt14    H/Zr2.05t
       Zr/H2.05t
m15     1001.53c  4.91576e-2
       6000.66c  1.78701e-3
      40000.58c  3.22796e-2
      68166.34c  7.71700e-5
      68167.34c  5.29900e-5
      92234.66c  8.23000e-6
      92235.14c  1.08197e-3
      92236.66c  1.21000e-5
      92238.14c  4.32127e-3
      72000.60c  1.93677e-6
      94238.60c  1.0e-30
      94239.14c  1.0e-30
      94240.60c  1.0e-30
      94241.60c  1.0e-30
      94242.60c  1.0e-30
mt15    H/Zr2.05t
       Zr/H2.05t
m16     1001.53c  4.91576e-2
```

```
        6000.66c  1.78701e-3
       40000.58c  3.22796e-2
       68166.34c  7.71700e-5
       68167.34c  5.29900e-5
       92234.66c  8.23000e-6
       92235.14c  1.08197e-3
       92236.66c  1.21000e-5
       92238.14c  4.32127e-3
       72000.60c  1.93677e-6
       94238.60c  1.0e-30
       94239.14c  1.0e-30
       94240.60c  1.0e-30
       94241.60c  1.0e-30
       94242.60c  1.0e-30
mt16    H/Zr2.05t
        Zr/H2.05t
m17     1001.53c  4.91576e-2
        6000.66c  1.78701e-3
       40000.58c  3.22796e-2
       68166.34c  7.71700e-5
       68167.34c  5.29900e-5
       92234.66c  8.23000e-6
       92235.14c  1.08197e-3
       92236.66c  1.21000e-5
       92238.14c  4.32127e-3
       72000.60c  1.93677e-6
       94238.60c  1.0e-30
       94239.14c  1.0e-30
       94240.60c  1.0e-30
       94241.60c  1.0e-30
       94242.60c  1.0e-30
mt17    H/Zr2.05t
        Zr/H2.05t
m18     1001.53c  4.91576e-2
        6000.66c  1.78701e-3
       40000.58c  3.22796e-2
       68166.34c  7.71700e-5
       68167.34c  5.29900e-5
       92234.66c  8.23000e-6
       92235.14c  1.08197e-3
       92236.66c  1.21000e-5
       92238.14c  4.32127e-3
       72000.60c  1.93677e-6
       94238.60c  1.0e-30
       94239.14c  1.0e-30
       94240.60c  1.0e-30
       94241.60c  1.0e-30
       94242.60c  1.0e-30
mt18    H/Zr2.05t
        Zr/H2.05t
m19     1001.53c  4.91576e-2
```

```
       6000.66c  1.78701e-3
      40000.58c  3.22796e-2
      68166.34c  7.71700e-5
      68167.34c  5.29900e-5
      92234.66c  8.23000e-6
      92235.14c  1.08197e-3
      92236.66c  1.21000e-5
      92238.14c  4.32127e-3
      72000.60c  1.93677e-6
      94238.60c  1.0e-30
      94239.14c  1.0e-30
      94240.60c  1.0e-30
      94241.60c  1.0e-30
      94242.60c  1.0e-30
mt19    H/Zr2.05t
       Zr/H2.05t
m20     1001.53c  4.91576e-2
       6000.66c  1.78701e-3
      40000.58c  3.22796e-2
      68166.34c  7.71700e-5
      68167.34c  5.29900e-5
      92234.66c  8.23000e-6
      92235.14c  1.08197e-3
      92236.66c  1.21000e-5
      92238.14c  4.32127e-3
      72000.60c  1.93677e-6
      94238.60c  1.0e-30
      94239.14c  1.0e-30
      94240.60c  1.0e-30
      94241.60c  1.0e-30
      94242.60c  1.0e-30
mt20    H/Zr2.05t
       Zr/H2.05t
m21     1001.53c  4.91576e-2
       6000.66c  1.78701e-3
      40000.58c  3.22796e-2
      68166.34c  7.71700e-5
      68167.34c  5.29900e-5
      92234.66c  8.23000e-6
      92235.14c  1.08197e-3
      92236.66c  1.21000e-5
      92238.14c  4.32127e-3
      72000.60c  1.93677e-6
      94238.60c  1.0e-30
      94239.14c  1.0e-30
      94240.60c  1.0e-30
      94241.60c  1.0e-30
      94242.60c  1.0e-30
mt21    H/Zr2.05t
       Zr/H2.05t
m22     1001.53c  4.91576e-2
```

```
       6000.66c  1.78701e-3
      40000.58c  3.22796e-2
      68166.34c  7.71700e-5
      68167.34c  5.29900e-5
      92234.66c  8.23000e-6
      92235.14c  1.08197e-3
      92236.66c  1.21000e-5
      92238.14c  4.32127e-3
      72000.60c  1.93677e-6
      94238.60c  1.0e-30
      94239.14c  1.0e-30
      94240.60c  1.0e-30
      94241.60c  1.0e-30
      94242.60c  1.0e-30
mt22    H/Zr2.05t
       Zr/H2.05t
m23     1001.53c  4.91576e-2
       6000.66c  1.78701e-3
      40000.58c  3.22796e-2
      68166.34c  7.71700e-5
      68167.34c  5.29900e-5
      92234.66c  8.23000e-6
      92235.14c  1.08197e-3
      92236.66c  1.21000e-5
      92238.14c  4.32127e-3
      72000.60c  1.93677e-6
      94238.60c  1.0e-30
      94239.14c  1.0e-30
      94240.60c  1.0e-30
      94241.60c  1.0e-30
      94242.60c  1.0e-30
mt23    H/Zr2.05t
       Zr/H2.05t
m24     1001.53c  4.91576e-2
       6000.66c  1.78701e-3
      40000.58c  3.22796e-2
      68166.34c  7.71700e-5
      68167.34c  5.29900e-5
      92234.66c  8.23000e-6
      92235.14c  1.08197e-3
      92236.66c  1.21000e-5
      92238.14c  4.32127e-3
      72000.60c  1.93677e-6
      94238.60c  1.0e-30
      94239.14c  1.0e-30
      94240.60c  1.0e-30
      94241.60c  1.0e-30
      94242.60c  1.0e-30
mt24    H/Zr2.05t
       Zr/H2.05t
m25     1001.53c  4.91576e-2
```

```
       6000.66c  1.78701e-3
      40000.58c  3.22796e-2
      68166.34c  7.71700e-5
      68167.34c  5.29900e-5
      92234.66c  8.23000e-6
      92235.14c  1.08197e-3
      92236.66c  1.21000e-5
      92238.14c  4.32127e-3
      72000.60c  1.93677e-6
      94238.60c  1.0e-30
      94239.14c  1.0e-30
      94240.60c  1.0e-30
      94241.60c  1.0e-30
      94242.60c  1.0e-30
mt25    H/Zr2.05t
       Zr/H2.05t
c        SS304
m3    24000.50c  1.7482e-2
      26000.50c  5.6730e-2
      28000.50c  7.9390e-3
      25055.66c  1.6970e-3
m4     1001.66c  6.6691E-2
       8016.66c  3.3346E-2 $ Light water
mt4    lwtr.60t
m5     6000.66c  1.0082E-1
       5010.66c  2.1824E-2
       5011.66c  5.1500E-3 $ Borated Graphite
mt5    grph.60t
m6     6000.66c  2.7247E-2
       5010.66c  2.0598E-2
       5011.66c  8.7298E-2 $ B4C
m7     6000.66c  8.7744665E-2 $ Graphite
mt7    grph.60t
m8    26000.50c  0.0146238
      24000.50c  0.0042940
      28000.50c  0.0019017
      25055.66c  0.0004278
      13027.66c  0.0107829
       1001.66c  0.0382806
       8016.66c  0.0191406 $ Mix of 24.7% SS, 17.9% Al, 57.4% Water
mt8    lwtr.60t
m9    26000.50c  0.0192419
      24000.50c  0.0056501
      28000.50c  0.0025023
      25055.66c  0.0005629
       1001.66c  0.0450164
       8016.66c  0.0225085 $ Mix of 32.5% SS and 67.5% Water
mt9    lwtr.60t
m10   13027.60c -0.9685
      26000.50c -0.0070
      29000.50c -0.0025
```

```
14000.60c -0.0060
12000.60c -0.0110
24000.50c -0.0035
25055.60c -0.0015    $ Structural Aluminum (type 6061)
```

C.2. Monteburns Input for NSCR with 15 Materials

```
DPRK Rod Irradiation
PC
15                    !Number of MCNP Materials to Burn
11                    !MCNP Material "m" Numbers
12
13
14
15
16
17
18
19
20
21
22
23
24
25
499.2732378           !Volume of material
499.2732378
499.2732378
499.2732378
499.2732378
1997.092951
1997.092951
1997.092951
1997.092951
1997.092951
3637.562161
3637.562161
3637.562161
3637.562161
3637.562161
1.00                  !Power in MWt
-196.0                !Q-value for Fission
4000.0                !Total Number of Days Burned
3                     !Number of Outer Burn Steps
2                     !Number of Inner Burn Steps
1                     !Number of Predictor Steps
0                     !Step to Restart After
candunau              !ORIGEN2 Library
/packages/origen/origen22/libs  !Location of ORIGEN2 Library
0.005                 !Fractional Importance Limit
1                     !Flag for Intermediate keff Calculations
24                     !Number of Automatic Tally Isotopes
92234.66c
92235.14c
92236.66c
92237.50c
```

```
92238.14c
92239.35c
93237.60c
94238.60c
94239.14c
94240.60c
94241.60c
94242.60c
95241.60c
95242.66c
95243.60c
62149.66c
62150.50c
62152.50c
40000.58c
1001.53c
68166.34c
68167.34c
6000.66c
72000.60c
24                    !Number of Automatic Tally Isotopes
92234.66c
92235.14c
92236.66c
92237.50c
92238.14c
92239.35c
93237.60c
94238.60c
94239.14c
94240.60c
94241.60c
94242.60c
95241.60c
95242.66c
95243.60c
62149.66c
62150.50c
62152.50c
40000.58c
1001.53c
68166.34c
68167.34c
6000.66c
72000.60c
24                     !Number of Automatic Tally Isotopes
92234.66c
92235.14c
92236.66c
92237.50c
92238.14c
```

```
92239.35c
93237.60c
94238.60c
94239.14c
94240.60c
94241.60c
94242.60c
95241.60c
95242.66c
95243.60c
62149.66c
62150.50c
62152.50c
40000.58c
1001.53c
68166.34c
68167.34c
6000.66c
72000.60c
24                    !Number of Automatic Tally Isotopes
92234.66c
92235.14c
92236.66c
92237.50c
92238.14c
92239.35c
93237.60c
94238.60c
94239.14c
94240.60c
94241.60c
94242.60c
95241.60c
95242.66c
95243.60c
62149.66c
62150.50c
62152.50c
40000.58c
1001.53c
68166.34c
68167.34c
6000.66c
72000.60c
24                    !Number of Automatic Tally Isotopes
92234.66c
92235.14c
92236.66c
92237.50c
92238.14c
92239.35c
```

```
93237.60c
94238.60c
94239.14c
94240.60c
94241.60c
94242.60c
95241.60c
95242.66c
95243.60c
62149.66c
62150.50c
62152.50c
40000.58c
1001.53c
68166.34c
68167.34c
6000.66c
72000.60c
24                    !Number of Automatic Tally Isotopes
92234.66c
92235.14c
92236.66c
92237.50c
92238.14c
92239.35c
93237.60c
94238.60c
94239.14c
94240.60c
94241.60c
94242.60c
95241.60c
95242.66c
95243.60c
62149.66c
62150.50c
62152.50c
40000.58c
1001.53c
68166.34c
68167.34c
6000.66c
72000.60c
24                    !Number of Automatic Tally Isotopes
92234.66c
92235.14c
92236.66c
92237.50c
92238.14c
92239.35c
93237.60c
```

```
94238.60c
94239.14c
94240.60c
94241.60c
94242.60c
95241.60c
95242.66c
95243.60c
62149.66c
62150.50c
62152.50c
40000.58c
1001.53c
68166.34c
68167.34c
6000.66c
72000.60c
24                    !Number of Automatic Tally Isotopes
92234.66c
92235.14c
92236.66c
92237.50c
92238.14c
92239.35c
93237.60c
94238.60c
94239.14c
94240.60c
94241.60c
94242.60c
95241.60c
95242.66c
95243.60c
62149.66c
62150.50c
62152.50c
40000.58c
1001.53c
68166.34c
68167.34c
6000.66c
72000.60c
24                    !Number of Automatic Tally Isotopes
92234.66c
92235.14c
92236.66c
92237.50c
92238.14c
92239.35c
93237.60c
94238.60c
```

```
94239.14c
94240.60c
94241.60c
94242.60c
95241.60c
95242.66c
95243.60c
62149.66c
62150.50c
62152.50c
40000.58c
1001.53c
68166.34c
68167.34c
6000.66c
72000.60c
24                    !Number of Automatic Tally Isotopes
92234.66c
92235.14c
92236.66c
92237.50c
92238.14c
92239.35c
93237.60c
94238.60c
94239.14c
94240.60c
94241.60c
94242.60c
95241.60c
95242.66c
95243.60c
62149.66c
62150.50c
62152.50c
40000.58c
1001.53c
68166.34c
68167.34c
6000.66c
72000.60c
24                    !Number of Automatic Tally Isotopes
92234.66c
92235.14c
92236.66c
92237.50c
92238.14c
92239.35c
93237.60c
94238.60c
94239.14c
```

```
94240.60c
94241.60c
94242.60c
95241.60c
95242.66c
95243.60c
62149.66c
62150.50c
62152.50c
40000.58c
1001.53c
68166.34c
68167.34c
6000.66c
72000.60c
24                    !Number of Automatic Tally Isotopes
92234.66c
92235.14c
92236.66c
92237.50c
92238.14c
92239.35c
93237.60c
94238.60c
94239.14c
94240.60c
94241.60c
94242.60c
95241.60c
95242.66c
95243.60c
62149.66c
62150.50c
62152.50c
40000.58c
1001.53c
68166.34c
68167.34c
6000.66c
72000.60c
24                    !Number of Automatic Tally Isotopes
92234.66c
92235.14c
92236.66c
92237.50c
92238.14c
92239.35c
93237.60c
94238.60c
94239.14c
94240.60c
```

```
94241.60c
94242.60c
95241.60c
95242.66c
95243.60c
62149.66c
62150.50c
62152.50c
40000.58c
1001.53c
68166.34c
68167.34c
6000.66c
72000.60c
24                    !Number of Automatic Tally Isotopes
92234.66c
92235.14c
92236.66c
92237.50c
92238.14c
92239.35c
93237.60c
94238.60c
94239.14c
94240.60c
94241.60c
94242.60c
95241.60c
95242.66c
95243.60c
62149.66c
62150.50c
62152.50c
40000.58c
1001.53c
68166.34c
68167.34c
6000.66c
72000.60c
24                   !Number of Automatic Tally Isotopes
92234.66c
92235.14c
92236.66c
92237.50c
92238.14c
92239.35c
93237.60c
94238.60c
94239.14c
94240.60c
94241.60c
```

```
94242.60c
95241.60c
95242.66c
95243.60c
62149.66c
62150.50c
62152.50c
40000.58c
1001.53c
68166.34c
68167.34c
6000.66c
72000.60c
```

C.3. MCNP Input for NSCR with 45 Cells

```
TRIGA Reactor 3D Core Lattice (no thermal column)
c
c   - Description -
c
c        This deck includes a full core simulation for the
c        TAMU NSC TRIGA. Rod-to-rod spacing is rod averages
c        in x- and y-dimensions. Spacing is rectangular (not
c        square).  Fuel and clad materials are from Rearden
c        Thesis (August 1995).  The grid plate is included as
c        a solid aluminum section beneath the core. Support
c        structure for the grid plate was not included. Also,
c        the beam ports and thermal column were not included.
c        Since the pool is essentially infinitely large, the
c        tank and tank liner were ignored.
c
c        Shim safety rods must be moved in bank using surfaces
c        200, 201, and 202. The transient rod can be moved using
c        surfaces 302, 303, 304, and 305.  The Regulating rod can
c        be moved using surfaces 402 and 403.  Fuel and rod
c        materials are all fresh.  Erbium cross sections are
c        from Charlton-3xc-library, all other cross sections
c        are ENDF/B-VI standard MCNP cross sections.
c
c        Modified for 30/20 fuel after 30 days of operation at 1MW.
c
c     -- Cell Cards --
c
c         - Fuel Pin -
09    1  0.04297569  -100 +111 -112      u=9 imp:n=1
101   11  -7.18153 +100 -101 +111 -1000 u=9 imp:n=1
102   11  -7.18153 +100 -101 +1000 -1001 u=9 imp:n=1
103   11  -7.18153 +100 -101 +1001 -1002 u=9 imp:n=1
104   12  -7.18120 +100 -101 +1002 -1003 u=9 imp:n=1
105   12  -7.18120 +100 -101 +1003 -1004 u=9 imp:n=1
106   12  -7.18120 +100 -101 +1004 -1005 u=9 imp:n=1
107   13  -7.18103 +100 -101 +1005 -1006 u=9 imp:n=1
108   13  -7.18103 +100 -101 +1006 -1007 u=9 imp:n=1
109   13  -7.18103 +100 -101 +1007 -1008 u=9 imp:n=1
110   14  -7.18125 +100 -101 +1008 -1009 u=9 imp:n=1
111   14  -7.18125 +100 -101 +1009 -1010 u=9 imp:n=1
112   14  -7.18125 +100 -101 +1010 -1011 u=9 imp:n=1
113   15  -7.18168 +100 -101 +1011 -1012 u=9 imp:n=1
114   15  -7.18168 +100 -101 +1012 -1013 u=9 imp:n=1
115   15  -7.18168 +100 -101 +1013 -112 u=9 imp:n=1
11    3  0.083848  +101 -102 +110 -113   u=9 imp:n=1
12    7  0.0878229  -101 +110 -111     u=9 imp:n=1
13    7  0.0878229  -101 +112 -113     u=9 imp:n=1
14    8  0.089452  -102 +113 -114        u=9 imp:n=1
15    9  0.095482  -102 -110 +109        u=9 imp:n=1
```

```
16   10  0.060220  -109 +108             u=9 imp:n=1
17    4  0.100040  +102 +109             u=9 imp:n=1
18    4  0.100040  -108                  u=9 imp:n=1
19    4  0.100040  -102 +114             u=9 imp:n=1
c
c         - Fuel Pin -
209    1  0.04297569  -100 +111 -112      u=10 imp:n=1
2101   16  -7.18186 +100 -101 +111 -1000 u=10 imp:n=1
2102   16  -7.18186 +100 -101 +1000 -1001 u=10 imp:n=1
2103   16  -7.18186 +100 -101 +1001 -1002 u=10 imp:n=1
2104   17  -7.18152 +100 -101 +1002 -1003 u=10 imp:n=1
2105   17  -7.18152 +100 -101 +1003 -1004 u=10 imp:n=1
2106   17  -7.18152 +100 -101 +1004 -1005 u=10 imp:n=1
2107   18  -7.18142 +100 -101 +1005 -1006 u=10 imp:n=1
2108   18  -7.18142 +100 -101 +1006 -1007 u=10 imp:n=1
2109   18  -7.18142 +100 -101 +1007 -1008 u=10 imp:n=1
2110   19  -7.18154 +100 -101 +1008 -1009 u=10 imp:n=1
2111   19  -7.18154 +100 -101 +1009 -1010 u=10 imp:n=1
2112   19  -7.18154 +100 -101 +1010 -1011 u=10 imp:n=1
2113   20  -7.18195 +100 -101 +1011 -1012 u=10 imp:n=1
2114   20  -7.18195 +100 -101 +1012 -1013 u=10 imp:n=1
2115   20  -7.18195 +100 -101 +1013 -112 u=10 imp:n=1
211    3  0.083848  +101 -102 +110 -113   u=10 imp:n=1
212    7  0.0878229  -101 +110 -111     u=10 imp:n=1
213    7  0.0878229  -101 +112 -113     u=10 imp:n=1
214    8  0.089452  -102 +113 -114        u=10 imp:n=1
215    9  0.095482  -102 -110 +109        u=10 imp:n=1
216   10  0.060220  -109 +108             u=10 imp:n=1
217    4  0.100040  +102 +109             u=10 imp:n=1
218    4  0.100040  -108                  u=10 imp:n=1
219    4  0.100040  -102 +114             u=10 imp:n=1
c
c         - Fuel Pin -
309    1  0.04297569  -100 +111 -112      u=11 imp:n=1
3101   21  -7.18200 +100 -101 +111 -1000 u=11 imp:n=1
3102   21  -7.18200 +100 -101 +1000 -1001 u=11 imp:n=1
3103   21  -7.18200 +100 -101 +1001 -1002 u=11 imp:n=1
3104   22  -7.18179 +100 -101 +1002 -1003 u=11 imp:n=1
3105   22  -7.18179 +100 -101 +1003 -1004 u=11 imp:n=1
3106   22  -7.18179 +100 -101 +1004 -1005 u=11 imp:n=1
3107   23  -7.18174 +100 -101 +1005 -1006 u=11 imp:n=1
3108   23  -7.18174 +100 -101 +1006 -1007 u=11 imp:n=1
3109   23  -7.18174 +100 -101 +1007 -1008 u=11 imp:n=1
3110   24  -7.18180 +100 -101 +1008 -1009 u=11 imp:n=1
3111   24  -7.18180 +100 -101 +1009 -1010 u=11 imp:n=1
3112   24  -7.18180 +100 -101 +1010 -1011 u=11 imp:n=1
3113   25  -7.18205 +100 -101 +1011 -1012 u=11 imp:n=1
3114   25  -7.18205 +100 -101 +1012 -1013 u=11 imp:n=1
3115   25  -7.18205 +100 -101 +1013 -112 u=11 imp:n=1
311    3  0.083848  +101 -102 +110 -113   u=11 imp:n=1
312    7  0.0878229  -101 +110 -111     u=11 imp:n=1
```

```
313    7  0.0878229  -101 +112 -113     u=11 imp:n=1
314    8  0.089452  -102 +113 -114        u=11 imp:n=1
315    9  0.095482  -102 -110 +109        u=11 imp:n=1
316   10  0.060220  -109 +108            u=11 imp:n=1
317    4  0.100040  +102 +109            u=11 imp:n=1
318    4  0.100040  -108                 u=11 imp:n=1
319    4  0.100040  -102 +114            u=11 imp:n=1
c
c         - Shim Safety Control Rod -
20     5  0.135143  -101 +201 -202        u=2 imp:n=1
21     3  0.083848  +101 -102 +200 -202   u=2 imp:n=1
22     1  0.04297569  -100 +200 -201      u=2 imp:n=1
23     2  0.0887799  +100 -101 +200 -201  u=2 imp:n=1
24     4  0.100040  +102 +109            u=2 imp:n=1
25     4  0.100040  -102 -200            u=2 imp:n=1
26     4  0.100040  -102 +202            u=2 imp:n=1
27    10  0.060220  +102 -109 +108        u=2 imp:n=1
28     4  0.100040  +102 -108            u=2 imp:n=1
c
c         - Transient Control Rod -
30     5  0.135143  -300 +303 -304        u=3 imp:n=1
31     3  0.083848  +300 -301 +302 -305   u=3 imp:n=1
32     0            -300 +302 -303        u=3 imp:n=1
33     4  0.100040  +301 +109            u=3 imp:n=1
34     4  0.100040  -301 -302            u=3 imp:n=1
35     0            -300 +304 -305        u=3 imp:n=1
36     4  0.100040  -301 +305            u=3 imp:n=1
37    10  0.060220  +301 -109 +108        u=3 imp:n=1
38     4  0.100040  +301 -108            u=3 imp:n=1
c
c         - Regulating Control Rod -
40     6  0.127794  -400 +402 -403        u=4 imp:n=1
41     3  0.083848  +400 -401 +402 -403   u=4 imp:n=1
42     4  0.100040  +401 +109            u=4 imp:n=1
43     4  0.100040  -401 -402            u=4 imp:n=1
44     4  0.100040  -401 +403            u=4 imp:n=1
45    10  0.060220  +401 -109 +108        u=4 imp:n=1
46     4  0.100040  +401 -108            u=4 imp:n=1
c
c         - Graphite Element -
50     7  0.0878229  -500 +109 -502     u=5 imp:n=1
51     7  0.0878229  +500 +109 -502     u=5 imp:n=1
52    10  0.060220  -500 -109 +108        u=5 imp:n=1
53     4  0.100040  -108                 u=5 imp:n=1
54     4  0.100040  +502                 u=5 imp:n=1
c
c         - Water Hole -
60     4  0.100040  -500 +109            u=6 imp:n=1
61     4  0.100040  +500                 u=6 imp:n=1
62    10  0.060220  -500 -109 +108        u=6 imp:n=1
63     4  0.100040  -500 -108            u=6 imp:n=1
```

```
c
c         - Water Hole with Tally Element -
70    4  0.100040  -500 +600 -601        u=7 imp:n=1 vol=156.1064 $
Tally vol in water
71    4  0.100040  -500 -600 +109        u=7 imp:n=1
72    4  0.100040  -500 +601             u=7 imp:n=1
73    4  0.100040  +500                  u=7 imp:n=1
74   10  0.060220  -500 -109 +108        u=7 imp:n=1
75    4  0.100040  -500 -108             u=7 imp:n=1
c
c         - Fuel Assembly  Lattice -
700   0        -702 +701 -704 +703 lat=1 u=8 fill=0:17 0:11 0:0
      5 5 11 11 11 11 11 11 11 11 11 11 11 5 5 5 5
      5 5 11 11 11 4 11 11 11 11 11 11 11 5 5 5 5
      5 5 5 5 11 10 10 10 10 10 10 10 11 11 5 5 5 5
      5 5 5 5 11 10 2 10 10 10 2 10 11 11 5 5 5 5
      5 5 6 6 7 7 10 9 9 9 9 10 6 6 5 5 5 5
      5 5 6 6 7 7 10 9 3 9 9 10 6 6 5 5 5 5
      5 5 5 5 11 10 10 10 10 10 10 10 11 11 5 5 5 5
      5 5 5 5 11 10 2 10 10 10 2 10 11 11 5 5 5 5
      7 7 5 5 11 11 11 11 11 11 11 11 11 11 5 5 5 5
      7 7 5 5 11 11 6 6 11 11 6 6 11 11 5 5 5 5
      6 6 6 6 6 6 6 6 6 6 6 6 6 6 6 6 6 6
      6 6 6 6 6 6 6 6 6 6 6 6 6 6 6 6 6 6    imp:n=1
801   0        +800 -801 +802 -803 +804 -805 fill=8  imp:n=1
c         - Thermal Colunm
80    7  8.1299E-2 -80 +81 -82 -83 -84 -85     imp:n=1
c
c         - Universe -
900   4  0.10004   #801 #80 -900 imp:n=1
999   0            +900                      imp:n=0

c
c     -- Surface Cards --
c
c         - Fuel Pin Surfaces -
100   c/z   2.025015 1.927225 0.2280
101   c/z   2.025015 1.927225 1.7411
102   c/z   2.025015 1.927225 1.7920
108   pz  -30.48
109   pz  -17.78
110   pz   -8.89
111   pz    0.00
112   pz   38.10
113   pz   46.99
114   pz   58.42
c     -- Inner fuel surfaces --
1000  pz 2.54
1001  pz 5.08
1002  pz 7.62
1003  pz 10.16
```

```
1004  pz 12.7
1005  pz 15.24
1006  pz 17.78
1007  pz 20.32
1008  pz 22.86
1009  pz 25.4
1010  pz 27.94
1011  pz 30.48
1012  pz 33.02
1013  pz 35.56
c
c         - Shim Safety Rod Surfaces -
200   pz   -22.1717 $(0.00 for full removal)
201   pz   15.92834 $(38.10 for full removal)
202   pz   51.48834 $(73.66 for full removal)
c
c         - Transient Rod Surfaces -
300   c/z   2.025015 1.927225 1.5164
301   c/z   2.025015 1.927225 1.5876
302   pz   -8.89
303   pz   38.10 $(38.10 for full removal)
304   pz   76.20 $(76.20 for full removal)
305   pz   80.00
c
c         -Regulating Rod Surfaces -
400   c/z   2.025015 1.927225 1.5164
401   c/z   2.025015 1.927225 1.5876
402   pz   38.10 $(38.10 for full removal)
403   pz   76.20 $(76.20 for full removal)
c
c         - Water Hole and Graphite Element Surfaces -
500   c/z   2.025015 1.927225 7.0000
501   pz   -8.89
502   pz   46.99
c
c         - Tally Element Surfaces -
600   pz   14.00
601   pz   24.00
c
c         - Pin Cell Surfaces -
701   px   0.00
702   px   4.05003
703   py   0.00
704   py   3.85445
c
c         - Core Surfaces -
800   px   0.0001
801   px  72.90053
802   py   0.0001
803   py  46.2533
804   pz -100.0
```

```
805   pz  100.0
c
c         - Thermal Colunm -
c     -  y-Planes that define the front and back
80     py    -1.2705
81     py -306.0705
c     -  Inclined planes, each plane is defined by 3 points
82     P -9.269735 -0.0005 41.91  82.170265 -0.0005 41.91
          97.410265 -304.8005 80.01                              $ Top
Plane
83     P 82.170265 -0.0005 41.91  97.410265 -304.8005 80.01
         82.170265 -0.0005 -3.81                               $ Right
Plane
84     P -9.269735 -0.0005 41.91  -9.269735 -0.0005 -3.81
         -24.509735 -304.8005 -41.91                            $ Left
Plane
85     P -9.269735 -0.0005 -3.81  82.170265 -0.0005 -3.81
          97.410265 -304.8005 -41.91                            $ Bottom
Plane
c
c         - Reflector and Universe Cells -
900   cz 1000.00

c
c     -- Data Cards --
c
mode  n
kcode 100000 1.0 20 400
ksrc  37.0 22.0 19.0
m1    40000.60c 4.29757e-2
c        U-ZrH Fuel
m2     1001.53c  4.91576e-2
       6000.66c  1.78701e-3
      40000.58c  3.22796e-2
      68166.34c  7.71700e-5
      68167.34c  5.29900e-5
      92234.66c  8.23000e-6
      92235.14c  1.08197e-3
      92236.66c  1.21000e-5
      92238.14c  4.32127e-3
      72000.60c  1.93677e-6
      94238.60c  1.0e-30
      94239.14c  1.0e-30
      94240.60c  1.0e-30
      94241.60c  1.0e-30
      94242.60c  1.0e-30
mt2    H/Zr2.05t
       Zr/H2.05t
mt11    H/Zr2.05t
       Zr/H2.05t
mt12    H/Zr2.05t
```

```
       Zr/H2.05t
mt13    H/Zr2.05t
       Zr/H2.05t
mt14    H/Zr2.05t
       Zr/H2.05t
mt15    H/Zr2.05t
       Zr/H2.05t
mt16    H/Zr2.05t
       Zr/H2.05t
mt17    H/Zr2.05t
       Zr/H2.05t
mt18    H/Zr2.05t
       Zr/H2.05t
mt19    H/Zr2.05t
       Zr/H2.05t
mt20    H/Zr2.05t
       Zr/H2.05t
mt21    H/Zr2.05t
       Zr/H2.05t
mt22    H/Zr2.05t
       Zr/H2.05t
mt23    H/Zr2.05t
       Zr/H2.05t
mt24    H/Zr2.05t
       Zr/H2.05t
mt25    H/Zr2.05t
       Zr/H2.05t
c        SS304
m3    24000.50c  1.7482e-2
      26000.50c  5.6730e-2
      28000.50c  7.9390e-3
      25055.66c  1.6970e-3
m4     1001.66c  6.6691E-2
       8016.66c  3.3346E-2 $ Light water
mt4    lwtr.60t
m5     6000.66c  1.0082E-1
       5010.66c  2.1824E-2
       5011.66c  5.1500E-3 $ Borated Graphite
mt5    grph.60t
m6     6000.66c  2.7247E-2
       5010.66c  2.0598E-2
       5011.66c  8.7298E-2 $ B4C
m7     6000.66c  8.7744665E-2 $ Graphite
mt7    grph.60t
m8    26000.50c  0.0146238
      24000.50c  0.0042940
      28000.50c  0.0019017
      25055.66c  0.0004278
      13027.66c  0.0107829
       1001.66c  0.0382806
       8016.66c  0.0191406 $ Mix of 24.7% SS, 17.9% Al, 57.4% Water
```

```
mt8    lwtr.60t
m9    26000.50c  0.0192419
      24000.50c  0.0056501
      28000.50c  0.0025023
      25055.66c  0.0005629
       1001.66c  0.0450164
       8016.66c  0.0225085 $ Mix of 32.5% SS and 67.5% Water
mt9    lwtr.60t
m10   13027.60c -0.9685
      26000.50c -0.0070
      29000.50c -0.0025
      14000.60c -0.0060
      12000.60c -0.0110
      24000.50c -0.0035
      25055.60c -0.0015    $ Structural Aluminum (type 6061)
m11
      92234.60c   -4.4485E-04
      92235.14c   -5.8649E-02
      92236.60c   -6.8854E-04
      92237.50c   -1.5323E-07
      92238.14c   -2.3783E-01
      92239.42c   -2.2552E-08
      93237.60c   -2.5682E-07
      94238.60c   -1.3045E-10
      94239.14c   -1.9624E-05
      94240.60c   -2.7840E-08
      94241.60c   -1.1782E-10
      94242.60c   -5.2198E-14
      95241.60c   -8.9193E-14
      95242.50c   -1.8287E-17
      95243.60c   -1.7665E-17
      62149.50c   -6.7225E-07
      62150.50c   -9.8265E-08
      62152.50c   -2.8603E-07
      40000.58c   -6.8088E-01
       1001.53c   -1.1455E-02
      68166.34c   -2.9601E-03
      68167.34c   -2.0279E-03
       6000.60c   -4.9630E-03
      72000.60c   -7.9933E-05
      54135.53c   -9.0028E-08
c
c
m12
      92234.60c   -4.4464E-04
      92235.14c   -5.8603E-02
      92236.60c   -6.9851E-04
      92237.50c   -2.1084E-07
      92238.14c   -2.3784E-01
      92239.42c   -3.1170E-08
      93237.60c   -3.5210E-07
```

```
      94238.60c   -2.5059E-10
      94239.14c   -2.7087E-05
      94240.60c   -5.3590E-08
      94241.60c   -2.8785E-10
      94242.60c   -1.7050E-13
      95241.60c   -2.1811E-13
      95242.50c   -6.2526E-17
      95243.60c   -9.0554E-17
      62149.50c   -8.5185E-07
      62150.50c   -1.6164E-07
      62152.50c   -4.0265E-07
      40000.58c   -6.8091E-01
       1001.53c   -1.1456E-02
      68166.34c   -2.9599E-03
      68167.34c   -2.0209E-03
       6000.60c   -4.9632E-03
      72000.60c   -7.9936E-05
      54135.53c   -1.1291E-07
c
c
m13
      92234.60c   -4.4452E-04
      92235.14c   -5.8583E-02
      92236.60c   -7.0235E-04
      92237.50c   -2.4430E-07
      92238.14c   -2.3783E-01
      92239.42c   -3.4960E-08
      93237.60c   -4.0741E-07
      94238.60c   -3.1332E-10
      94239.14c   -3.0365E-05
      94240.60c   -6.6644E-08
      94241.60c   -4.3015E-10
      94242.60c   -2.8264E-13
      95241.60c   -3.2580E-13
      95242.50c   -1.0327E-16
      95243.60c   -1.5095E-16
      62149.50c   -9.2642E-07
      62150.50c   -1.9527E-07
      62152.50c   -4.5439E-07
      40000.58c   -6.8093E-01
       1001.53c   -1.1456E-02
      68166.34c   -2.9599E-03
      68167.34c   -2.0183E-03
       6000.60c   -4.9633E-03
      72000.60c   -7.9939E-05
      54135.53c   -1.2210E-07
c
c
m14
      92234.60c   -4.4470E-04
      92235.14c   -5.8610E-02
```

```
        92236.60c   -6.9680E-04
        92237.50c   -2.0884E-07
        92238.14c   -2.3783E-01
        92239.42c   -3.0242E-08
        93237.60c   -3.4894E-07
        94238.60c   -2.3860E-10
        94239.14c   -2.6287E-05
        94240.60c   -4.9502E-08
        94241.60c   -2.8650E-10
        94242.60c   -1.6266E-13
        95241.60c   -2.1725E-13
        95242.50c   -5.9494E-17
        95243.60c   -8.7328E-17
        62149.50c   -8.2508E-07
        62150.50c   -1.4902E-07
        62152.50c   -3.8411E-07
        40000.58c   -6.8091E-01
         1001.53c   -1.1456E-02
        68166.34c   -2.9599E-03
        68167.34c   -2.0216E-03
         6000.60c   -4.9632E-03
        72000.60c   -7.9936E-05
        54135.53c   -1.0961E-07
c
c
m15
        92234.60c   -4.4488E-04
        92235.14c   -5.8667E-02
        92236.60c   -6.8517E-04
        92237.50c   -1.3590E-07
        92238.14c   -2.3783E-01
        92239.42c   -2.0362E-08
        93237.60c   -2.2801E-07
        94238.60c   -1.0173E-10
        94239.14c   -1.7725E-05
        94240.60c   -2.2879E-08
        94241.60c   -8.5273E-11
        94242.60c   -3.3346E-14
        95241.60c   -6.4547E-14
        95242.50c   -1.1951E-17
        95243.60c   -1.1537E-17
        62149.50c   -5.9876E-07
        62150.50c   -7.5246E-08
        62152.50c   -2.4627E-07
        40000.58c   -6.8086E-01
         1001.53c   -1.1455E-02
        68166.34c   -2.9601E-03
        68167.34c   -2.0294E-03
         6000.60c   -4.9629E-03
        72000.60c   -7.9931E-05
        54135.53c   -8.0862E-08
```

```
c
c
m16
      92234.60c   -4.4487E-04
      92235.14c   -5.8668E-02
      92236.60c   -6.8458E-04
      92237.50c   -1.3135E-07
      92238.14c   -2.3784E-01
      92239.42c   -1.9031E-08
      93237.60c   -2.2043E-07
      94238.60c   -9.4048E-11
      94239.14c   -1.6568E-05
      94240.60c   -2.0485E-08
      94241.60c   -7.1022E-11
      94242.60c   -2.7205E-14
      95241.60c   -5.3685E-14
      95242.50c   -9.5129E-18
      95243.60c   -8.5055E-18
      62149.50c   -5.9235E-07
      62150.50c   -7.4266E-08
      62152.50c   -2.4061E-07
      40000.58c   -6.8086E-01
       1001.53c   -1.1455E-02
      68166.34c   -2.9601E-03
      68167.34c   -2.0302E-03
       6000.60c   -4.9628E-03
      72000.60c   -7.9929E-05
      54135.53c   -7.9862E-08
c
c
m17
      92234.60c   -4.4473E-04
      92235.14c   -5.8631E-02
      92236.60c   -6.9251E-04
      92237.50c   -1.8362E-07
      92238.14c   -2.3783E-01
      92239.42c   -2.6451E-08
      93237.60c   -3.0728E-07
      94238.60c   -1.7919E-10
      94239.14c   -2.3003E-05
      94240.60c   -3.8237E-08
      94241.60c   -1.8916E-10
      94242.60c   -9.4835E-14
      95241.60c   -1.4337E-13
      95242.50c   -3.4653E-17
      95243.60c   -4.1302E-17
      62149.50c   -7.4159E-07
      62150.50c   -1.2029E-07
      62152.50c   -3.3100E-07
      40000.58c   -6.8089E-01
       1001.53c   -1.1456E-02
```

```
      68166.34c   -2.9600E-03
      68167.34c   -2.0248E-03
       6000.60c   -4.9631E-03
      72000.60c   -7.9935E-05
      54135.53c   -9.9117E-08
c
c
m18
      92234.60c   -4.4469E-04
      92235.14c   -5.8614E-02
      92236.60c   -6.9573E-04
      92237.50c   -1.9828E-07
      92238.14c   -2.3783E-01
      92239.42c   -2.9364E-08
      93237.60c   -3.3147E-07
      94238.60c   -2.1274E-10
      94239.14c   -2.5528E-05
      94240.60c   -4.6638E-08
      94241.60c   -2.5090E-10
      94242.60c   -1.3863E-13
      95241.60c   -1.9012E-13
      95242.50c   -5.0184E-17
      95243.60c   -6.7084E-17
      62149.50c   -8.0671E-07
      62150.50c   -1.4447E-07
      62152.50c   -3.7183E-07
      40000.58c   -6.8090E-01
       1001.53c   -1.1456E-02
      68166.34c   -2.9599E-03
      68167.34c   -2.0229E-03
       6000.60c   -4.9631E-03
      72000.60c   -7.9936E-05
      54135.53c   -1.0715E-07
c
c
m19
      92234.60c   -4.4479E-04
      92235.14c   -5.8634E-02
      92236.60c   -6.9162E-04
      92237.50c   -1.7361E-07
      92238.14c   -2.3783E-01
      92239.42c   -2.5548E-08
      93237.60c   -2.9064E-07
      94238.60c   -1.6554E-10
      94239.14c   -2.2222E-05
      94240.60c   -3.5794E-08
      94241.60c   -1.6793E-10
      94242.60c   -8.1846E-14
      95241.60c   -1.2725E-13
      95242.50c   -2.9758E-17
      95243.60c   -3.3469E-17
```

```
      62149.50c   -7.2492E-07
      62150.50c   -1.1294E-07
      62152.50c   -3.1964E-07
      40000.58c   -6.8089E-01
       1001.53c   -1.1456E-02
      68166.34c   -2.9600E-03
      68167.34c   -2.0256E-03
       6000.60c   -4.9630E-03
      72000.60c   -7.9934E-05
      54135.53c   -9.6952E-08
c
c
m20
      92234.60c   -4.4495E-04
      92235.14c   -5.8684E-02
      92236.60c   -6.8162E-04
      92237.50c   -1.1824E-07
      92238.14c   -2.3783E-01
      92239.42c   -1.7181E-08
      93237.60c   -1.9865E-07
      94238.60c   -7.5303E-11
      94239.14c   -1.4963E-05
      94240.60c   -1.6274E-08
      94241.60c   -5.0480E-11
      94242.60c   -1.6955E-14
      95241.60c   -3.8204E-14
      95242.50c   -5.9718E-18
      95243.60c   -4.7051E-18
      62149.50c   -5.2320E-07
      62150.50c   -5.6301E-08
      62152.50c   -2.0597E-07
      40000.58c   -6.8085E-01
       1001.53c   -1.1455E-02
      68166.34c   -2.9601E-03
      68167.34c   -2.0321E-03
       6000.60c   -4.9628E-03
      72000.60c   -7.9929E-05
      54135.53c   -7.1064E-08
c
c
m21
      92234.60c   -4.4503E-04
      92235.14c   -5.8702E-02
      92236.60c   -6.7779E-04
      92237.50c   -8.5573E-08
      92238.14c   -2.3784E-01
      92239.42c   -1.2148E-08
      93237.60c   -1.4398E-07
      94238.60c   -4.2474E-11
      94239.14c   -1.0586E-05
      94240.60c   -9.1669E-09
```

```
      94241.60c   -2.0580E-11
      94242.60c   -5.7217E-15
      95241.60c   -1.5513E-14
      95242.50c   -1.9177E-18
      95243.60c   -1.1178E-18
      62149.50c   -4.5064E-07
      62150.50c   -4.2164E-08
      62152.50c   -1.6777E-07
      40000.58c   -6.8083E-01
       1001.53c   -1.1455E-02
      68166.34c   -2.9602E-03
      68167.34c   -2.0349E-03
       6000.60c   -4.9625E-03
      72000.60c   -7.9929E-05
      54135.53c   -6.1369E-08
c
c
m22
      92234.60c   -4.4494E-04
      92235.14c   -5.8677E-02
      92236.60c   -6.8301E-04
      92237.50c   -1.1645E-07
      92238.14c   -2.3783E-01
      92239.42c   -1.7427E-08
      93237.60c   -1.9554E-07
      94238.60c   -7.7907E-11
      94239.14c   -1.5175E-05
      94240.60c   -1.7350E-08
      94241.60c   -5.5518E-11
      94242.60c   -1.9905E-14
      95241.60c   -4.1950E-14
      95242.50c   -6.8807E-18
      95243.60c   -5.5722E-18
      62149.50c   -5.6039E-07
      62150.50c   -6.7179E-08
      62152.50c   -2.2351E-07
      40000.58c   -6.8086E-01
       1001.53c   -1.1455E-02
      68166.34c   -2.9601E-03
      68167.34c   -2.0313E-03
       6000.60c   -4.9627E-03
      72000.60c   -7.9930E-05
      54135.53c   -7.5721E-08
c
c
m23
      92234.60c   -4.4489E-04
      92235.14c   -5.8664E-02
      92236.60c   -6.8527E-04
      92237.50c   -1.2647E-07
      92238.14c   -2.3784E-01
```

```
      92239.42c   -1.8937E-08
      93237.60c   -2.1221E-07
      94238.60c   -9.2653E-11
      94239.14c   -1.6485E-05
      94240.60c   -2.0758E-08
      94241.60c   -7.2027E-11
      94242.60c   -2.8377E-14
      95241.60c   -5.4433E-14
      95242.50c   -9.8341E-18
      95243.60c   -8.8334E-18
      62149.50c   -6.0960E-07
      62150.50c   -8.0076E-08
      62152.50c   -2.4946E-07
      40000.58c   -6.8086E-01
       1001.53c   -1.1455E-02
      68166.34c   -2.9601E-03
      68167.34c   -2.0301E-03
       6000.60c   -4.9627E-03
      72000.60c   -7.9932E-05
      54135.53c   -8.1985E-08
c
c
m24
      92234.60c   -4.4496E-04
      92235.14c   -5.8678E-02
      92236.60c   -6.8267E-04
      92237.50c   -1.1107E-07
      92238.14c   -2.3783E-01
      92239.42c   -1.6804E-08
      93237.60c   -1.8656E-07
      94238.60c   -7.3481E-11
      94239.14c   -1.4633E-05
      94240.60c   -1.6580E-08
      94241.60c   -5.1223E-11
      94242.60c   -1.8132E-14
      95241.60c   -3.8684E-14
      95242.50c   -6.3067E-18
      95243.60c   -5.0321E-18
      62149.50c   -5.5303E-07
      62150.50c   -6.4951E-08
      62152.50c   -2.1941E-07
      40000.58c   -6.8085E-01
       1001.53c   -1.1455E-02
      68166.34c   -2.9601E-03
      68167.34c   -2.0316E-03
       6000.60c   -4.9627E-03
      72000.60c   -7.9931E-05
      54135.53c   -7.4755E-08
c
c
m25
```

```
       92234.60c   -4.4506E-04
       92235.14c   -5.8709E-02
       92236.60c   -6.7655E-04
       92237.50c   -7.2419E-08
       92238.14c   -2.3783E-01
       92239.42c   -1.1512E-08
       93237.60c   -1.2192E-07
       94238.60c   -3.3577E-11
       94239.14c   -1.0033E-05
       94240.60c   -8.0300E-09
       94241.60c   -1.6803E-11
       94242.60c   -4.3033E-15
       95241.60c   -1.2669E-14
       95242.50c   -1.4447E-18
       95243.60c   -7.7063E-19
       62149.50c   -4.1919E-07
       62150.50c   -3.6453E-08
       62152.50c   -1.5386E-07
       40000.58c   -6.8083E-01
        1001.53c   -1.1455E-02
       68166.34c   -2.9602E-03
       68167.34c   -2.0356E-03
        6000.60c   -4.9625E-03
       72000.60c   -7.9928E-05
       54135.53c   -5.7297E-08
f17:n  (101 < 700 [7 4 0, 8 4 0, 9 4 0, 10 4 0,
        7 5 0, 9 5 0, 10 5 0])
f27:n  (102 < 700 [7 4 0, 8 4 0, 9 4 0, 10 4 0,
        7 5 0, 9 5 0, 10 5 0])
f37:n  (103 < 700 [7 4 0, 8 4 0, 9 4 0, 10 4 0,
        7 5 0, 9 5 0, 10 5 0])
f47:n  (104 < 700 [7 4 0, 8 4 0, 9 4 0, 10 4 0,
        7 5 0, 9 5 0, 10 5 0])
f57:n  (105 < 700 [7 4 0, 8 4 0, 9 4 0, 10 4 0,
        7 5 0, 9 5 0, 10 5 0])
f67:n  (106 < 700 [7 4 0, 8 4 0, 9 4 0, 10 4 0,
        7 5 0, 9 5 0, 10 5 0])
f77:n  (107 < 700 [7 4 0, 8 4 0, 9 4 0, 10 4 0,
        7 5 0, 9 5 0, 10 5 0])
f87:n  (108 < 700 [7 4 0, 8 4 0, 9 4 0, 10 4 0,
        7 5 0, 9 5 0, 10 5 0])
f97:n  (109 < 700 [7 4 0, 8 4 0, 9 4 0, 10 4 0,
        7 5 0, 9 5 0, 10 5 0])
f107:n  (110 < 700 [7 4 0, 8 4 0, 9 4 0, 10 4 0,
        7 5 0, 9 5 0, 10 5 0])
f117:n  (111 < 700 [7 4 0, 8 4 0, 9 4 0, 10 4 0,
        7 5 0, 9 5 0, 10 5 0])
f127:n  (112 < 700 [7 4 0, 8 4 0, 9 4 0, 10 4 0,
        7 5 0, 9 5 0, 10 5 0])
f137:n  (113 < 700 [7 4 0, 8 4 0, 9 4 0, 10 4 0,
        7 5 0, 9 5 0, 10 5 0])
```

```
f147:n  (114 < 700 [7 4 0, 8 4 0, 9 4 0, 10 4 0,
        7 5 0, 9 5 0, 10 5 0])
f157:n  (115 < 700 [7 4 0, 8 4 0, 9 4 0, 10 4 0,
        7 5 0, 9 5 0, 10 5 0])
f167:n  (2101 < 700 [5 2 0, 6 2 0, 7 2 0, 8 2 0,
         9 2 0, 10 2 0, 11 2 0,
         5 3 0, 7 3 0, 8 3 0, 9 3 0, 11 3 0,
         6 4 0, 11 4 0, 6 5 0, 11 5 0,
         5 6 0, 6 6 0, 7 6 0, 8 6 0, 9 6 0, 10 6 0,
         11 6 0, 5 7 0, 7 7 0, 8 7 0, 9 7 0, 11 7 0])
f177:n  (2102 < 700 [5 2 0, 6 2 0, 7 2 0, 8 2 0,
         9 2 0, 10 2 0, 11 2 0,
         5 3 0, 7 3 0, 8 3 0, 9 3 0, 11 3 0,
         6 4 0, 11 4 0, 6 5 0, 11 5 0,
         5 6 0, 6 6 0, 7 6 0, 8 6 0, 9 6 0, 10 6 0,
         11 6 0, 5 7 0, 7 7 0, 8 7 0, 9 7 0, 11 7 0])
f187:n  (2103 < 700 [5 2 0, 6 2 0, 7 2 0, 8 2 0,
         9 2 0, 10 2 0, 11 2 0,
         5 3 0, 7 3 0, 8 3 0, 9 3 0, 11 3 0,
         6 4 0, 11 4 0, 6 5 0, 11 5 0,
         5 6 0, 6 6 0, 7 6 0, 8 6 0, 9 6 0, 10 6 0,
         11 6 0, 5 7 0, 7 7 0, 8 7 0, 9 7 0, 11 7 0])
f197:n  (2104 < 700 [5 2 0, 6 2 0, 7 2 0, 8 2 0,
         9 2 0, 10 2 0, 11 2 0,
         5 3 0, 7 3 0, 8 3 0, 9 3 0, 11 3 0,
         6 4 0, 11 4 0, 6 5 0, 11 5 0,
         5 6 0, 6 6 0, 7 6 0, 8 6 0, 9 6 0, 10 6 0,
         11 6 0, 5 7 0, 7 7 0, 8 7 0, 9 7 0, 11 7 0])
f207:n  (2105 < 700 [5 2 0, 6 2 0, 7 2 0, 8 2 0,
         9 2 0, 10 2 0, 11 2 0,
         5 3 0, 7 3 0, 8 3 0, 9 3 0, 11 3 0,
         6 4 0, 11 4 0, 6 5 0, 11 5 0,
         5 6 0, 6 6 0, 7 6 0, 8 6 0, 9 6 0, 10 6 0,
         11 6 0, 5 7 0, 7 7 0, 8 7 0, 9 7 0, 11 7 0])
f217:n  (2106 < 700 [5 2 0, 6 2 0, 7 2 0, 8 2 0,
         9 2 0, 10 2 0, 11 2 0,
         5 3 0, 7 3 0, 8 3 0, 9 3 0, 11 3 0,
         6 4 0, 11 4 0, 6 5 0, 11 5 0,
         5 6 0, 6 6 0, 7 6 0, 8 6 0, 9 6 0, 10 6 0,
         11 6 0, 5 7 0, 7 7 0, 8 7 0, 9 7 0, 11 7 0])
f227:n  (2107 < 700 [5 2 0, 6 2 0, 7 2 0, 8 2 0,
         9 2 0, 10 2 0, 11 2 0,
         5 3 0, 7 3 0, 8 3 0, 9 3 0, 11 3 0,
         6 4 0, 11 4 0, 6 5 0, 11 5 0,
         5 6 0, 6 6 0, 7 6 0, 8 6 0, 9 6 0, 10 6 0,
         11 6 0, 5 7 0, 7 7 0, 8 7 0, 9 7 0, 11 7 0])
f237:n  (2108 < 700 [5 2 0, 6 2 0, 7 2 0, 8 2 0,
         9 2 0, 10 2 0, 11 2 0,
         5 3 0, 7 3 0, 8 3 0, 9 3 0, 11 3 0,
         6 4 0, 11 4 0, 6 5 0, 11 5 0,
         5 6 0, 6 6 0, 7 6 0, 8 6 0, 9 6 0, 10 6 0,
```

```
         11 6 0, 5 7 0, 7 7 0, 8 7 0, 9 7 0, 11 7 0])
f247:n  (2109 < 700 [5 2 0, 6 2 0, 7 2 0, 8 2 0,
         9 2 0, 10 2 0, 11 2 0,
         5 3 0, 7 3 0, 8 3 0, 9 3 0, 11 3 0,
         6 4 0, 11 4 0, 6 5 0, 11 5 0,
         5 6 0, 6 6 0, 7 6 0, 8 6 0, 9 6 0, 10 6 0,
         11 6 0, 5 7 0, 7 7 0, 8 7 0, 9 7 0, 11 7 0])
f257:n  (2110 < 700 [5 2 0, 6 2 0, 7 2 0, 8 2 0,
         9 2 0, 10 2 0, 11 2 0,
         5 3 0, 7 3 0, 8 3 0, 9 3 0, 11 3 0,
         6 4 0, 11 4 0, 6 5 0, 11 5 0,
         5 6 0, 6 6 0, 7 6 0, 8 6 0, 9 6 0, 10 6 0,
         11 6 0, 5 7 0, 7 7 0, 8 7 0, 9 7 0, 11 7 0])
f267:n  (2111 < 700 [5 2 0, 6 2 0, 7 2 0, 8 2 0,
         9 2 0, 10 2 0, 11 2 0,
         5 3 0, 7 3 0, 8 3 0, 9 3 0, 11 3 0,
         6 4 0, 11 4 0, 6 5 0, 11 5 0,
         5 6 0, 6 6 0, 7 6 0, 8 6 0, 9 6 0, 10 6 0,
         11 6 0, 5 7 0, 7 7 0, 8 7 0, 9 7 0, 11 7 0])
f277:n  (2112 < 700 [5 2 0, 6 2 0, 7 2 0, 8 2 0,
         9 2 0, 10 2 0, 11 2 0,
         5 3 0, 7 3 0, 8 3 0, 9 3 0, 11 3 0,
         6 4 0, 11 4 0, 6 5 0, 11 5 0,
         5 6 0, 6 6 0, 7 6 0, 8 6 0, 9 6 0, 10 6 0,
         11 6 0, 5 7 0, 7 7 0, 8 7 0, 9 7 0, 11 7 0])
f287:n  (2113 < 700 [5 2 0, 6 2 0, 7 2 0, 8 2 0,
         9 2 0, 10 2 0, 11 2 0,
         5 3 0, 7 3 0, 8 3 0, 9 3 0, 11 3 0,
         6 4 0, 11 4 0, 6 5 0, 11 5 0,
         5 6 0, 6 6 0, 7 6 0, 8 6 0, 9 6 0, 10 6 0,
         11 6 0, 5 7 0, 7 7 0, 8 7 0, 9 7 0, 11 7 0])
f297:n  (2114 < 700 [5 2 0, 6 2 0, 7 2 0, 8 2 0,
         9 2 0, 10 2 0, 11 2 0,
         5 3 0, 7 3 0, 8 3 0, 9 3 0, 11 3 0,
         6 4 0, 11 4 0, 6 5 0, 11 5 0,
         5 6 0, 6 6 0, 7 6 0, 8 6 0, 9 6 0, 10 6 0,
         11 6 0, 5 7 0, 7 7 0, 8 7 0, 9 7 0, 11 7 0])
f307:n  (2115 < 700 [5 2 0, 6 2 0, 7 2 0, 8 2 0,
         9 2 0, 10 2 0, 11 2 0,
         5 3 0, 7 3 0, 8 3 0, 9 3 0, 11 3 0,
         6 4 0, 11 4 0, 6 5 0, 11 5 0,
         5 6 0, 6 6 0, 7 6 0, 8 6 0, 9 6 0, 10 6 0,
         11 6 0, 5 7 0, 7 7 0, 8 7 0, 9 7 0, 11 7 0])
f317:n   (3101 < 700 [2 0 0, 3 0 0, 4 0 0, 5 0 0,
          6 0 0, 7 0 0, 8 0 0, 9 0 0, 10 0 0,
          11 0 0, 12 0 0, 13 0 0, 2 1 0, 3 1 0,
          4 1 0, 6 1 0, 7 1 0, 8 1 0, 9 1 0, 10 1 0,
          11 1 0, 12 1 0, 13 1 0, 4 2 0, 12 2 0,
          13 2 0, 4 3 0, 12 3 0,13 3 0, 4 6 0,
          12 6 0, 13 6 0, 4 7 0, 12 7 0, 13 7 0,
          4 8 0, 5 8 0, 6 8 0, 7 8 0, 8 8 0,
```

```
          9 8 0, 10 8 0, 11 8 0, 12 8 0, 13 8 0,
          4 9 0, 5 9 0, 8 9 0, 9 9 0, 12 9 0,
          13 9 0])
f327:n   (3102 < 700 [2 0 0, 3 0 0, 4 0 0, 5 0 0,
          6 0 0, 7 0 0, 8 0 0, 9 0 0, 10 0 0,
          11 0 0, 12 0 0, 13 0 0, 2 1 0, 3 1 0,
          4 1 0, 6 1 0, 7 1 0, 8 1 0, 9 1 0, 10 1 0,
          11 1 0, 12 1 0, 13 1 0, 4 2 0, 12 2 0,
          13 2 0, 4 3 0, 12 3 0,13 3 0, 4 6 0,
          12 6 0, 13 6 0, 4 7 0, 12 7 0, 13 7 0,
          4 8 0, 5 8 0, 6 8 0, 7 8 0, 8 8 0,
          9 8 0, 10 8 0, 11 8 0, 12 8 0, 13 8 0,
          4 9 0, 5 9 0, 8 9 0, 9 9 0, 12 9 0,
          13 9 0])
f337:n   (3103 < 700 [2 0 0, 3 0 0, 4 0 0, 5 0 0,
          6 0 0, 7 0 0, 8 0 0, 9 0 0, 10 0 0,
          11 0 0, 12 0 0, 13 0 0, 2 1 0, 3 1 0,
          4 1 0, 6 1 0, 7 1 0, 8 1 0, 9 1 0, 10 1 0,
          11 1 0, 12 1 0, 13 1 0, 4 2 0, 12 2 0,
          13 2 0, 4 3 0, 12 3 0,13 3 0, 4 6 0,
          12 6 0, 13 6 0, 4 7 0, 12 7 0, 13 7 0,
          4 8 0, 5 8 0, 6 8 0, 7 8 0, 8 8 0,
          9 8 0, 10 8 0, 11 8 0, 12 8 0, 13 8 0,
          4 9 0, 5 9 0, 8 9 0, 9 9 0, 12 9 0,
          13 9 0])
f347:n   (3104 < 700 [2 0 0, 3 0 0, 4 0 0, 5 0 0,
          6 0 0, 7 0 0, 8 0 0, 9 0 0, 10 0 0,
          11 0 0, 12 0 0, 13 0 0, 2 1 0, 3 1 0,
          4 1 0, 6 1 0, 7 1 0, 8 1 0, 9 1 0, 10 1 0,
          11 1 0, 12 1 0, 13 1 0, 4 2 0, 12 2 0,
          13 2 0, 4 3 0, 12 3 0,13 3 0, 4 6 0,
          12 6 0, 13 6 0, 4 7 0, 12 7 0, 13 7 0,
          4 8 0, 5 8 0, 6 8 0, 7 8 0, 8 8 0,
          9 8 0, 10 8 0, 11 8 0, 12 8 0, 13 8 0,
          4 9 0, 5 9 0, 8 9 0, 9 9 0, 12 9 0,
          13 9 0])
f357:n   (3105 < 700 [2 0 0, 3 0 0, 4 0 0, 5 0 0,
          6 0 0, 7 0 0, 8 0 0, 9 0 0, 10 0 0,
          11 0 0, 12 0 0, 13 0 0, 2 1 0, 3 1 0,
          4 1 0, 6 1 0, 7 1 0, 8 1 0, 9 1 0, 10 1 0,
          11 1 0, 12 1 0, 13 1 0, 4 2 0, 12 2 0,
          13 2 0, 4 3 0, 12 3 0,13 3 0, 4 6 0,
          12 6 0, 13 6 0, 4 7 0, 12 7 0, 13 7 0,
          4 8 0, 5 8 0, 6 8 0, 7 8 0, 8 8 0,
          9 8 0, 10 8 0, 11 8 0, 12 8 0, 13 8 0,
          4 9 0, 5 9 0, 8 9 0, 9 9 0, 12 9 0,
          13 9 0])
f367:n   (3106 < 700 [2 0 0, 3 0 0, 4 0 0, 5 0 0,
          6 0 0, 7 0 0, 8 0 0, 9 0 0, 10 0 0,
          11 0 0, 12 0 0, 13 0 0, 2 1 0, 3 1 0,
          4 1 0, 6 1 0, 7 1 0, 8 1 0, 9 1 0, 10 1 0,
```

```
          11 1 0, 12 1 0, 13 1 0, 4 2 0, 12 2 0,
          13 2 0, 4 3 0, 12 3 0,13 3 0, 4 6 0,
          12 6 0, 13 6 0, 4 7 0, 12 7 0, 13 7 0,
          4 8 0, 5 8 0, 6 8 0, 7 8 0, 8 8 0,
          9 8 0, 10 8 0, 11 8 0, 12 8 0, 13 8 0,
          4 9 0, 5 9 0, 8 9 0, 9 9 0, 12 9 0,
          13 9 0])
f377:n   (3107 < 700 [2 0 0, 3 0 0, 4 0 0, 5 0 0,
          6 0 0, 7 0 0, 8 0 0, 9 0 0, 10 0 0,
          11 0 0, 12 0 0, 13 0 0, 2 1 0, 3 1 0,
          4 1 0, 6 1 0, 7 1 0, 8 1 0, 9 1 0, 10 1 0,
          11 1 0, 12 1 0, 13 1 0, 4 2 0, 12 2 0,
          13 2 0, 4 3 0, 12 3 0,13 3 0, 4 6 0,
          12 6 0, 13 6 0, 4 7 0, 12 7 0, 13 7 0,
          4 8 0, 5 8 0, 6 8 0, 7 8 0, 8 8 0,
          9 8 0, 10 8 0, 11 8 0, 12 8 0, 13 8 0,
          4 9 0, 5 9 0, 8 9 0, 9 9 0, 12 9 0,
          13 9 0])
f387:n   (3108 < 700 [2 0 0, 3 0 0, 4 0 0, 5 0 0,
          6 0 0, 7 0 0, 8 0 0, 9 0 0, 10 0 0,
          11 0 0, 12 0 0, 13 0 0, 2 1 0, 3 1 0,
          4 1 0, 6 1 0, 7 1 0, 8 1 0, 9 1 0, 10 1 0,
          11 1 0, 12 1 0, 13 1 0, 4 2 0, 12 2 0,
          13 2 0, 4 3 0, 12 3 0,13 3 0, 4 6 0,
          12 6 0, 13 6 0, 4 7 0, 12 7 0, 13 7 0,
          4 8 0, 5 8 0, 6 8 0, 7 8 0, 8 8 0,
          9 8 0, 10 8 0, 11 8 0, 12 8 0, 13 8 0,
          4 9 0, 5 9 0, 8 9 0, 9 9 0, 12 9 0,
          13 9 0])
f397:n   (3109 < 700 [2 0 0, 3 0 0, 4 0 0, 5 0 0,
          6 0 0, 7 0 0, 8 0 0, 9 0 0, 10 0 0,
          11 0 0, 12 0 0, 13 0 0, 2 1 0, 3 1 0,
          4 1 0, 6 1 0, 7 1 0, 8 1 0, 9 1 0, 10 1 0,
          11 1 0, 12 1 0, 13 1 0, 4 2 0, 12 2 0,
          13 2 0, 4 3 0, 12 3 0,13 3 0, 4 6 0,
          12 6 0, 13 6 0, 4 7 0, 12 7 0, 13 7 0,
          4 8 0, 5 8 0, 6 8 0, 7 8 0, 8 8 0,
          9 8 0, 10 8 0, 11 8 0, 12 8 0, 13 8 0,
          4 9 0, 5 9 0, 8 9 0, 9 9 0, 12 9 0,
          13 9 0])
f407:n   (3110 < 700 [2 0 0, 3 0 0, 4 0 0, 5 0 0,
          6 0 0, 7 0 0, 8 0 0, 9 0 0, 10 0 0,
          11 0 0, 12 0 0, 13 0 0, 2 1 0, 3 1 0,
          4 1 0, 6 1 0, 7 1 0, 8 1 0, 9 1 0, 10 1 0,
          11 1 0, 12 1 0, 13 1 0, 4 2 0, 12 2 0,
          13 2 0, 4 3 0, 12 3 0,13 3 0, 4 6 0,
          12 6 0, 13 6 0, 4 7 0, 12 7 0, 13 7 0,
          4 8 0, 5 8 0, 6 8 0, 7 8 0, 8 8 0,
          9 8 0, 10 8 0, 11 8 0, 12 8 0, 13 8 0,
          4 9 0, 5 9 0, 8 9 0, 9 9 0, 12 9 0,
          13 9 0])
```

```
f417:n   (3111 < 700 [2 0 0, 3 0 0, 4 0 0, 5 0 0,
          6 0 0, 7 0 0, 8 0 0, 9 0 0, 10 0 0,
          11 0 0, 12 0 0, 13 0 0, 2 1 0, 3 1 0,
          4 1 0, 6 1 0, 7 1 0, 8 1 0, 9 1 0, 10 1 0,
          11 1 0, 12 1 0, 13 1 0, 4 2 0, 12 2 0,
          13 2 0, 4 3 0, 12 3 0,13 3 0, 4 6 0,
          12 6 0, 13 6 0, 4 7 0, 12 7 0, 13 7 0,
          4 8 0, 5 8 0, 6 8 0, 7 8 0, 8 8 0,
          9 8 0, 10 8 0, 11 8 0, 12 8 0, 13 8 0,
          4 9 0, 5 9 0, 8 9 0, 9 9 0, 12 9 0,
          13 9 0])
f427:n   (3112 < 700 [2 0 0, 3 0 0, 4 0 0, 5 0 0,
          6 0 0, 7 0 0, 8 0 0, 9 0 0, 10 0 0,
          11 0 0, 12 0 0, 13 0 0, 2 1 0, 3 1 0,
          4 1 0, 6 1 0, 7 1 0, 8 1 0, 9 1 0, 10 1 0,
          11 1 0, 12 1 0, 13 1 0, 4 2 0, 12 2 0,
          13 2 0, 4 3 0, 12 3 0,13 3 0, 4 6 0,
          12 6 0, 13 6 0, 4 7 0, 12 7 0, 13 7 0,
          4 8 0, 5 8 0, 6 8 0, 7 8 0, 8 8 0,
          9 8 0, 10 8 0, 11 8 0, 12 8 0, 13 8 0,
          4 9 0, 5 9 0, 8 9 0, 9 9 0, 12 9 0,
          13 9 0])
f437:n   (3113 < 700 [2 0 0, 3 0 0, 4 0 0, 5 0 0,
          6 0 0, 7 0 0, 8 0 0, 9 0 0, 10 0 0,
          11 0 0, 12 0 0, 13 0 0, 2 1 0, 3 1 0,
          4 1 0, 6 1 0, 7 1 0, 8 1 0, 9 1 0, 10 1 0,
          11 1 0, 12 1 0, 13 1 0, 4 2 0, 12 2 0,
          13 2 0, 4 3 0, 12 3 0,13 3 0, 4 6 0,
          12 6 0, 13 6 0, 4 7 0, 12 7 0, 13 7 0,
          4 8 0, 5 8 0, 6 8 0, 7 8 0, 8 8 0,
          9 8 0, 10 8 0, 11 8 0, 12 8 0, 13 8 0,
          4 9 0, 5 9 0, 8 9 0, 9 9 0, 12 9 0,
          13 9 0])
f447:n   (3114 < 700 [2 0 0, 3 0 0, 4 0 0, 5 0 0,
          6 0 0, 7 0 0, 8 0 0, 9 0 0, 10 0 0,
          11 0 0, 12 0 0, 13 0 0, 2 1 0, 3 1 0,
          4 1 0, 6 1 0, 7 1 0, 8 1 0, 9 1 0, 10 1 0,
          11 1 0, 12 1 0, 13 1 0, 4 2 0, 12 2 0,
          13 2 0, 4 3 0, 12 3 0,13 3 0, 4 6 0,
          12 6 0, 13 6 0, 4 7 0, 12 7 0, 13 7 0,
          4 8 0, 5 8 0, 6 8 0, 7 8 0, 8 8 0,
          9 8 0, 10 8 0, 11 8 0, 12 8 0, 13 8 0,
          4 9 0, 5 9 0, 8 9 0, 9 9 0, 12 9 0,
          13 9 0])
f457:n   (3115 < 700 [2 0 0, 3 0 0, 4 0 0, 5 0 0,
          6 0 0, 7 0 0, 8 0 0, 9 0 0, 10 0 0,
          11 0 0, 12 0 0, 13 0 0, 2 1 0, 3 1 0,
          4 1 0, 6 1 0, 7 1 0, 8 1 0, 9 1 0, 10 1 0,
          11 1 0, 12 1 0, 13 1 0, 4 2 0, 12 2 0,
          13 2 0, 4 3 0, 12 3 0,13 3 0, 4 6 0,
          12 6 0, 13 6 0, 4 7 0, 12 7 0, 13 7 0,
```

```
4 8 0, 5 8 0, 6 8 0, 7 8 0, 8 8 0,
9 8 0, 10 8 0, 11 8 0, 12 8 0, 13 8 0,
4 9 0, 5 9 0, 8 9 0, 9 9 0, 12 9 0,
13 9 0])
```

C.4. PARET Input for Region 1 with Thermal Column

```
     0
*PARET:  TRIGA Steady State at 1MW, therm column, burn 30 days, region1
1001,      -2    16     7     1     1     1
1002,       0     0     6    -1     0    75
1003,    1.0         0.032656    1.78211+5 -21.11        1.79200-2
1004,    1.74110-2   1.74200-2   0.0         0.0         0.4064
0.1016
1005,    0.1016      0.0071     27.900-6   9.80664     0.00679
1006     0.00         0.80        1.0       988.67      -0.47296
1007,   -2.02010-3   1.15817-5   0.00        0.00        1.00
0.001
1008,    0.00        0.001       0.001       0.05        0.05
0.05
1009,    1.4         0.33
1111,    0.050804    1.00         1.00
1112,       0     1     1     6     1     5+5
1113,    3.81         0.2       10000.0      0.00
1114,    0.0889      0.0889
2001,    0.0         0.0        18.00        0.00        0.00
2002,    0.0         0.4059+4    2.0600+6    0.00       -273.0
2003,    0.0         0.0         0.199000    0.00        0.00
2004,    0.0         0.0         6.66340+2   0.00        0.00
2005,    0.0         0.0        16.8         0.00        0.00
2006,    0.0         0.0         3.975+6     0.00        0.00
3001,   4.35275-3      5     1   0.980
3002,      9.0-6       6     2   0.00
3003,      5.00-4      7     3   0.000
4001,    0.02540      16
5100,       1     0  0.02794      0.08140    0.5         0.55       1.0
5100,    1.00        0.00        0.00
5101,    1.1         1.1         4.38511-2   4.38511-2  1.3818
1.250
5102,    0.001       1.00        1.00        1.00
5103,    1.412       1.00        1.00        1.00
5104,    1.324       1.00        1.00        1.00
5105,    1.489       1.00        1.00        1.00
5106,    1.607       1.00        1.00        1.00
5107,    1.674       1.00        1.00        1.00
5108,    1.670       1.00        1.00        1.00
5109,    1.599       1.00        1.00        1.00
5110,    1.502       1.00        1.00        1.00
5111,    1.412       1.00        1.00        1.00
5112,    1.305       1.00        1.00        1.00
5113,    1.184       1.00        1.00        1.00
5114,    1.045       1.00        1.00        1.00
5115,    0.904       1.00        1.00        1.00
5116,    0.738       1.00        1.00        1.00
5117,    0.682       1.00        1.00        1.00
```

```
5200,      1     0  0.02794      0.91860     0.5         0.55
1.00
5200,    1.00         0.0         0.0
5201,    1.1          1.1         4.38511-2   4.38511-2 1.3818
1.250
5202,    0.001        1.00        1.00        1.00
5203,    1.056        1.00        1.00        1.00
5204,    0.981        1.00        1.00        1.00
5205,    1.105        1.00        1.00        1.00
5206,    1.195        1.00        1.00        1.00
5207,    1.245        1.00        1.00        1.00
5208,    1.251        1.00        1.00        1.00
5209,    1.210        1.00        1.00        1.00
5210,    1.154        1.00        1.00        1.00
5211,    1.090        1.00        1.00        1.00
5212,    1.016        1.00        1.00        1.00
5213,    0.928        1.00        1.00        1.00
5214,    0.830        1.00        1.00        1.00
5215,    0.724        1.00        1.00        1.00
5216,    0.608        1.00        1.00        1.00
5217,    0.606        1.00        1.00        1.00
6001,    0.3824-1     0.12722-1   0.21194     0.31737-1   0.1878
0.1161
6002,    0.40684      0.31137     0.12879     1.4001      0.2639-1
3.8706
9000,      6
9001,    0.000        0.000       0.000         0.15        1.80
0.20
9002,    1.80         2.00        0.00          2.20        0.00
1000.0
10000,     6
10001,   166.46       0.00        300.0        0.300        300.0
0.500
10002,   100.0        5.00        10.49        45.00        10.49
1000.0
11000,     2
11001,   0.0         10.00         0.5        1000.0
12000,     2
12001,   0.0          0.0          0.00          0.0
14000,     6
14001,   0.001       0.0          0.0001      0.20          0.00005
0.25
14002,   0.0005      0.28         0.001       1.00          0.005
1.50
16000,     6
16001,   0.1           50         0.0         0.02           10
0.20
16002,   0.005          1         0.25        0.10           10
0.28
16003,   0.50          25         1.00        1.00           10
1.50
```

```
17000,     2
17001,   1.0          0.0        1.00000   455.0
18000,     2
18001,   0.0         0.0       -4.00         0.381
```

APPENDIX D

MCNP INPUT DECK FOR RACE SIMULATION

```
TRIGA Reactor 3D Core Lattice (no thermal column)
c
c   - Description -
c
c        This deck includes a full core simulation for the
c        TAMU NSC TRIGA. Rod-to-rod spacing is rod averages
c        in x- and y-dimensions. Spacing is rectangular (not
c        square).  Fuel and clad materials are from Rearden
c        Thesis (August 1995).  The grid plate is included as
c        a solid aluminum section beneath the core. Support
c        structure for the grid plate was not included. Also,
c        the beam ports and thermal column were not included.
c        Since the pool is essentially infinitely large, the
c        tank and tank liner were ignored.
c
c        Shim safety rods must be moved in bank using surfaces
c        200, 201, and 202. The transient rod can be moved using
c        surfaces 302, 303, 304, and 305.  The Regulating rod can
c        be moved using surfaces 402 and 403.  Fuel and rod
c        materials are all fresh.  Erbium cross sections are
c        from Charlton-3xc-library, all other cross sections
c        are ENDF/B-VI standard MCNP cross sections.
c
c        Modified for 30/20 fuel.
c
c     -- Cell Cards --
c
c         - Fuel Pin -
09    1  0.04297569  -100 +111 -112      u=1 imp:n=1 imp:p=1  imp:e=0
10    2  0.0887799  +100 -101 +111 -112  u=1 imp:n=1 imp:p=1  imp:e=0
11    3  0.083848  +101 -102 +110 -113   u=1 imp:n=1 imp:p=1  imp:e=0
12    7  0.0878229  -101 +110 -111       u=1 imp:n=1 imp:p=1  imp:e=0
13    7  0.0878229  -101 +112 -113       u=1 imp:n=1 imp:p=1  imp:e=0
14    8  0.089452  -102 +113 -114        u=1 imp:n=1 imp:p=1  imp:e=0
15    9  0.095482  -102 -110 +109        u=1 imp:n=1 imp:p=1  imp:e=0
16   10  0.060220  -109 +108            u=1 imp:n=1 imp:p=1  imp:e=0
17    4  0.100040  +102 +109            u=1 imp:n=1 imp:p=1  imp:e=0
18    4  0.100040  -108                 u=1 imp:n=1 imp:p=1  imp:e=0
19    4  0.100040  -102 +114            u=1 imp:n=1 imp:p=1  imp:e=0
c
c         - Shim Safety Control Rod -
20    5  0.135143  -101 +201 -202       u=2 imp:n=1 imp:p=1  imp:e=0
21    3  0.083848  +101 -102 +200 -202  u=2 imp:n=1 imp:p=1  imp:e=0
22    1  0.04297569  -100 +200 -201     u=2 imp:n=1 imp:p=1  imp:e=0
23    2  0.0887799  +100 -101 +200 -201  u=2 imp:n=1 imp:p=1  imp:e=0
```

```
24    4  0.100040  +102 +109             u=2 imp:n=1 imp:p=1  imp:e=0
25    4  0.100040  -102 -200             u=2 imp:n=1 imp:p=1  imp:e=0
26    4  0.100040  -102 +202             u=2 imp:n=1 imp:p=1  imp:e=0
27   10  0.060220  +102 -109 +108        u=2 imp:n=1 imp:p=1  imp:e=0
28    4  0.100040  +102 -108             u=2 imp:n=1 imp:p=1  imp:e=0
c
c         - Transient Control Rod -
30    5  0.135143  -300 +303 -304        u=3 imp:n=1 imp:p=1  imp:e=0
31    3  0.083848  +300 -301 +302 -305   u=3 imp:n=1 imp:p=1  imp:e=0
32    0            -300 +302 -303        u=3 imp:n=1 imp:p=1  imp:e=0
33    4  0.100040  +301 +109             u=3 imp:n=1 imp:p=1  imp:e=0
34    4  0.100040  -301 -302             u=3 imp:n=1 imp:p=1  imp:e=0
35    0            -300 +304 -305        u=3 imp:n=1 imp:p=1  imp:e=0
36    4  0.100040  -301 +305             u=3 imp:n=1 imp:p=1  imp:e=0
37   10  0.060220  +301 -109 +108        u=3 imp:n=1 imp:p=1  imp:e=0
38    4  0.100040  +301 -108             u=3 imp:n=1 imp:p=1  imp:e=0
c
c         - Regulating Control Rod -
40    6  0.127794  -400 +402 -403        u=4 imp:n=1 imp:p=1  imp:e=0
41    3  0.083848  +400 -401 +402 -403   u=4 imp:n=1 imp:p=1  imp:e=0
42    4  0.100040  +401 +109             u=4 imp:n=1 imp:p=1  imp:e=0
43    4  0.100040  -401 -402             u=4 imp:n=1 imp:p=1  imp:e=0
44    4  0.100040  -401 +403             u=4 imp:n=1 imp:p=1  imp:e=0
45   10  0.060220  +401 -109 +108        u=4 imp:n=1 imp:p=1  imp:e=0
46    4  0.100040  +401 -108             u=4 imp:n=1 imp:p=1  imp:e=0
c
c         - Graphite Element -
50    7  0.0878229  -500 +109 -502       u=5 imp:n=1 imp:p=1  imp:e=0
51    7  0.0878229  +500 +109 -502       u=5 imp:n=1 imp:p=1  imp:e=0
52   10  0.060220  -500 -109 +108        u=5 imp:n=1 imp:p=1  imp:e=0
53    4  0.100040  -108                  u=5 imp:n=1 imp:p=1  imp:e=0
54    4  0.100040  +502                  u=5 imp:n=1 imp:p=1  imp:e=0
c
c         - Water Hole -
60    4  0.100040  -500 +109             u=6 imp:n=1 imp:p=1  imp:e=0
61    4  0.100040  +500                  u=6 imp:n=1 imp:p=1  imp:e=0
62   10  0.060220  -500 -109 +108        u=6 imp:n=1 imp:p=1  imp:e=0
63    4  0.100040  -500 -108             u=6 imp:n=1 imp:p=1  imp:e=0
c
c
c         - Water Hole with Tally Element - $ Tally vol in water
70    4  0.100040  -500 +600 -601 u=7 imp:n=1 imp:p=1  imp:e=0
vol=156.1064
71    4  0.100040  -500 -600 +109        u=7 imp:n=1 imp:p=1  imp:e=0
72    4  0.100040  -500 +601             u=7 imp:n=1 imp:p=1  imp:e=0
73    4  0.100040  +500                  u=7 imp:n=1 imp:p=1  imp:e=0
74   10  0.060220  -500 -109 +108        u=7 imp:n=1 imp:p=1  imp:e=0
75    4  0.100040  -500 -108             u=7 imp:n=1 imp:p=1  imp:e=0
c
c         - Tungsten Target -
90    11 -19.24     -1100 +1101 -1102    u=9 imp:n=1 imp:p=1  imp:e=1
```

```
91    7  0.087822   -1100 +109 -1101     u=9 imp:n=1 imp:p=1  imp:e=0
92    0             -1100 +1102         u=9 imp:n=1 imp:p=1  imp:e=0
93    4  0.100040   +1100 +1102         u=9 imp:n=1 imp:p=1  imp:e=0
94    4  0.100040   +1100 +1101 -1102    u=9 imp:n=1 imp:p=1  imp:e=0
95    4  0.100040   +1100 +109 -1101     u=9 imp:n=1 imp:p=1  imp:e=0
96   10  0.060220   -1100 +108 -109      u=9 imp:n=1 imp:p=1  imp:e=0
97   10  0.060220   +1100 +108 -109      u=9 imp:n=1 imp:p=1  imp:e=0
98    4  0.100040   -108                 u=9 imp:n=1 imp:p=1  imp:e=0
c
190    11 -19.24     -1103 +1101 -1102    u=10 imp:n=1 imp:p=1  imp:e=1
191    7  0.087822   -1103 +109 -1101     u=10 imp:n=1 imp:p=1  imp:e=0
192    0             -1103 +1102         u=10 imp:n=1 imp:p=1  imp:e=0
193    4  0.100040   +1103 +1102         u=10 imp:n=1 imp:p=1  imp:e=0
194    4  0.100040   +1103 +1101 -1102    u=10 imp:n=1 imp:p=1  imp:e=0
195    4  0.100040   +1103 +109 -1101     u=10 imp:n=1 imp:p=1  imp:e=0
196   10  0.060220   -1103 +108 -109      u=10 imp:n=1 imp:p=1  imp:e=0
197   10  0.060220   +1103 +108 -109      u=10 imp:n=1 imp:p=1  imp:e=0
198    4  0.100040   -108                 u=10 imp:n=1 imp:p=1  imp:e=0
c
290    11 -19.24     -1104 +1101 -1102    u=11 imp:n=1 imp:p=1  imp:e=1
291    7  0.087822   -1104 +109 -1101     u=11 imp:n=1 imp:p=1  imp:e=0
292    0             -1104 +1102         u=11 imp:n=1 imp:p=1  imp:e=0
293    4  0.100040   +1104 +1102         u=11 imp:n=1 imp:p=1  imp:e=0
294    4  0.100040   +1104 +1101 -1102    u=11 imp:n=1 imp:p=1  imp:e=0
295    4  0.100040   +1104 +109 -1101     u=11 imp:n=1 imp:p=1  imp:e=0
296   10  0.060220   -1104 +108 -109      u=11 imp:n=1 imp:p=1  imp:e=0
297   10  0.060220   +1104 +108 -109      u=11 imp:n=1 imp:p=1  imp:e=0
298    4  0.100040   -108                 u=11 imp:n=1 imp:p=1  imp:e=0
c
390    11 -19.24     -1105 +1101 -1102    u=12 imp:n=1 imp:p=1  imp:e=1
391    7  0.087822   -1105 +109 -1101     u=12 imp:n=1 imp:p=1  imp:e=0
392    0             -1105 +1102         u=12 imp:n=1 imp:p=1  imp:e=0
393    4  0.100040   +1105 +1102         u=12 imp:n=1 imp:p=1  imp:e=0
394    4  0.100040   +1105 +1101 -1102    u=12 imp:n=1 imp:p=1  imp:e=0
395    4  0.100040   +1105 +109 -1101     u=12 imp:n=1 imp:p=1  imp:e=0
396   10  0.060220   -1105 +108 -109      u=12 imp:n=1 imp:p=1  imp:e=0
397   10  0.060220   +1105 +108 -109      u=12 imp:n=1 imp:p=1  imp:e=0
398    4  0.100040   -108                 u=12 imp:n=1 imp:p=1  imp:e=0
c
c         - Fuel Assembly  Lattice -
700   0        -702 +701 -704 +703 lat=1 u=8 fill=0:17 0:11 0:0
      5 5 1 1 1 1 1 1 1 1 1 1 1 5 5 5 5
      5 5 1 1 1 4 1 1 1 1 1 1 1 5 5 5 5
      5 5 5 5 1 1 1 1 1 1 1 1 1 5 5 5 5
      5 5 5 5 1 1 2 1 1 1 2 1 1 1 5 5 5 5
      5 5 6 6 7 7 1 1 1 1 1 1 9 10 5 5 5 5
      5 5 6 6 7 7 1 1 3 1 1 1 11 12 5 5 5 5
      5 5 5 5 1 1 1 1 1 1 1 1 1 1 5 5 5 5
      5 5 5 5 1 1 2 1 1 1 2 1 1 1 5 5 5 5
      7 7 5 5 1 1 1 1 1 1 1 1 1 1 5 5 5 5
      7 7 5 5 1 1 6 6 1 1 6 6 1 1 5 5 5 5
```

```
      6 6 6 6 6 6 6 6 6 6 6 6 6 6 6 6 6
      6 6 6 6 6 6 6 6 6 6 6 6 6 6 6 6 6    imp:n=1 imp:p=1  imp:e=1
801   0        +800 -801 +802 -803 +804 -805 fill=8  imp:n=1 imp:p=1
imp:e=1
c
c         - Universe -
900   4  0.10004   #801 -900                imp:n=1 imp:p=0  imp:e=0
999   0            +900                     imp:n=0 imp:p=0  imp:e=0

c
c     -- Surface Cards --
c
c         - Fuel Pin Surfaces -
100   c/z   2.025015 1.927225 0.2280
101   c/z   2.025015 1.927225 1.7411
102   c/z   2.025015 1.927225 1.7920
108   pz  -30.48
109   pz  -17.78
110   pz   -8.89
111   pz    0.00
112   pz   38.10
113   pz   46.99
114   pz   58.42
c
c         - Shim Safety Rod Surfaces -
200   pz   -22.86 $(0.00 for full removal)
201   pz   15.24 $(38.10 for full removal)
202   pz   50.80 $(73.66 for full removal)
c
c         - Transient Rod Surfaces -
300   c/z   2.025015 1.927225 1.5164
301   c/z   2.025015 1.927225 1.5876
302   pz   -8.89
303   pz   38.10 $(38.10 for full removal)
304   pz   76.20 $(76.20 for full removal)
305   pz   80.00
c
c         -Regulating Rod Surfaces -
400   c/z   2.025015 1.927225 1.5164
401   c/z   2.025015 1.927225 1.5876
402   pz   38.10 $(38.10 for full removal)
403   pz   76.20 $(76.20 for full removal)
c
c         - Water Hole and Graphite Element Surfaces -
500   c/z   2.025015 1.927225 7.0000
501   pz   -8.89
502   pz   46.99
c
c         - Tally Element Surfaces -
600   pz   14.00
601   pz   24.00
```

```
c
c         - Pin Cell Surfaces -
701   px   0.00
702   px   4.05003
703   py   0.00
704   py   3.85445
c
c         - Core Surfaces -
800   px   0.0001
801   px  72.90053
802   py   0.0001
803   py  46.2533
804   pz -100.0
805   pz  100.0
c
c         - Reflector and Universe Cells -
900   cz 1000.00
c
c         - Tungsten Target -
1100   c/z 4.05003 3.85445 3.55
1101   pz  12.05
1102   pz  22.05
1103   c/z 0.0 3.85445 3.55
1104   c/z 4.05003 0.0 3.55
1105   c/z 0.0 0.0 3.55

c
c     -- Data Cards --
c
mode n p e
c
c  neutron, photon and electron mode code
c
nps 100000
c  number of electrons to start with is '1000'
c
rand seed=1
c  random number to start with
c
sdef  sur=1102 pos=52.585 19.237 +22.05 vec=0 0 1 dir=-1 rad=d1
      erg=20.0 par=3
c  electrons hit surface 1102
si1   0 0.5
sp1   -21 1
phys:p 100 0 0 1 0
phys:e 50   0 0 0 0 10 1 0 1 0
cut:n  1e+33   0.0    0.0  0.0
cut:p  1e+33   0.001  0.0  0.0
cut:e  1e+33   0.001  0.0  0.0
c
m1    40000.60c 4.29757e-2
```

```
mpn1  0
c        U-ZrH Fuel
m2     1001.53c  4.91576e-2
       6000.66c  1.78701e-3
      40000.58c  3.22796e-2
      68166.34c  7.71700e-5
      68167.34c  5.29900e-5
      92234.66c  8.23000e-6
      92235.14c  1.08197e-3
      92236.66c  1.21000e-5
      92238.14c  4.32127e-3
      72000.60c  1.93677e-6
      94238.60c  1.0e-30
      94239.14c  1.0e-30
      94240.60c  1.0e-30
      94241.60c  1.0e-30
      94242.60c  1.0e-30
mt2    H/Zr2.05t
       Zr/H2.05t
mpn2  0  0  0  0  0  0  0  0  0  0  0  0  0  0  0
c        SS304
m3    24000.50c  1.7482e-2
      26000.50c  5.6730e-2
      28000.50c  7.9390e-3
      25055.66c  1.6970e-3
mpn3  0  0  0  0
m4     1001.66c  6.6691E-2
       8016.66c  3.3346E-2 $ Light water
mt4    lwtr.60t
mpn4   0  0
m5     6000.66c  1.0082E-1
       5010.66c  2.1824E-2
       5011.66c  5.1500E-3 $ Borated Graphite
mt5    grph.60t
mpn5   0  0  0
m6     6000.66c  2.7247E-2
       5010.66c  2.0598E-2
       5011.66c  8.7298E-2 $ B4C
mpn6   0  0  0
m7     6000.66c  8.7744665E-2 $ Graphite
mt7    grph.60t
mpn7   0
m8    26000.50c  0.0146238
      24000.50c  0.0042940
      28000.50c  0.0019017
      25055.66c  0.0004278
      13027.66c  0.0107829
       1001.66c  0.0382806
       8016.66c  0.0191406 $ Mix of 24.7% SS, 17.9% Al, 57.4% Water
mt8    lwtr.60t
mpn8  0  0  0  0  0  0  0
```

```
m9    26000.50c  0.0192419
      24000.50c  0.0056501
      28000.50c  0.0025023
      25055.66c  0.0005629
       1001.66c  0.0450164
       8016.66c  0.0225085 $ Mix of 32.5% SS and 67.5% Water
mt9    lwtr.60t
mpn9  0  0  0  0  0  0
m10   13027.60c -0.9685
      26000.50c -0.0070
      29000.50c -0.0025
      14000.60c -0.0060
      12000.60c -0.0110
      24000.50c -0.0035
      25055.60c -0.0015    $ Structural Aluminum (type 6061)
mpn10 0  0  0  0  0  0  0
m11   74182.66c  0.2653
      74183.66c  0.1434
      74184.66c  0.3067
      74186.66c  0.2846
mpn11 74182
      74183
      74184
      74186
f16:n  (10 < 700 [2 0 0,3 0 0,4 0 0,5 0 0,6 0 0,
       7 0 0,8 0 0,9 0 0,10 0 0,11 0 0,12 0 0,13 0 0,
       2 1 0,3 1 0,4 1 0,6 1 0,7 1 0,8 1 0,9 1 0,
       10 1 0,11 1 0,12 1 0,13 1 0,
       4 2 0,5 2 0,6 2 0,7 2 0,8 2 0,9 2 0,
       10 2 0,11 2 0,12 2 0,13 2 0,
       4 3 0,5 3 0,7 3 0,8 3 0,9 3 0,
       11 3 0,12 3 0,13 3 0,
       6 4 0,7 4 0,8 4 0,9 4 0,10 4 0,11 4 0,
       6 5 0,7 5 0,9 5 0,10 5 0,11 5 0,
       4 6 0,5 6 0,6 6 0,7 6 0,8 6 0,9 6 0,10 6 0,
       11 6 0,12 6 0,13 6 0,
       4 7 0,5 7 0,7 7 0,8 7 0,9 7 0,11 7 0,12 7 0,13 7 0,
       4 8 0,5 8 0,6 8 0,7 8 0,8 8 0,9 8 0,10 8 0,
       11 8 0,12 8 0,13 8 0,
       4 9 0,5 9 0,8 9 0,9 9 0,12 9 0,13 9 0])
f26:n (23 < 700 [6 3 0, 10 3 0, 6 7 0, 10 7 0])
f36:p  (10 < 700 [2 0 0,3 0 0,4 0 0,5 0 0,6 0 0,
       7 0 0,8 0 0,9 0 0,10 0 0,11 0 0,12 0 0,13 0 0,
       2 1 0,3 1 0,4 1 0,6 1 0,7 1 0,8 1 0,9 1 0,
       10 1 0,11 1 0,12 1 0,13 1 0,
       4 2 0,5 2 0,6 2 0,7 2 0,8 2 0,9 2 0,
       10 2 0,11 2 0,12 2 0,13 2 0,
       4 3 0,5 3 0,7 3 0,8 3 0,9 3 0,
       11 3 0,12 3 0,13 3 0,
       6 4 0,7 4 0,8 4 0,9 4 0,10 4 0,11 4 0,
       6 5 0,7 5 0,9 5 0,10 5 0,11 5 0,
```

```
       4 6 0,5 6 0,6 6 0,7 6 0,8 6 0,9 6 0,10 6 0,
       11 6 0,12 6 0,13 6 0,
       4 7 0,5 7 0,7 7 0,8 7 0,9 7 0,11 7 0,12 7 0,13 7 0,
       4 8 0,5 8 0,6 8 0,7 8 0,8 8 0,9 8 0,10 8 0,
       11 8 0,12 8 0,13 8 0,
       4 9 0,5 9 0,8 9 0,9 9 0,12 9 0,13 9 0])
f46:p (23 < 700 [6 3 0, 10 3 0, 6 7 0, 10 7 0])
f57:n  (10 < 700 [2 0 0,3 0 0,4 0 0,5 0 0,6 0 0,
       7 0 0,8 0 0,9 0 0,10 0 0,11 0 0,12 0 0,13 0 0,
       2 1 0,3 1 0,4 1 0,6 1 0,7 1 0,8 1 0,9 1 0,
       10 1 0,11 1 0,12 1 0,13 1 0,
       4 2 0,5 2 0,6 2 0,7 2 0,8 2 0,9 2 0,
       10 2 0,11 2 0,12 2 0,13 2 0,
       4 3 0,5 3 0,7 3 0,8 3 0,9 3 0,
       11 3 0,12 3 0,13 3 0,
       6 4 0,7 4 0,8 4 0,9 4 0,10 4 0,11 4 0,
       6 5 0,7 5 0,9 5 0,10 5 0,11 5 0,
       4 6 0,5 6 0,6 6 0,7 6 0,8 6 0,9 6 0,10 6 0,
       11 6 0,12 6 0,13 6 0,
       4 7 0,5 7 0,7 7 0,8 7 0,9 7 0,11 7 0,12 7 0,13 7 0,
       4 8 0,5 8 0,6 8 0,7 8 0,8 8 0,9 8 0,10 8 0,
       11 8 0,12 8 0,13 8 0,
       4 9 0,5 9 0,8 9 0,9 9 0,12 9 0,13 9 0])
f67:n (23 < 700 [6 3 0, 10 3 0, 6 7 0, 10 7 0])
f76:n 90
f86:n 190
f96:n 290
f106:n 390
f116:p 90
f126:p 190
f136:p 290
f146:p 390
```

VITA

Robert Wilcox Candalino was born in Fort Worth, Texas on April 29, 1981. He is the son of Thomas and Roberta Candalino who reside in Bedford, Texas. After graduating from L.D. Bell High School in 1999, he attended Texas A&M University and received a B.S. in nuclear engineering in 2004. He continued his education at Texas A&M University for a M.S. in nuclear engineering and graduated in August of 2006.

His permanent address is the following:

3409 Blue Quail Lane

Bedford, TX 76021